SANAE 52 OCEANOGRAPHIC REPORT

Participants: Sebastiaan Swart1,2,*, Gerda Du Plessis, Giuseppe Aulicino, Samuel Eberenz, Laura Braby, Beanca van den Berg, Stephen Broccardo, Bakomoso Lebepe, Kagiso Mokalane, Baxolele Mdokwana, Mthetho Sovara, Khaya Siswana, Precious Mongwe, Andrew Schoffield, Helm van Zyl, Keith Soal, Brendan Boulle.

Principal Investigators: Dr Pedro Monteiro (CSIR), Dr Isabelle Ansorge (UCT), Dr Hans Verheye (DEA)
Mr Mthuthuzeli Gulekana (DEA), Mr Mutshutshu Tsanwani (DEA), Dr. Annette Bekker, Dr. Sandy Thomalla, Dr. Sebastiaan Swart.

CSIR, Natural Resources and the Environment, Rosebank, South Africa
Department of Oceanography, University of Cape Town, Rondebosch, South Africa
Oceans and Coasts, Department of Environmental Affairs, Roggebaai, South Africa
University of Stellenbosch, Stellenbosch, South Africa

SOCCO
Southern Ocean Carbon and Climate Observatory

MV SA AGULHAS II
VOYAGE 005 SANAE IV,
ANTARCTICA RELIEF VOYAGE SOUTH GEORGIA & SOUTH SANDWICH ISLANDS

Table of Contents

FIGURES AND TABLES

Synopsis of events and cruise track information

The SANAE 52 voyage departed Cape Town on the 6th December 2012 and returned to Cape Town on February 2013. Delays in the voyage are included where necessary. The voyage can be separated into 6 scientific legs. Figure 1 displays the GoodHope line. The begin and end dates of these legs and their heading information is given as follows:

Leg1. 6 December 2012 – 15 December 2013: GoodHope Line South

Completion of the GoodHope line as per normal waypoints with hydrographic stations occurring every ~20nm using XBT deployments. Biological stations occurring either every 20 or 40nm. Microbiology stations were conducted on fronts and zones. Deviation from the GH line occurs south of ~60°S.

Leg 2. 15 December 2012 – 12 January 2013: Logistical operations at Akta and RSA bukta

Only stations at RSA Bukta were conducted. A series of 14 CTD's were conducted and biological samples were taken at 10 successful casts. Salinity samples were only taken at every second CTD due to the limitation of sampling bottles. All casts were done down to 200m at ~12:00 and ~00:00 when logistics allowed.

Leg 3. 13 January 2013 – 22 January 2013: Buoy run North

Underway stations were conducted at a high resolution (~10-15 nm) between ~68 °S and 50°S. CTD's were done at every degree. The proposed CTD at 70 °S occupied a position within the continental shelf and 69°S was completely ice-locked (not allowing us to stop for a day to break into the ice). All CTD casts were 500m casts and conducted through the moonpool. At 50°S we turned due West and biological stations were decreased to every 2 to 4 hours till we reached South Georgia. No XBT or physical oceanography stations were done. Buoy's 3-6 were deployed during this leg.

Leg 4. 22 January 2013 – 29 January 2013: Buoy run South

Underway biological stations were conducted every 4 hours and salinities every 8 hours for the leg South. No oceanographic stations were completed. Buoy's 7-10 were deployed during this leg.

Leg 5. 29 January 2013 – 10 February 2013: Shelf backloading at Akta bukta

Upon return to Akta bay, 7 CTDs were completed at midday and midnight stations to an approximate depth of 250m. Full biological sampling was conducted on CTDs with the exception of Chlorophyll, where we ran out of filters.

Leg 6. 10 February 2013 – 19 February 2013:

Due to delays in the MV SA AGULHAS I's cruise plans, CSIR representative, Dr. Sebastiaan Swart requested the retrieval of two gliders at ~41 S 3W. As a result of bad weather and the extended trip to fetch the gliders the GoodHope line was cut completely. A northerly track 3W was roughly followed directly to the two gliders at an average speed of 15 knots. Stations were conducted every 90 min as per GoodHope South. Both gliders, deployed during the 2012 Gough takeover voyage, were retrieved within 4 hours and a direct track back to Cape Town was followed. As an addition, the CPR was towed continuously during ice-free conditions.

1. INTRODUCTION

1.1 Physical Oceanography

The global oceanic thermohaline circulation, often referred to as the Meridional Overturning Circulation, is a vital link in the global transport of heat from the tropics to higher latitudes. The physical structure of this circulation belt and its efficiency in regulating climate is substantially influenced by the nature of water mass exchange between ocean basins (Gordon, 1986; Rintoul, 1991; Speich et al., 2001). The Antarctic Circumpolar Current (ACC) is by far the largest conduit for such exchange. Extending unbroken around Antarctica it is the primary means by which water, heat and salt are transferred between different ocean basins.

The Southern Ocean plays a unique role in coupling the ocean to the atmosphere and cryosphere. Variations in these aspects of the global climate system may be expected to be linked to and perhaps drive global climate variability. The most relevant processes occurring in the Southern Ocean that may have a large influence in the global ocean circulation and possibly on the evolution of our climate include:

. (1) The Antarctic Circumpolar Current (ACC) is the only current that connects all three major ocean basins, thereby providing an essential heat and fresh water conduit.

. (2) The Southern Ocean provides a strong coupling of the ocean and atmosphere within the Subantarctic belt and its polar-extrapolar communication of heat, freshwater and CO2 through the production of Antarctic Intermediate Water and Subantarctic Mode Water. These water masses spread northwards injecting cool low salinity water into and along the base of the main thermocline.

. (3) The upwelling of Circumpolar Deep Water south of the Antarctic Circumpolar Current provides a pathway in the transport heat from of >2000 m into the atmosphere and cryosphere.

. (4) The production of very cold dense Antarctic Bottom Water.

. (5) The Antarctic sea ice fields represent a highly mobile and mutable surface property whose distribution and characteristics may play a major role in the global radiative budget and thus global climate.

. (6) The large-scale coherent variability of the atmospheric circulation over the Southern Ocean and the mechanisms of these variations and their geographic communication, are directly involved in the propagation of anomalies across the various climate zones.

Interpreting the causes of temperature and salinity variability observed in the ocean interior requires an understanding of the formation of Southern Ocean water masses and the circulation paths they follow. Changes in heat supplied by the deep ocean may influence the atmosphere directly or through changes in sea ice. As these exchanges play an important role in regulating mean global climate, sustained hydrographic observations are essential in order to describe and better understand the physical and dynamic processes, which are responsible for the variability of the ACC (Budillon and Rintoul, 2003). The major part of the flow associated with the ACC is concentrated at a number of circumpolar fronts, which act as boundaries separating zones of uniform water masses. From north to south the fronts and associated zones of the Southern Ocean are: Subtropical Convergence (STC), Subantarctic Zone (SAZ), Subantarctic Front (SAF), Polar Frontal Zone (PFZ), Antarctic Polar Front (APF), Antarctic Zone (AAZ) and Antarctic Divergence (AAD).

South of Africa, the Southern Ocean plays a unique role in providing a source for the equatorward flux of heat into the South Atlantic. However, it has been suggested (Speich et al., 2001; 2002) that water mass differences between the South Indian and Atlantic Ocean basins would be far more prominent were it not for various smaller inter-ocean links. South of Africa, water masses originating in the Indian Ocean are injected into the South Atlantic both by anticyclonic ring shedding processes at the Agulhas Retroflection region and by filaments of Agulhas Current water (Lutjeharms and Cooper, 1996).

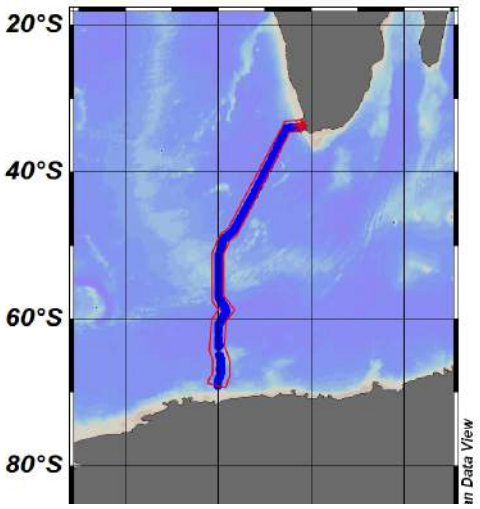

Figure 1. The GoodHope Line indicating the track followed with blue circles denoting individual stations.

Recent modeling studies on the global ocean circulation suggest that Indo-Atlantic interocean exchanges through the Agulhas Current system are far more important for the thermohaline circulation than the direct input of water from the Drake Passage (Speich et al., 2001; 2002). Estimates of the percentage of mode and intermediate waters entering the Atlantic via the Agulhas region is highly variable ranging from 0% (Rintoul, 1991) to 50% (Gordon et al., 1992). Therefore, in order to understand the role of this key component of the MOC on the global ocean circulation and its possible role in climate it is critical that the inflow of Indian waters into the Atlantic Ocean be properly quantified, and monitored.

The aim of the GoodHope programme is to establish an intensive monitoring platform that will provide detailed information on the physical structure and volume flux of waters south of South Africa, where the interbasin exchanges occur. A key component of this programme is the implementation of the high-density XBT line AX25 that runs from Cape Town to Antarctica. The advantages of the GoodHope programme are four-fold: (1) It runs approximately along with the TOPEX/POSEIDON – JASON 1 altimeter ground-tracks and will serve for ground-truthing of altimetry-derived sea height anomaly data (2) The southern fraction of this line (south of 50oS) is currently monitored by a mooring array aimed at investigating the formation of deep and bottom water in the Weddell Sea deployed during the WECCON project by the Alfred Wegener Institute for Polar and Marine Research. (3) The northern section of the GoodHope line also overlaps the region being studied by the USA - ASTTEX programme, enabling observations in the Southern Ocean to be linked with data collected within the Benguela region and the west coast of Southern Africa. (3) GoodHope will support and contribute to the data collected by numerous Pressure Inverted Echo Sounder (PIES) moorings already deployed and retrieved along this line.

Sustained observations such as repeat transects along AX25 will provide the only means to monitor the vertical structure and to investigate the variability of the fronts in this region. The GoodHope programme will investigate year-to-year and longer period variability in the fluxes, such as those related to the Antarctic Circumpolar Wave. Such intense and periodic monitoring has been underway in the Drake Passage (Sprintall et al., 1997) and south of Tasmania (Budillon and Rintoul, 2003) since the 1970s. A repeat transect between South Africa and

Antarctica, the third Southern Ocean “choke point”, was only implemented during the first GoodHope cruise in 2004.

1.2. Carbon & Climate change

Changes in the Earth’s climate are the result of both internal variability within the climate system and external factors, such as anthropogenic emissions of long-lived greenhouse gases. Greenhouse gases, such as carbon dioxide (CO2), have a lasting effect on the Earth System through both global warming and ocean acidification (Caldeira and Wickett, 2005). Since 1750,

the atmospheric CO2 concentration has been rising steadily and anthropogenic activities presently add approximately 7.1 Pg C y-1 (1015g) CO2 to the atmosphere. Of the long lived greenhouse gases, CO2 is the most important manageable driving agent for climate change. The ocean has the most significant overall potential as a sink for anthropogenic CO2 and it is currently estimated to take up 30% (2 – 2.4 Pg C y-1) (Takahashi et al., 2002). This oceanic CO2 uptake slows the build up of atmospheric CO2 reducing the magnitude of human-driven climate change (Fung et al., 2005, Friedlingstein et al., 2006). The uptake of atmospheric CO2 by the oceans however lowers the surface water pH with the potential for the resultant ocean acidification to disrupt marine ecosystems (Feely et al., 2004; Orr et al., 2005; Doney et al., 2009a). Climate change is predicted to impact the biology as well as the physics of the ocean driving both positive and negative feedbacks on the global carbon pump (Boyd and Doney, 2003). Meaningful projections of the future behavior of the oceanic carbon sink will ultimately depend on an improved understanding and prediction ability for the ocean mechanisms regulating CO2 uptake and its evolution under a future altered climate (Doney et al., 2009b).

Present work that combines modeling and observations on a global scale emphasizes the climatological scale of the Southern Ocean CO2 sink (Caldeira and Duffy, 2000; Takahashi et al., 2002). It shows that this region is characterized by a net atmosphere – ocean sink flux of 1 – 5 moles CO2 m-2 y-1 and that this flux is predominantly driven by biogeochemical processes (biological pump) as opposed to physical solubility processes (solubility pump) (Takahashi et al., 2002).

The Southern Ocean to the south of South Africa is a particularly interesting part of the Ocean - Atmosphere System because of the high energy meso-scale eddy activity linked to the convergence and exchange between basins (Lutjeharms et al., 2000). The combination of convergence and high energy mixing gives rise to two biogeochemically important features of the sub-Antarctic:

1) The production of sub Antarctic Mode Water (SAMW) and Antarctic intermediate water (AAIW) which are then advected into most of the oceans thermocline domain.

2) Elevated New production fluxes south of the sub-tropical frontal zone.

Combined these two features make this region one of the most important ocean sinks of anthropogenic CO2 (Sigman and Boyle, 2000; Sarmiento and Orr, 2004; Marinov et al., 2006). In contrast, south of 50°S lies a zone which is linked to the thermohaline deep ocean circulation (Marinov et al., 2006), where Circumpolar Deep Water upwells and outcrops and where Antarctic Bottom water is formed. The role of the Southern Ocean as a net CO2 sink is controlled by the interaction between the Sub-Antarctic CO2 sink and the out-gassing linked to upwelling of Circumpolar Deep Water (CDW) south of 50°S (Sigman and Boyle, 2000; Toggweiler et al., 2003; 2006). This coupled behavior is sensitive to changes in the characteristics of the westerly wind stress over the Southern Ocean which responds to changes in the characteristics of the Southern Annular Mode (SAM)(Hall and Visbeck, 2002) as well as the long term change in the pCO2 gradient between the atmosphere and the ocean (Bellerby et al., 2004; Toggweiler et al., 2006). Recent studies have suggested that although the CO2 sink characteristics of the Sub-Antarctic Zone may remain strong the overall sink characteristics of the Southern Ocean may have been weakened by increased upwelling rates of CO2 rich CDW (LeQuéré et al., 2007; Baker, 2007).

Despite the Southern Ocean being one of the most important sinks of anthropogenic CO2 (Berger and Wefer, 1991; Caldeira and Duffy, 2000; Sigman and Boyle, 2000), it remains one of the least sampled and understood ocean domains. The basis for the focus of SOCCO is to better understand the knowledge gaps in the CO2 sink dynamics of the Southern Ocean south of Africa. One of the important knowledge gaps lies in linking the physical driver scales with those of the biogeochemical response, particularly the balance between export and total production. Recent innovations around observational capabilities to measure production (NCP & GPP) underway have opened the possibilities to close that gap (Cassar et al., 2007). South Africa has a comparative geographic advantage in respect of the Southern Ocean, the South Atlantic sector in particular. We aim to combine this with scientific questions of global significance to set up a strong programme that will both strengthen South Africa contribution to global climate knowledge and attract the best young scientists to this field.

1.3. Rationale

On average, the Southern Ocean is characterized by abundant macronutrients coupled with low annual average net primary production rates making it a predominantly high nutrient-low chlorophyll (HNLC) ecosystem (Moore and Abbott, 2000). Intense phytoplankton blooms however occasionally develop, making productivity in the Southern ocean both temporally and spatially variable. In addition, these localized phytoplankton blooms account for the importance of the Southern Ocean in global biogeochemical cycling. Low production rates are generally associated with the permanently open ocean zone north of the sea ice, whereas high rates of production tend to be associated with frontal regions where divergence of surface waters brings high nutrient waters to the surface, fueling productivity (Moore and Abott, 2000). Other exceptions of high productivity within the Southern Ocean are near offshore islands and in the marginal ice zone.

The role of various biogeochemical controls on phytoplankton production in the high nutrient low chlorophyll (HNLC) Southern Ocean have been well established (for review see Boyd 2002; Cochlan, 2008). However our understanding of the interaction between the various biogeochemical controls and the regional variability of these controls remains incomplete. The role of Fe and light in particular are thought to play a crucial role in the vicinity of sub-Antarctic islands due to the 'island-mass effect'. In such cases iron stress is relieved from benthic and surface run-off sources up stream of the islands. Furthermore, the light environment in the vicinity of the islands is enhanced by stabilization of the water column through increased buoyancy in the surface layer caused by glacial melt water (south of PAF) or rain-water run-off (north of APF). The increased stability enhances stratification, causing a shoaling of the upper mixed layer wherein the phytoplankton can experience a more favorable light environment and minimize respiratory losses. The relationship between these and other controls (such as Si limitation and grazing) and the degree of co-limitation on phytoplankton production is not well understood. A study by Perissinotto et al. (1992) suggests stabilization by melt water to be the main cause of phytoplankton bloom formation in the vicinity of the South Sandwich Islands whereas Holeton et al. (2005) found natural Fe fertilization to be the dominant control on a bloom at the nearby South Georgia Island.

In addition to the large influence these parameters have on phytoplankton blooms, we do not fully yet understand its impact on the higher and lower order biomes. It is impossible to study a bloom without taking into account the predation qualities of bacterioplankton or the influence of viral growth in certain populations. With the change in sea surface temperatures, both viral and bacterial influence on phytoplankton growth and multiplication could drastically alter the diversity and hierarchy with which such a bloom is formed. The only way to be able to fully understand interactions however, is to know what is present. A start to this was the International polar year project, which utilized the collaborative efforts of laboratories all over the world to increase our knowledge of the Polar Regions. One such an example is presented in Fig.2. The diagram indicates both the areas, which were under sampled for all species monitored during the course of 2007-2008, and the density of a said species in specific quadrants. Clearly the area South of South Africa has a large potential to be sampled and may still contain some unknown species or novel bacterial biodiversity. This is the main motivation behind the large scale biodiversity study currently underway. It is only possible to predict a physical or biological response when all parameters are considered and we are lacking several.

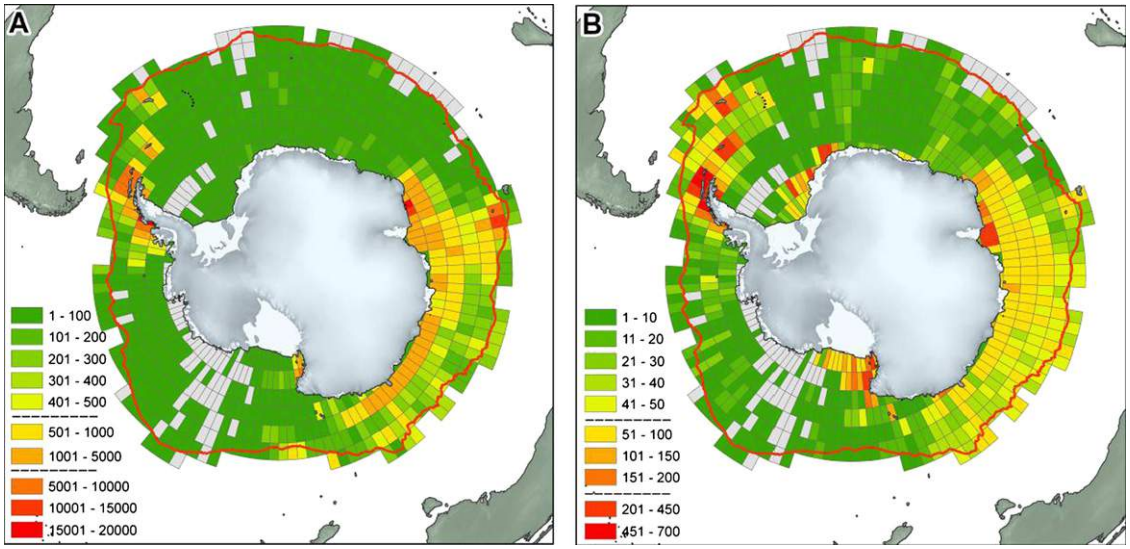

Figure 2. An overview of total marine sampling sites and frequency sampled (A) as well as species richness (B) across a 3° latitude/longitude grid around Antarctica. The distribution records give an indication of areas low in sampling efficiency and coverage. Image from Griffiths *et al.,* (2010).

The SANAE cruise track crossed four distinct oceanic domains: the seasonal marginal ice-edge zone, the permanently open ocean zone, the shelf zone of the South Sandwich and South Georgia Islands and the frontal zones of the Antarctic Polar Front, the Subantarctic Front and the Subtropical Front. This cruise therefore provided a perfect opportunity for comparing regional differences in the controls on phytoplankton populations and primary production and export as well as studying the interactions of controls on phytoplankton production in the various oceanographic regions. This information will allow a better understanding of the main drivers in the variability of surface CO2 flux so that the role of the Southern Ocean in a changing climate can be better predicted.

The Southern Ocean Carbon and Climate Observatory is now the largest and sustained carbon biogeochemistry observational programme in the South Atlantic.

1.4. Aims

The main aims of the SANAE cruise were as follows:

- To extend the long-term time series of Southern Ocean underway observations through a more comprehensive set process oriented observations complemented by the Marion Is and Gough Is underway observations.
- To continue hydrographic measurements at the GoodHope line for long term monitoring of the physical state of the ocean and conduct measurements of the oceanography in the Scotia Sea.
- To understand the link between surface pCO2 variability and the underlying physical and biogeochemical drivers in response to climate: Carbon – Climate system.

- To characterise phytoplankton community structure and investigate the biogeochemical controls of primary production and export

- To enable model and remote sensing verification.

2. STANDARD OPERATING PROCEDURES

2.1. OCEANOGRAPHY

2.1.1. EXPENDABLE BATHYTHERMOGRAPH (XBT)

To effectively measure oceanic changes of heat fluxes, in particular across regions of inter-basin exchange, high- density observations need to be undertaken. Repeat XBT sections across “choke-point” sections provide measurements of changes in upper ocean heat content and SST on both seasonal and inter-annual time scales. In addition, by exploiting the relationship between upper ocean temperature and dynamic height, XBTs can be used to infer velocities even in the Southern Ocean where salinity changes are important (Rintoul and Sokolov, 2001). In this way, XBT sections serve as a useful tool in measuring changes in the inter-ocean exchange of heat.

In the framework of the GoodHope program XBTs were funded by the NOAA's Office of Global Programs as part of their High Density XBT project at NOAA/AOML. A total of 159 XBT’s were deployed with a spatial resolution of ~20 nautical miles (1.5 hours of navigation). Most deployments reached a maximum working depth of the Sippican Deep Blue XBT, which is in the order of 800 m, but slower ship speed allowed data collection up to 900 m depth.

In total, 15 XBTs (~8%) failed mainly as a result of strong winds and sea swell blowing the running signal wire against the ship’s hull, which resulted in the XBT wire stretching and thus insulation leakages. On the return leg back to Cape Town, 125 XBT’s were deployed of which 41 (~32.8%) malfunctioned. It appeared that most XBTs failed during the night when visibility was hampered, swell and wind direction was harder to determine and the CPR was being towed. The deployment position, either side or back quarter, did not seem to remedy the situation. Although perfect profiles could be obtained, it is suggested that the continuous plankton recorder (CPR) together with bad weather contributes to enhanced XBT failures.

The XBT temperature data for both legs is displayed in Figure 3. Data pertaining to the GoodHope XBT transects can be obtained at: http://www.aoml.noaa.gov/phod/hdenxbt/high_density_home.html

.

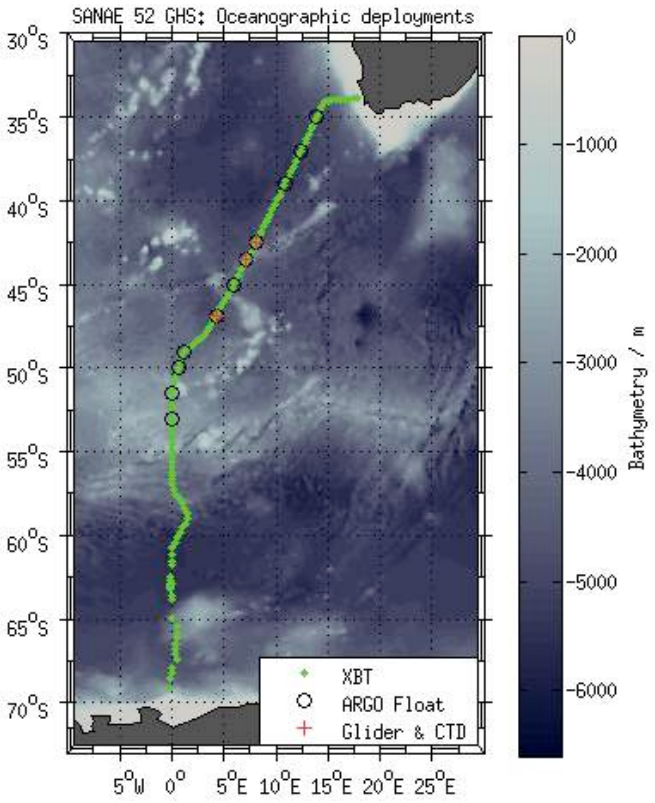

Figure 3. The GoodHope Line as followed during SANAE52. Green dots: XBT stations; Black circles: ARGO float deployments; Red cross: Glider and CTD deployments.

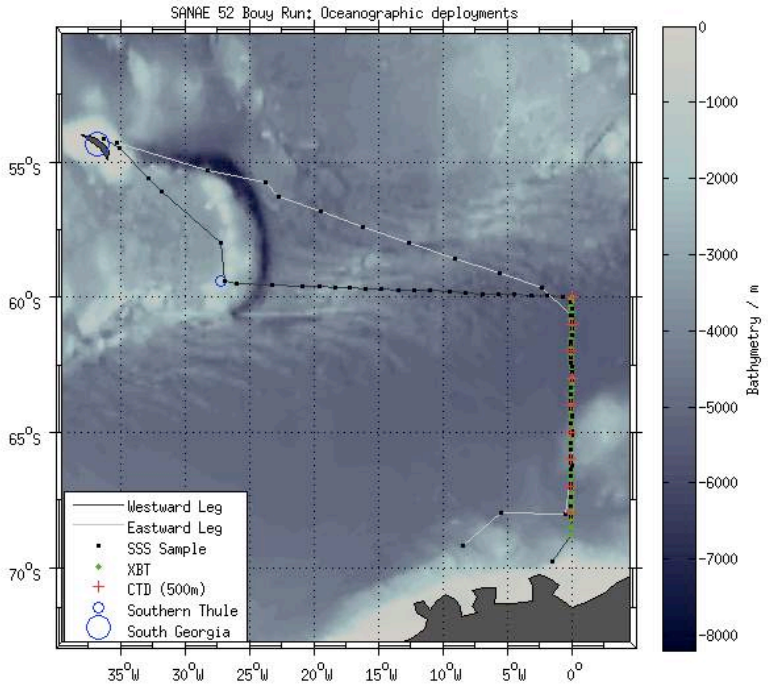

Figure 4. Sampling positions during the Buoy run between Antarctica and South Georgia. A high resolution transect was performed between 68S and 50S. SSS: Salinity sampling stations.

2.1.2. ARGO PROFILING FLOATS

During the voyage between Cape Town and SANAE eleven Argo profiling floats were deployed (Figure 3 and Table 1). These deployments hope to improve the state of the hydrographically data sparse region of the South Atlantic. Data can be obtained from:

Coriolis: **http://www.coriolis.eu.org/**

USGODAE: **http://www.usgodae.org/argo/argo.html**

Profiles are available within 24-48 hours of the float surfacing and data can be accessed either using the Argos numbers or WMO numbers.

All floats were inspected for damages after transport. No oil or residue were visible upon opening of crates and all floats were intact. The CTD protection was intact and all sensor cells had distilled water. All floats were prepared at least 24-1 hour before deployment which followed the manufacturer's instructions. Almost all deployments were done via the aft deck hydraulic crane using a trigger snap shackle. Float AR1224 was deployed manualy after the snap shakle failed two release twice. This is also the same float that was deployed with the glider retrievals.

Table 1. ARGO floats deployed during the SANAE52 takeover voyage.

FLOAT SAIL ID	ID ARGOS	MODEL	ARGO WMO NO	DATE	TIME (GMT)	LATITUDE	LONGITUDE
AR1211	117961	ARVOR	6901422	07/12/2012	15:00:00	35° 00.022'' S	013° 54.536'' E
AR1212	117962	ARVOR	6901423	08/12/2012	01:42:00	37° 00.300'' S	012° 23.700'' E
AR1213	117963	ARVOR	6901424	08/12/2012	12:03:00	39° 00.031'' S	010° 50.950'' W
AR1214	117964	ARVOR	6901425	09/12/2012	09:25:00	42° 29.970'' S	008° 01.917'' E
AR1215	120816	ARVOR	6901426	09/12/2012	17:14:00	43° 30.013'' S	007° 11.176'' E
AR1216	120817	ARVOR	6901427	10/12/2012	03:17:00	45° 00.228'' S	005° 54.567'' E
AR1217	120818	ARVOR	6901428	11/12/2012	13:37:00	46° 51.134'' S	004° 16.946'' W
AR1218	120819	ARVOR	6901429	11/12/2012	07:08:00	49° 00.470'' S	001° 13.750'' W
AR1228	120829	ARVOR	6901444	11/12/2012	12:07:00	49° 59.916'' S	000° 39.325'' W
AR1220	120821	ARVOR	6901431	11/12/2012	19:10:00	51° 30.200'' S	000° 00.400'' W
AR1221	120822	ARVOR	6901432	11/12/2012	01:58:00	53° 01.300'' S	000° 00.010'' W
***AR1222**	120823	ARVOR	6901433	14/02/2013	04:17:00	49° 59.202'' S	004° 05.286'' W
***AR1223**	120824	ARVOR	6901434	14/02/2013	24:25:00	44° 59.007'' S	003° 23.295'' W
***AR1224**	120825	ARVOR	6901435	15/02/2013	19:55:00	41° 31.353'' S	003° 05.367'' W
***AR1225**	120826	ARVOR	6901436	17/02/2013	17:22:00	37° 00.128'' S	010° 03.380'' W

***DEPLOYED ON NORTHBOUND VOYAGE BACK TO CAPE TOWN-NOT ON GOODHOPE LINE.**

2.1.3 GLIDERS

During the southward passage along the GoodHope line three autonomous ocean Seagliders were deployed. These gliders were deployed as part of the Southern Ocean Seasonal Cycle Experiment (SOSCEx) that supplemented the first two gliders deployed on the Gough Island take over voyage in September 2012. Each glider was equipped with a CTD, dissolved oxygen and Wetlabs puck (BB2Fl) sensors. Seagliders 543 and 542 had additional PAR (light) sensors.

All gliders were deployed successfully off the SA Agulhas II stern A-frame using a quick release to deploy the glider while the ship was progressing at approximately 1 knot. The first two gliders were deployed 1 degree apart in the central region of the Subantarctic Zone and the final third glider was deployed in the Polar Frontal Zone (see Table 2).

Following each glider deployment, the ship remained on station until the glider had completed one shallow dive. Following the first glider dive, the ship proceeded to deploy the CTD to 1100m in order to provide calibration data for the sensors housed on the glider (such as CTD, bio-optics and dissolved oxygen data). Once the CTD was completed, the ship then proceeded away from the glider deployment location.

The path of all the gliders and the progress of the experiment can be followed using this link: http://access.oceansafrica.org. For more information, contact Dr Seb Swart on seb.swart@gmail.com.

On the return leg between Antarctica and Cape Town, two Seagliders (SG 573 and SG 574) were retrieved. These two gliders were initially deployed during the Gough Island take over voyage in September 2012 that culminated in the start of SOSCEx. Three techniques were tested to retrieve the gliders (see Fig.5). Due to 40-knot winds and swell of roughly 4m, no FRS boat could be deployed. The first method involved lassoing the glider from the aft deck with a 6 m hollow aluminum pole with a nylon rope threaded through to hook the glider. After several attempts it was clear that this was too tricky and the glider had slipped underneath the ship twice due to wave and ship movement. Secondly, we tried to lasso it through the environmental hangar door, but this proved to be just as difficult. Thirdly we tried a cargo net waited down at two ends with ropes attached to each end. The weights were thrown over the glider and the glider pulled up with the net. On the first attempt the glider rolled out and was successfully retrieved on the second attempt.

During the course of the retrieval process we lost sight of the gliders. The hydrophone was used to give an approximate distance but varied between 4000m, 500m and 50m even when constantly submerged under water, suggesting its efficiency at finding the gliders is negotiable. Volunteers, in most instances, easily spotted both gliders from the bridge or aft deck.

The second glider was retrieved using the starboard quarter crane to lift part of the cargo net so that the net made a 90degree angle with the ship and the weights placed in the water with ropes so as to 'scoop' the glider. This worked on the first attempt and the glider seemed unharmed. The only problem being the cargo net was made of polypropylene and would not sink thus getting the net under the glider was difficult. I would advise that a net of nylon fiber be acquired for the retrieval of the other gliders. Both gliders were thoroughly photographed and rapped in plastic bags before being stored in the 4 °C walk in fridge. Both retrieval positions are documented in Table 3.

Table 2. Deployment information for each Seaglider during the SANAE 52 voyage

Glider ID	Glider Generation	Date	Time (GMT)	Latitude	Longitude	Transponder interrogate
SG 543	Standard	09/12/2012	07:53	-42 30.053 S	08 01.672 E	Not done
SG 575	Ogive	09/12/2012	16:54	-43 30.026 S	07 11.184 E	Yes, good response
SG 542	Standard	10/12/2012	13:32	-46 51.127 S	04 16.956 E	Yes, good response

Table 3. Retrieval information for each Seaglider during SANAE 52 voyage.

Glider ID	Date	Time (GMT)	Latitude	Longitude	Retrieval method	State
SG 573	15/02/2013	17:41	-41 32.963 S	003 07.883 W	Lassoing and net	Damaged
SG 574	15/02/2013	16:42	-41 30.623 S	003 06.677 W	Net through environmental hangar door	Good

Figure 5. Deployment methods used for glider retrieval. Top left: Lassoing through hangar door. Top right: lassoing from aft deck. Middle left/right: Manual deployment of cargo net. Bottom: Using starboard quarter crane to 'scoop' glider.

2.1.4. BOUY DEPLOYMENTS

As a member of the Data Buoy Coorperation Panel (DBCP), SAWS participates in the International South Atlantic Buoy Programme (ISABP), International Buoy Programme for the Indian Ocean (ISABP) and the International Programme for Antarctic Buoys (IPAB). As part of this programme SAWS is required to deploy buoys during relief voyages. Ideally all buoys need to be deployed as far South and West as possible in order to collect information on data sparse areas.

All buoy deployments were conducted on the Southward leg of the GoodHope line and on the Buoy run between 50 °S 0°W and South Georgia. A total of eleven buoys were deployed as seen in Fig.6.

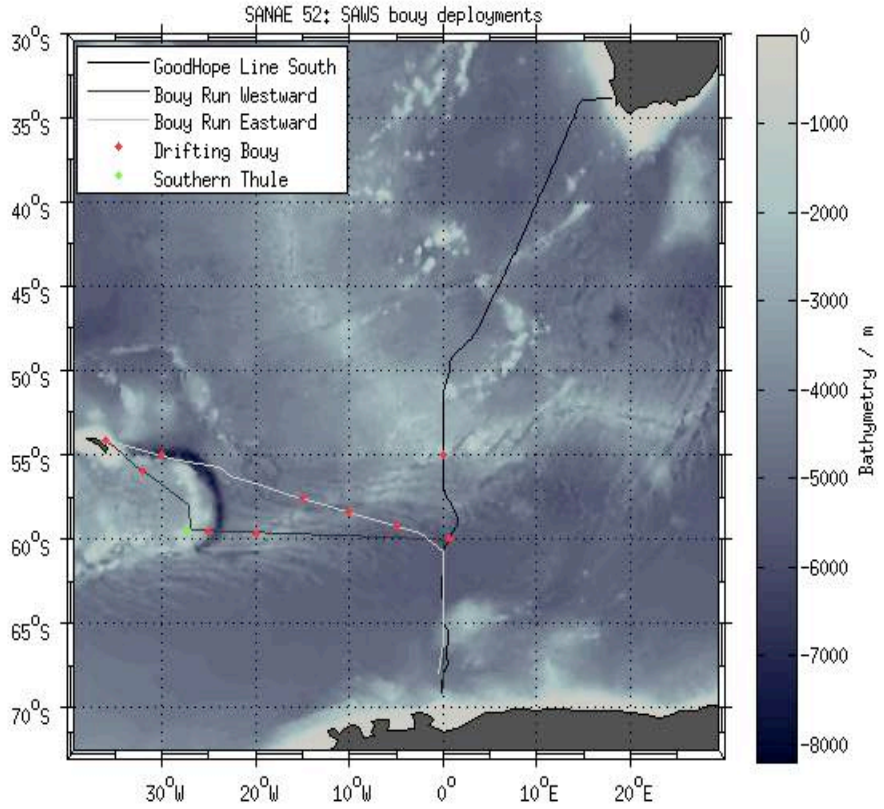

Figure 6. Drifter buoy deployment sites during the 2013 buoy run and Southbound Goodhope line.

2.1.5. CONDUCTIVITY TEMPERATURE AND DEPTH (CTD)

A SeaBird 911plus CTD, together with a sampling carousel of 24 x 20 liter Niskin bottles and auxiliary sensors, were deployed at the ice shelf and on the northward bound leg of buoy run between 68°S and 50°S (SANAE, Antarctica). The auxiliary sensors include an SBE 43 Dissolved Oxygen Sensor, Flourometre and Turbidity sensor, Transmissometre Red, Transmissometre Blue, Altimeter, Scatterometre, an underwater PAR and surface reference PAR sensor.

All CTD deployments can be divided into three categories based on location. These include: Akta Bay, RSA Bukta and buoy run deployments. During our logistical operations at either Bukta, a log CTD system was followed whereby, if logistics allowed it, midday and midnight CTD's would be conducted at predefined locations. These would allow us to build up a

Table 4. CTD's performed during the course of SANAE 52 with corresponding sampling strategy.

CTD FILENAME	Location	Date	Time (GMT)	Latitude	Longitude	*DO	*TCO_2	*Salinity	*Chla	*Nutrient	*P
SANAE 12-13 CTD01	SAZ	09/12/12	11:10:00	42 30.134S	008 01.864 E	4	5 /		5	23	1
SANAE 12-13 CTD02	SAZ	09/12/12	17:47:00	43 30.010 S	007 11.174 E	4	13 /		5	13	1
SANAE 12-13 CTD03	SAZ	10/12/12	14:45:00	46 51.080 S	004 16.830 E		13 /		5	13	1
SANAE 12-13 CTD04	TEST	24/12/12	23:55:00	70 15.608 S	002 44.246 W		/				1
SANAE 12-13 CTD05	TEST	25/12/12	10:05:00	70 15.590 S	002 43.909 W	5	5 /		5	5	1
SANAE 12-13 CTD06	RSA BUKTA	26/12/12	23:58:00	70 15.602 S	002 44.270 W	3	/		5	7	1
SANAE 12-13 CTD07	TEST	27/12/12	12:49:00	70 15.603 S	002 48.007 W		/				1
SANAE 12-13 CTD07	RSA BUKTA	27/12/12	23:55:00	70 15.615S	002 44.238 W	3	7 /		4	7	1
SANAE 12-13 CTD08	RSA BUKTA	28/12/12	00:02:00	70 15.645 S	002 44.17 W	6	3	6	5	6	1
SANAE 12-13 CTD09	RSA BUKTA	29/12/12	00:12:00	70 15.608 S	002 44.501 W	3	7	3	5	7	1
SANAE 12-13 CTD10	RSA BUKTA	30/12/12	00:15:00	70 15.603 S	002 44.242 W	3	7	3	5	7	1
SANAE 12-13 CTD11	RSA BUKTA	30/12/12	23:54:00	70 15.602 S	002 44.331 W		6	3		6	1
SANAE 12-13 CTD12	RSA BUKTA	31/12/12	12:02:00	70 15.578 S	002 44.362 W	3	6	3	5	6	1
SANAE 12-13 CTD13	RSA BUKTA	02/01/13	12:21:00	70 14.703 S	002 44.462 W	3	6	3	5	6	1
SANAE 12-13 CTD14	RSA BUKTA	02/01/13	23:59:00	70 15.566 S	002 44.456 W	2	6	3	5	6	1
SANAE 12-13 CTD15	RSA BUKTA	03/01/13	12:02:00	70 15.53 S	002 44.11 W	2	6	3	5	6	1
SANAE 12-13 CTD16	RSA BUKTA	04/01/13	00:02:00	70 15.484 S	002 44.221 W	2	6	3	5	6	1
SANAE 12-13 CTD17	RSA BUKTA	04/01/13	11:50:00	70 15.531 S	002 44.280 W	2	6	3	5	6	1
SANAE 12-13 CTD18	RSA BUKTA	05/01/13	00:06:00	70 15.585 S	002 44.334 W	2	6	3	5	6	1
SANAE 12-13 CTD19	RSA BUKTA	09/01/13	00:05:00	70 15.588 S	002 44.271 W	/	/	/	/	/	/
SANAE 12-13 CTD20	TEST	10/01/13	12:06:00	70 15.571 S	002 44.315 W	/	/	/	/	/	/
SANAE 12-13 CTD21	BUOY RUN	14/01/13	10:03:00	67 57.98 S	000 00.140 W	5	9	5	5	9	1
SANAE 12-13 CTD22	BUOY RUN	15/01/13	03:29:00	66 59.834 S	000 00.066 W	5	9 /		5	9	1
SANAE 12-13 CTD23	BUOY RUN	13/01/13	09:55:00	66 00.017 S	000 00.008 W	5	9	5	5	9	1
SANAE 12-13 CTD24	BUOY RUN	14/01/13	04:41:00	65 00.013 S	000 00.229 W	5	9 /		5	9	1
SANAE 12-13 CTD25	BUOY RUN	15/01/13	11:30:00	63 59.987 S	000 00.076 W	5	9	5	5	9	1
SANAE 12-13 CTD26	BUOY RUN	15/01/13	18:42:00	62 59.871 S	000 00.078 W	5	9 /		5	9	1
SANAE 12-13 CTD27	BUOY RUN	16/01/13	01:41:00	62 00.021 S	000 00.048 W	5	9	5	5	9	1
SANAE 12-13 CTD28	BUOY RUN	16/01/13	09:03:00	60 59.945 S	000 00.010 E	5	9 /		5	9	1
SANAE 12-13 CTD29	BUOY RUN	16/01/13	16:28:00	60 00.034 S	000 00.182 E	5	9	5	5	9	1
SANAE 12-13 CTD30	TEST	29/01/13	13:30:00	70 32.014 S	007 51.934 W	/	/	/	/	/	/
SANAE 12-13 CTD31	AKTA BAY	29/01/13	23:53:00	70 32.015 S	007 51.937 W	5	7	3	5	7	1
SANAE 12-13 CTD32	AKTA BAY	30/01/13	12:06:00	70 32.014 S	007 51.884 W	3	7 /		5	7	1
SANAE 12-13 CTD33	AKTA BAY	31/01/13	00:00:00	70 32.016 S	007 51.920 W	2	7	3	5	7	1
SANAE 12-13 CTD34	AKTA BAY	31/01/13	12:53:00	70 32.014 S	007 51.885 W	2	7 /	/		7	1
SANAE 12-13 CTD35	AKTA BAY	07/02/13	23:57:00	70 32.009 S	007 51.862 W	2 /		3 /		7	1
SANAE 12-13 CTD36	AKTA BAY	09/01/13	12:09:00	70 32.004 S	007 51.862 W	2	7 /	/		7	1
SANAE 12-13 CTD37	AKTA BAY	09/01/13	00:03:00	70 32.004 S	007 51.836 W	3	7	3 /		7	1
SANAE 12-13 CTD38	GLIDER	15/02/13	18:46:00	41 32.967 S	003 07.904 W	6	8	8	8	8	1

/ refers to stations where the corresponding parameter was not sampled * The amount of bottles sampled for each parameter

record of anomalies at each sight. Documenting any changes, year by year. All CTD's performed at RSA bukta were done to a depth of 200 m and biological samples were taken at critical depths for further analyses. All RSA bukta CTD's were done using the environmental hangar door in order to get a better resolution of the top 20 m profile. A single cast was performed to accommodate Dr. Pedro Monteiro's sampling efforts for 11 surface bottles and an additional 18 CTD's were conducted at this site (10 full biological, 3 test casts during which the pump failed).

All CTD's at Akta bay were done post-buoy run during backloading operations and the same protocol was followed with the exception of using the moonpool for deployments. The position used in previous years was in the pack ice and therefore did not allow CTDs to be conducted over the side of the ship. The depth of the CTD's were 250m and biological samples were taken at all CTDs as indicated in Table 4. In the cases where chlorophyll samples were not included resulted from a lack of filter paper. This was resolved for the leg back home by punching new filters from larger stocks provided by UCT and Rhodes.

On the Southbound leg of the Buoy run a total of 8 CTDs were deployed to 500m, every degree. The location of 70°S was within the continental ice shelf and 69°S were in bay ice that would have added an extra day to operations and was cut. Biological (DO, Chla, nutrients,TCO2,NCP,) samples were collected at each station and salinities every second station.

2.1.5.1. CTD QUALITY CONTROL

The data acquired during the cast (raw data) needs to be converted from binary to engineering units and then processed in order to improve the quality of the data. The data can be affected by different errors that can be accidental (example, the momentary closure of the sensor) or inherent (example, related to the inherent time delay of the temperature and the conductivity sensor responses that can affect the measure of the salinity). In order to process the data, the software *SEASOFT-Win32: SBE Data Processing* is used. The software is composed of different modules, each one with a singular function. The different modules are applied in sequence one per execution. In order to automatize this process a DOS batch file: Postpro.bat is used.

copy D:\CTDdata50Process\leg2\%1.con D:\CTDdata50Process\processedData sbebatch D:\CTDdata50Process\dataProcessing\Postpro.txt %1

The first line copies the configuration file (".con") to the folder where the processed data are stored for the CTD data only. This is important because some of the modules ("derive" and "bottle summary") need the configuration files in the folder where the processed file is stored. The second line launches a ".txt" file where the instruction needed to launch the different modules of the software are written. An example of the ".txt" is:

datcnv /pD:\CTDdata50Process\dataProcessing\DatCnv.psa /iD:\CTDdata50Process\leg2\%1.dat /oD:\CTDdata50Process\processedData /f%1.cnvwildedit /pD:\CTDdata50Process\dataProcessing\WildEdit.psa /iD:\CTDdata50Process\processedData\ %1.cnv /oD:\CTDdata50Process\processedData /f%1.cnv

celltm /pD:\CTDdata50Process\dataProcessing\CellTM.psa /iD:\CTDdata50Process\processedData\ %1.cnv /oD:\CTDdata50Process\processedData /f%1.cnvfilter /pD:\CTDdata50Process\dataProcessing\Filter.psa /iD:\CTDdata50Process\processedData\%1.cnv /oD:\CTDdata50Process\processedData /f%1.cnv

loopedit /pD:\CTDdata50Process\dataProcessing\LoopEdit.psa /iD:\CTDdata50Process\processedData\ %1.cnv /oD:\CTDdata50Process\processedData /f%1.cnvderive /pD:\CTDdata50Process\dataProcessing\Derive.psa /iD:\CTDdata50Process\processedData\%1.cnv /oD:\CTDdata50Process\processedData /f%1.cnv

Split /pD:\CTDdata50Process\dataProcessing\Split.psa /iD:\CTDdata50Process\processedData\%1.cnv /oD:\CTDdata50Process\processedData /f%1.cnvsection /pD:\CTDdata50Process\dataProcessing\Section.psa /iD:\CTDdata50Process\processedData\d %1.cnv /oD:\CTDdata50Process\processedData /fd%1.cnv

binavg /pD:\CTDdata50Process\dataProcessing\BinAvg.psa /iD:\CTDdata50Process\processedData\d %1.cnv /oD:\CTDdata50Process\processedData /fd%1.cnvBottleSum /pD:\CTDdata50Process\dataProcessing\BottleSum.psa /iD:\CTDdata50Process\processedData\%1.ros /oD:\CTDdata50Process\processedData /f%1.btl SeaPlot /pD:\CTDdata50Process\dataProcessing\SeaPlot.psa /iD:\CTDdata50Process\processedData\d %1.cnv /oD:\CTDdata50Process\processedData /f%1.Jpeg

Each line corresponds to a different module that is applied. The first part of each line gives the instruction of which module to use and where it is stored. The second part is for the input file and the third part tells one where to store the output file. In order to start the data processing, one must run the batch file, giving the position where it is stored and the file name of the cast that is required to be processed.

For example: OPEN: **D:\CTDdata50Process\dataProcessing\Postpro.bat SANAE50CTD_BR164**

The modules used during this campaign for the UCTD are in sequence:

- Ascii in
- Align ctd
- Section
- Filter
- Derive

The modules used during this campaign for the CTD are in sequence:

- Data Conversion
- Wild Edit (The rest of the conversions can be done in matlab using a script-please enquire if this is required)
- Cell Thermal Mass
- Filter
- Loopedit
- Derive
- Split
- Section
- Bin Average
- Bottle Summary

Data Conversion: convert raw data from CTD (".hex" or ".dat" file) to engineering units, storing the converted data in ".cnv" file (all data) and ".ros" file (water bottle data).

Align CTD: aligns parameter data in time, relative to pressure. This ensures that calculations of salinity, dissolved oxygen concentration, and other parameters are made using measurements from the same parcel of water . Three principal causes of misalignment of CTD measurements are: • physical misalignment of the sensors in depth • inherent time delay (time constants) of the sensor responses • water transit time delay in the pumped plumbing line - the time it takes the parcel of water to go through the plumbing to each sensor Typical temperature alignment are: For the UCTD the best alignment was to give 0.095 s of advance of the temperature relative to pressure. For the CTD the best alignment was to give 0 s of advance of the temperature relative to pressure.

Wild Edit: Compute mean and standard deviation of data in block (100 per block) for each selected variable. Temporarily flag values that differ from mean by more than 2 times the standard deviations for pass 1; then recompute mean and standard deviation, excluding temporarily flagged values from step 1 and mark values that differ from mean by more than 10 times the standard deviations replacing data value with badflag.

Cell Thermal Mass: Cell Thermal Mass uses a recursive filter to remove conductivity cell thermal mass effects from the measured conductivity. In areas with steep temperature gradients, the correction is on the order of 0.005 PSU. In other areas the correction is negligible. ***Filter:*** Filter runs a low-pass filter on one or more columns of data. A low-pass filter smooths high frequency (rapidly changing) data. To produce zero phase (no time shift), the filter is first run forward through the data and then run backward through the data. This removes any delays caused by the filter.

Instrument	Advance of Temperature Relative to Pressure (seconds)
9*plus*	0
19 and 19*plus*	+ 0.5
25	0
49 *	+ 0.0625

Loopedit: Loop Edit marks scans bad by setting the flag value associated with the scan to badflag in input ".cnv" files that have pressure slowdowns or reversals (typically caused by ship heave). The minimum velocity used in this case is 0.05 m s-1

Derive: uses pressure, temperature and conductivity from the input ".cnv" file to compute the following oceanographic parameters: Depth (salt water, m), Salinity, Density (sigma-theta Kg m-3), Potential Temperature (ITS-90, deg C), Density (density, Kg m-3), Dynamic Meters (10 J Kg-1), Geopotential Anomaly (J Kg-1) . When use the batch file remember to check the match instrument configuration to input file box only for the CTD file.

Split: separates the data from an input ".cnv" file into upcast (pressure decreasing) and downcast (pressure increasing) files. Split writes the data to an output ".cnv" file(s). The upcast output file name is the input file name prefixed by u. The downcast output file name is the input file name prefixed by d.

Section: extracts rows of data from the input ".cnv" file, based on a pressure range or scan number range, and writes the rows to an output ".cnv" file. Section has been used to remove the first 5 m of data from the downcast output file. ***Bin Average:*** averages data, using averaging intervals based on: pressure range; depth range; scan number range; or time range. Bin Average has been used only for the downcast output file using the depth range to average the data.

Bottle Summary: reads a "ros" file created by Data Conversion and writes a bottle data summary to a ".btl" file. The ".ros" file must contain (as a minimum) temperature, pressure, and conductivity (or salinity). The output ".btl" file includes: • Bottle position, optional bottle serial number, and date/time

• User-selected variables - computed for each bottle from mean values of input variables. In our case the variables are: salinity, density, pressure, temperature, conductivity, dissolved oxygen, fluorescence and PAR/Irradiance. When use the batch file remember to check the match instrument configuration to input file box.

ASCII: adds a header to a .asc file that contains rows of ASCII data. The data can be separated by spaces, commas, or tabs (or any combination of spaces, commas, and tabs). The output file, which contains both the header and the data, is a ".cnv" file.

CONDUCTIVITY SENSOR DATA QUALITY CHECK

Salinity samples were collected from the uncontaminated underway lab supply for all underway legs of the voyage. Samples were also collected from selected depths from the CTD casts. Some of the preliminary quality checks are described below.

Figure 7 depicts the real-time TSG data as a black line and the bottled samples analyzed via the Portasal as crosses with 5 outliers distributed at the start and end of the voyage. Overall there is a good correlation between the TSG system and the bottled samples with an error rate of 8.4%. The offset between salinity values as graphed in Fig.8 shows that the average standard deviation, correcting for the outlier, would result in a $p<0.01$.

For the CTD stations it was not possible to do an accurate prediction based on three CTDs and would therefore have to be conducted once in Cape Town.

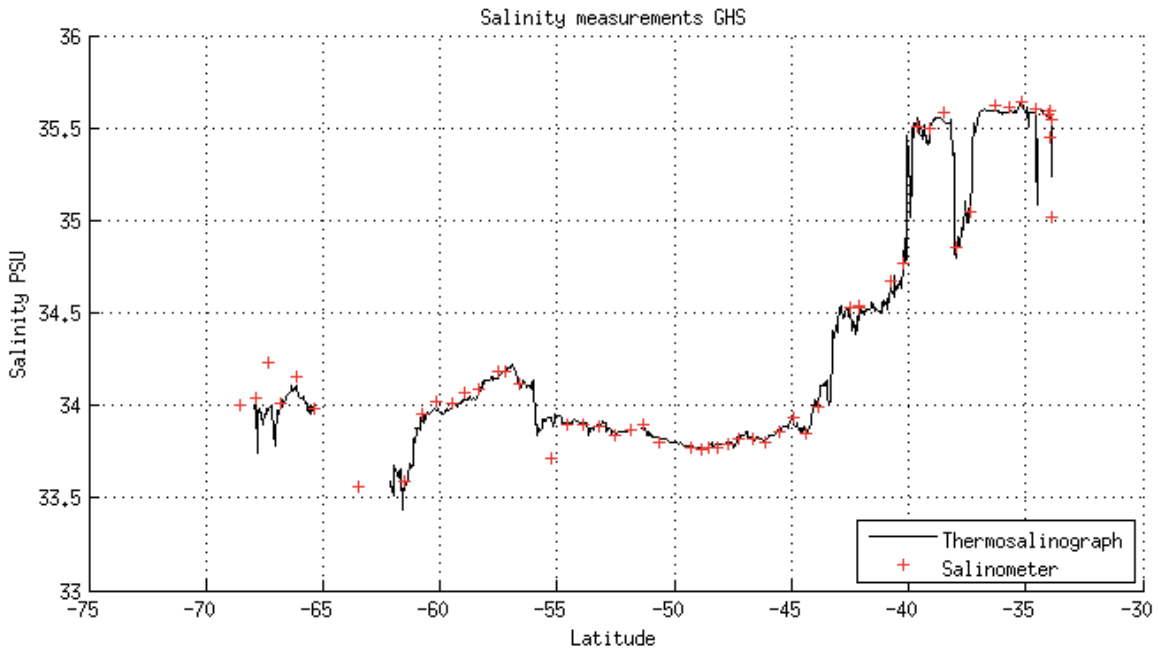

Figure 7. A comparison between TSG underway salinity calculations and bottle samples measured by the Portasal salinometer.

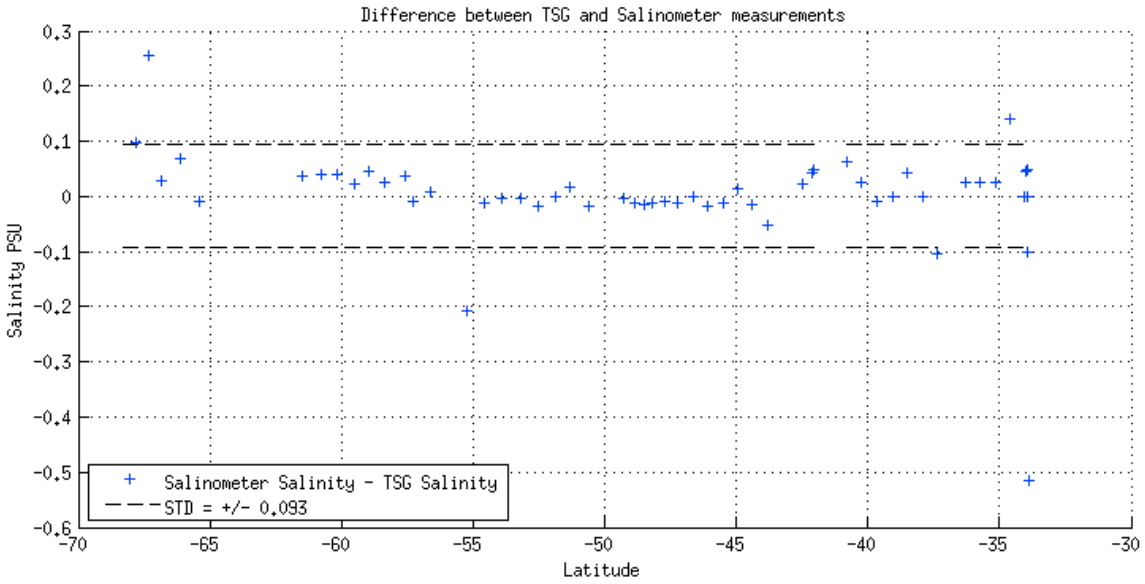

Figure 8. A diagram showing the difference in salinity values between the TSG and the Portasal salinometer.

DISSOLVED OXYGEN SENSOR DATA QUALITY CHECK

As dissolved oxygen was measured throughout the voyage, the DO values between all 38 CTDs were compared to determine the accuracy of the sensor onboard the system. A scatter plot is an effective tool for viewing the strength and direction of the correlation that exist two variables. From **Figure 9** it appears that there is a strong positive correlation (R^2=98.3) between the titrated dissolved oxygen concentration and the CTD detected oxygen values. This means that the CTD sensors were comparing (98.3%) very well from the Winkler titration method.

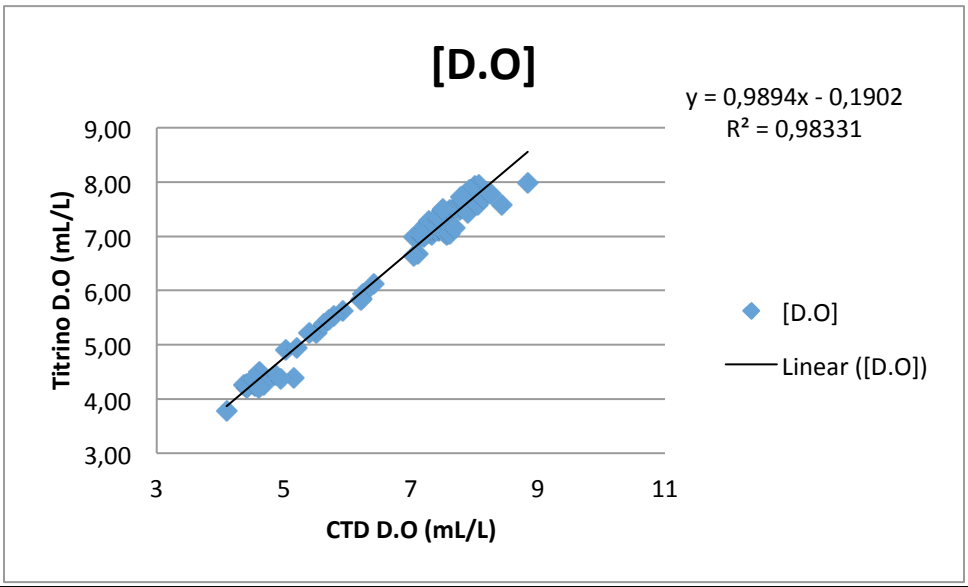

Figure 9. A diagram displaying the correlation between dissolved oxygen titration values and the CTD oxygen sensor.

2.1.6. THERMOSALINOGRAPH (TSG)

The TSG system is a continuous underway-monitoring system connected to the scientific seawater supply. It also supplies the onboard SDS system with real-time seawater temperature and conductivity/salinity values. The system was switched on underway, however ice flows tended to block the scientific water supply quickly and repeatedly hampering data collection in all bay ice/ice flow areas. Pumps blocked and no alarm was attached to the system therefore monitoring when the system would block is both time consuming and damaging to the pumps. All the data was stored and is available at 1min intervals from the ships system on request.

2.1.7. UNDERWAY SALINITY

During the course of the voyage salinity samples were taken at several underway stations. These samples were taken in 250 ml glass bottles with rubber stoppers and completely filled to minimize evaporative error. On The Southbound leg of the GoodHope line, samples were taken every 3 hours (~20 nm) and analyzed onboard along with CTD cast 1, 2 and 3 with a Portasal Salinometer 8410A for the GoodHope Line South (GHS). After completing the GHS, the Portasal was removed from the ship. From each CTD cast, five water samples from Niskin bottles at different depths were measured with the Portasal, after it was calibrated using Standard Seawater.

A total of 58 salinity samples were processed and a further 166 salinity samples were taken for analyses back in Cape Town. Please note that the Portasal Salinometer was recalibrated after the first 45 surface samples were analyzed (Sample 45 was taken at 57°15.475' S, 000°12.190' E). The recalibration had to be repeated three times, because the bottle of Standard Seawater ran dry during the first attempt and air was sucked into the conductivity cell. All samples analyzed after the recalibration show an overestimation compared to the TSG measurements.

Please refer to station sheets for salinity sampling sites.

2.1.8. DISSOLVED OXYGEN

The concentration of dissolved oxygen was readily, and accurately, measured by the method originally developed by Winkler in 1888. The principle of this Winkler method is that oxygen in the water sample oxidizes iodide ion (I^-) to iodine (I_2) quantitatively and the amount of iodine generated is then determined by titration with a standard thiosulfate ($S_2O_3^{-2}$) solution. A precise concentration of thiosulfate in the titrating solution was determined before titration by following a standardization procedure. The dissolved oxygen samples were titrated using a Metrohm 806 Change Unit. Preparation of chemical reagents, fixation of oxygen, standardization of working solution of sodium thiosulfate, and acidification of the sample were made following Carpenter (1965b). Reagent blanks were corrected also after Carpenter (1965b). The CSK standard solution of KIO3 was used for the standardization of sodium thiosulfate solution. Precise dispensers were used for the addition of alkaline iodide and manganese (II) chloride into the 200–220-mL BOD bottles. The titration was performed within the BOD bottles without transferring the whole sample to a titration vessel, as the transfer is a major source of errors due to volatilization of iodide (Carpenter, 1965a).

2.1.9. TCO2

Total dissolved inorganic carbon and total alkalinity samples were collected from the wet biology lab, from the same underway water supply where the TSG water is sampled. Intake temperature, salinity and atmospheric pressure were recorded at each point underway samples were collected. CTD samples were collected from nine depths with increased

resolution in shallower depths. Samples collected for ship based analysis were stored in 500mL bottles (identical to CRM bottles as supplied by A Dickson) with 200µL of concentrated HgCl (Mercuric Chloride). The 500mL samples were analyzed on board using Mirianda's VINDTA 3C (Versatile Instrument for the Determination of Titration Alkalinity). The VINDTA determines total alkalinity by potentiometric titration and also colometrically measures CO_2 from the same sample. Accuracy of the VINDTA was determined by running a Dickson's CRM's before and after each batch. Consistency was often difficult to achieve for entire batches. Alkalinity post calibration was performed using the CRMs samples as references.

At 45°S the nitrogen gas cylinder used for the DIC compartment run out and the spare cylinder was empty as well. Thus from this point until almost end of the buoy run DIC was not measured from the VINDTA, however the VINDTA was running only in the alkalinity run. The unmeasured DIC will be recalculating from the alkalinity and nutrients data after the cruise. A full gas cylinder was obtained from the German base, however our gas regulator could not fit to the German standard gas cylinder. At a later stage during the buoy run, the engine room offered a gas regulator that could fit to the German gas, hence DIC measurement where resumed.

2.1.10. UNDERWAY pCO2

The partial pressure of Carbon dioxide in the ocean and the atmosphere was measured throughout the cruise expect for regions where the underway water supply was clocked. Between 62S and 65S the underway water supply was clocked with ice hence the pCO_2 system was switched off. At the ice self the instrument was as well switched off.

The instrument is a General Oceanics equilibrator-based system with a Licor LI-7000 infrared gas analyzer, described by Pierrot,D.,et al. (2009). Four reference gases were used: 0.00 , 357.32, 377.8 and 427.83 ppm, provided and cross calibrated to international standards by the GAW station at Cape Point. The instrument cycle included returning to these gases followed by atmospheric measurements once every six hours. All times and dates are UTM (GMT). At about 60S the 0.00 reference gas run out, thus from this point to the end of the buoy run the pCO_2 was running with an empty 0.00 ppm reference standard. Due to the importance of the 0.00 ppm reference standard in calibrating the data, a CO_2 striper was sent from Cape Town and the 357 ppm reference gas was connected to the striper, striping all the CO2 and use it as the 0.00 ppm reference standard gas.

The pCO2 system logged on the log sheet the data from the TSG, underway 10 AU fluorometer, a Fluke digital thermometer for the equilibrator temperature, atmosphere CO_2 and the equilibrator measurement. For atmospheric CO_2, atmospheric air was sampled outside the ship at the bridge using a line going to the underway lab connected to the instrument.

2.2. BIOLOGICAL

2.2.1. NUTRIENTS

SOP for underway GoodHope line stations

Nutrient sampling sites mirrored that of XBT stations (i.e. every 90 min; ~10nm) and were collected straight after gas samples. All underway seawater sampling was done using the same scientific seawater supply split by two pumps and also feeds the onboard TSG system.

SOP for Buoy run underway stations and CTDs

Nutrient samples were collected every 90 minutes at all the underway stations except for the first leg of Buoy Run where it was at 45minutes, whereas the chl-a samples were collected every three hours (90 minutes for Buoy Run 1st leg). The nutrient sampling was always performed immediately after the gas (Dissolved oxygen and Dissolved Inorganic Carbon)

samples were taken. Nutrient bottles were rinsed three times and ultimately filled ¾ of the volume and the samples were stored at -80^{o}C freezer. The chlorophyll bottles were rinsed three times with the surface seawater intended to sample, and 400ml of that water was collected. The water was filtered through 25mm GFF at a vacuum. The filter paper was then folded in half using tweezers, thus encasing the sample on the inside. .The samples were then stored at -80^{o}C freezer. All the samples collected were labeled clearly, the station number, date and grid number and cruise name were noted down on a book .The results will be obtained at a later stage.

2.2.2. CHLOROPHYLL a

Underway chlorophyll samples were taken at every station, corresponding to ~10 nm (90 min). A 400ml seawater sample was collected from the onboard scientific water supply and vacuum filtered through a 0.45 µm 25mm Millipore GF/F filter before being stored at -80 °C for analysis after the voyage. Standard analytical procedures will be used to analyze the filters and data will be available through DEA request. During the course of the northbound trip between Antarctica and Cape Town, the filters ran out and were supplemented with 25mm HVLP grade 0.45 µm Millipore filters for the last stations.

2.2.3. MICROBIOLOGY

2.2.3.1. Viral/Phage biodiversity

All viral samples were collected for Dr. Ed Ryckibi at MCB (University of Cape Town) as part of their phage biodiversity study. Samples were collected in conjunction with bacterial samples at prominent frontal features and zones on the South- and North-bound legs of the cruise. Seawater was collected via the onboard pump system (MONO® S61M-0314R pump) at a constant pressure of 1 bar and a flow rate of between 15-35 dm^3/min. The pump system was flushed for 48 hours prior to sample collection and pumped through a 1 µm, 0.45 µm and 0.22 µm PVDF Millipore filter before being collected in a HCl washed (distilled water rinsed) 20 L polypropylene drum. The viral precipitation and filtering followed the protocols as published by John *et al.,* (2011). In short, 20 L/or 10L of prefiltered seawater was treated with 1mg/l $FeCl_3$ (dissolved in a volume of 0.8 ml dH_2O and filter sterilized) and stored at 4 °C for 1 hour prior to being filtered through a 0.8 µm polycarbonate filter and stored in falcon tubes at 4 °C. As a control reference, 50 ml of unfiltered seawater was fixed with Paraformaldehyde and stored at 4 °C for 20 min prior to long term storage at -20 °C.

2.2.3.2. Bacterial biodiversity

Bacterial samples consisted of a total of 9 stations (Fig.10). Each station corresponded to a front or zone and was identified based on seasonal isotherm data in association with XBT underway measurements and TSG data. Seawater was filtered through an onboard pump system (MONO® S61M-0314R pump) at a constant pressure of 1 bar and a flow rate of between 15-35 dm^3/min. All biological material for a 500 L seawater sample was collected on a 0.45 µm PVDF filter and stored at -80 °C in RNAlater (SIGMA®). A further size fractioned 300 L sample was taken and prefiltered through a 1.0 µm Millipore filter before collecting on a 0.45 µm PVDF filter. The second filter was stored the same. Two 0.75 x 0.75 cm sections of the 500 L filter were cut and resuspended in 0.22 µm filtered seawater before being treated with 0.1% buffered formalin or 0.5 % glutaldehyde for flow cytometry analysis. All fixed samples were incubated at 4 °C for 30 min prior to long term storage at -80°C . A 1 ml filtered and resuspended seawater sample was distributed between 4 media plates consisting of Seawater agar (75% autoclaved seawater, 5% Wolf's Mineral Mix and 5% Wolf's Vitamin Mix), Marine Agar (Difco Marine Broth 2216), GYM Streptomyces Medium and Ashby's nitrogen free agar (for a detailed protocol please refer to Appendix A).

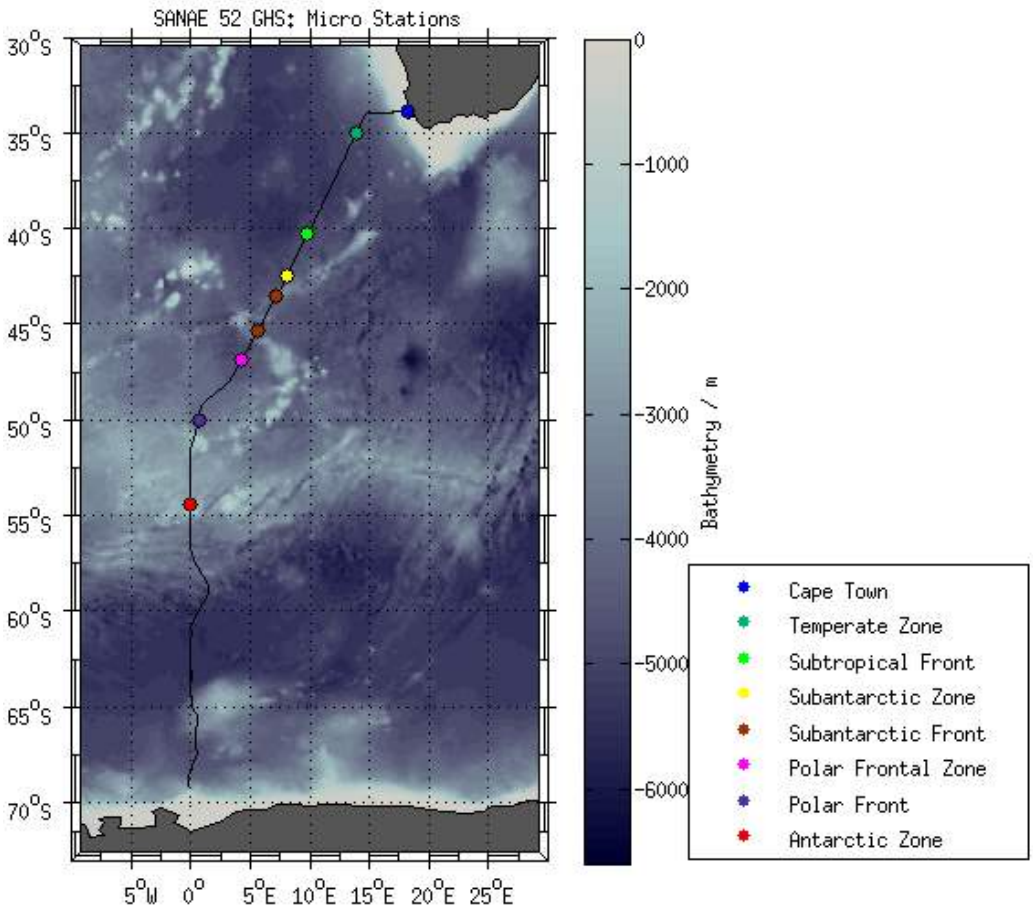

Figure 10. Microbiological stations on the Southward leg of the GoodHope line.

2.2.4. ORNITHOLOGICAL OBSERVATIONS

Bird observations were carried out underway in 10min intervals. At the start of the ten minute period the GPS co-ordinates were noted using a handheld GPS (There was no access to the SDS system from the Monkey Deck) and the number of bird observations were catalogued for either 90 degrees or 180 degrees depending on the observers quatran. Both species and total counts were recorded.

Factors taken into consideration are as follows:

Wind direction: The prevailing direction during the count
Wind strength: Taken from ship's instruments (accounting for ship speed)
Cloud cover: Rounded to the nearest 10%
Visibility: Starting with a value of +500 down to 30 m from the ship.
Swell height: A value to the nearest 1 m.
**No ship followers are counted.

Most observations were done from the Monkey bridge viewing platform and in the case of extreme cold and weather the lounge on the seventh floor forward facing windows were used.

Due to the fact that the ship is not always in motion or following a straight line a decision was made by the monitoring team to do extra observations whenever possible and to record data such as species and numbers over time periods as and when possible. So over and above the standard monitoring methodology used when the ship was sailing we created a system of

observing when the ship was stationary. A word document with the date and GPS position of where the observations were made and what and how many of each species was noted. In some of the notes even breeding activity is noted.

Recommendations for future observations would be a modified data capturing process. The excell based system currently used is outdated and modifying data for processing is laborous and time consuming. On average data capturing took 3 hours dayly, which could be drastically reduced if a better system was in place.

2.2.5. Continuous Plankton Recorder (CPR)

The CPR was towed behind the ship at a constant depth of about 10 m for the continuous and simultaneous collection of both phytoplankton and zooplankton material over large spatial scales. To allow the CPR to efficiently collect plankton the ship maintained a speed of a minimum of 10 knots. As the CPR is towed, water entered the CPR through an aperture at the front, and plankton present in the water is trapped onto a 270-µm silk mesh (the filtering mesh) inside the internal plankton sampling mechanism (PSM), while another 270-µm silk mesh (the covering mesh) then sandwiched the plankton. The speed of water flow was reduced to minimise clogging by an increase in the filtering area of the silk relative to the entrance aperture by a ratio of 29–1. Through a gearing system powered by a small impellor at the rear of the CPR, the silk was moved forward in proportion to the speed of the towing ship, such that typically 4 inches (10 cm) of silk corresponds to 10 nautical miles of tow. (Reid *et al, 2003*)

The filtering silk and a covering silk are wound together into a storage tank containing formaldehyde for fixation and preservation within the plankton sampling mechanism (PSM) until subsequent analysis in the laboratory. A log on the bridge should be kept of the position (latitude, longitude), course, date and time (UTC) of when the CPR was put into the water, updated every time the ship changes course, and when the CPR is retrieved on board. A full cassette of silk provided up to 500 nautical miles of samples with 5 cassettes with a total mileage of 2500 nautical miles. The first cassette to be deployed was cassette no. 189-0 which was deployed at 6720.400S 00719.000W and recovered at 5912.100 S 00536.200 W. The second cassette to be deployed was cassette no. 189-1 which was deployed at 5907.900S 00535.400W and recovered at 5103.700S 00414.800W. The third cassette to be deployed was cassette no. 189-2 which was deployed at 5100.900S 00414.400W and recovered at 4251.200S 00314.500W. The third cassette to be deployed was cassette no.189-3 which was deployed at 4130.700S 00304.100W and recovered at 3813.200S 00634.400E. The last cassette to be deployed was cassette no.189-4 which was deployed at 3811.900S 00638.300 and recovered a 3454.100S 01555.200W. The total mileage which was towed was 2443.5 nautical Miles. All cassettes where towed successfully.

RBR concerto™ CTD logger was used to measure the conductivity, temperature, and pressure (depth) when the CPR was deployed and the RBR log files recovered with each CPR cassette change. These physical parameters were measured with exceptional accuracy in the harshest of conditions with long deployment times. The Conductivity was measured with an inductive sensor, suitable for deployment in marine, estuarine, or fresh water. There are no exposed contacts to avoid susceptibility to corrosion, and the housing was frozen into ice without damage. The temperature sensor was calibrated in-house using an aged thermistor. The temperature channel was calibrated to an accuracy of ± 0.002°C (ITS-90) over the range -5 to +35°C. The pressure was measured with a piezo-resistive transducer with nickel based super alloy diaphragm to avoid corrosion. Accuracy was 0.05% of the full scale rating and achievable resolution was 0.001%. The pressure sensor had a range between 10dbar to 740dbar. The RRB log files for cassette no. 189-1, 189-2, 189-3 and 189-4 where recovered successfully with the exception of cassette 189-0 which failed to log the data properly.

2.3 ATMOSPHERIC

2.3.1. Atmospheric precipitation

An OTT Parsivel 2 disdrometer was mounted on the ship's mast (Figure 11). This is a commercially available disdrometer commonly used for calibration and ground-truthing of weather radar. Precipitation particle sizes up to 25mm and particle velocity up to 20m/s are measured. The instrument provides outputs of precipitation rate and type, particle count, present weather, predicted radar reflectivity, as well as housekeeping variables. These variables, as well as the raw size- and velocity spectrum data were logged on a laptop computer.

Figure 11. The Parsivel 2 disdrometer and 3D sonic anemometer mounted on the ship's mast.

Figure 12. The SVI camera clamped to the railing on the lower radar platform.

The Snowflake Video Imager was on loan from the National Center for Atmospheric Research in Boulder Colorado. This instrument is described in Newman *et al.* 2009. Presenting the Snowflake Video Imager. *Journal of Oceanic and Atmospheric Technology*, 26(2): 167-179. The instrument comprises a high-speed video camera (Figure 12) and a halogen floodlight. These were clamped to the railings on the ice radar platform, and cables run into the computer space described above. Images from the camera are captured by a video capture card on a PC. Custom software detects particles in real-time and saves the images to file. Post-processing software applies an image recognition algorithm to detect in-focus particles and provides particle size statistics.

The Aventech AIMMS-20 Attitude and Heading Reference System consists of 3 modules communicating over a CAN bus. Ship heading is measured by real-time kinematic GPS using two antenna's mounted on the railing of the crow's nest platform (Figure 13). Attitude is measured by a solid-state gyro module. A processing module provides either a real-time attitude solution, or streams the raw CAN bus data for logging and post-processing. Raw CAN bus data was logged on an embedded PC.

An RM Young 81000 3-d sonic anemometer was mounted on the ship's mast (Figure 11). Measurements of wind speed and direction relative to the ship, as well as wind elevation angle were sampled at 0.5 hertz, and logged on a Campbell Scientific CR1000 logger.

Figure 13. The location of the AIMMS GPS antennas.

Figure 64. Sun photometer measurement at SANAE.

A summary of data available is shown in Appendix A. Note that this only includes data that was available at the time of writing, some of the gaps in the measurements may be recoverable through post-processing.

2.3.2. Sun-photometry readings

A Microtops hand-held sun photometer was on loan from NASA Goddard Space Flight Center (GSFC). Measurements were made during cloud-free conditions, taking care to avoid measurements when the ship's exhaust plume would interfere with the measurement. In addition to ship-based measurements, two days of measurements at SANAE IV were made (Figure 14). Data was geolocated using a GPS receiver connected to the sun photometer. Data was sent to NASA GSFC, where quality assurance and a suite of corrections are made before making the measurements publically available on their website (aeronet.gsfc.nasa.gov)

3. RESULTS AND DISCUSSION

3.1. OCEANOGRAPHY

3.1.1. EXPENDABLE BATHYTHERMOGRAPH (XBT)

Responsible party: G. Du Plessis
Organization/group: Department of Oceanography, UCT in collaboration with NOAA
PI: Dr. Isabelle Ansorge

NOAA rationale:

XBT data are used in ocean analysis and in climate model initialization. For instance, for El Ninno prediction XBT data complement that from the TAO array and from satellite-derived sea surface temperature and sea height observations. The use of XBT data serves to measure the seasonal and interannual fluctuations in the upper layer heat storage, now being complemented by profiling float measurements. Heat transport and geostrophic ocean circulation can be measured using the high-density XBT data that determines the mesoscale field.

The XBT data also helps to document the ocean heat storage and global transport of heat and fresh water, which is crucial to improve climate prediction models that are initialized with temperature profiles. One primary objective of the XBT program is to provide oceanographic data needed to initialize the operational climate forecasts prepared by NCEP. Global coverage is now required as the forecast models not only simulate Pacific conditions but global conditions to improve prediction skill.

The operation at AOML is designed to measure the upper ocean thermal structure in key regions of the Atlantic ocean. XBT transects in HD mode are repeated approximately every three months in order to measure the mesoscale structure of the ocean to diagnose the ocean circulation responsible for redistributing heat and other water properties globally.

The HD XBT transect AX25 was implemented to monitor the variability in the upper layer interocean exchanges between South Africa and Antarctica on seasonal and interannual time scales. In addition, by exploiting the relationship between upper ocean temperature and dynamic height, XBTs are used to infer velocities and to monitor the various frontal locations in the region.

Table 5. The definitions used for the fronts bordering the Antarctic Circumpolar Current (ACC).

FRONT	TEMPERATURE	Subsurface T_{200}
Subtropical front (STF)	T_{100} = 12-10°C	8.0 -11.3 °C 34.42-35.18 Axial Value: 10°C, 34.8
Subantarctic front (SAF)	T_0 = 8°C, T_{100} = 7°C	4.8-8.4°C 34.11-34.47 Axial Value: 6°C, 34.3
Antarctic Polar Front (APF)	T_{200} = 2°C	Axial Value: 2°C
Antarctic Divergence (AAD)	Region of (upwelled) water warmer than 1°C	

GoodHope South

The 2012 Southbound leg of the GoodHope line was conducted as per NOAA prerequisites. Some changes with regards to the new vessel and transit time due to an increased average speed (13 knots) resulted in 90 min stations being conducted with an average spatial resolution of ~20nm. In all instances, deployments over the back of the aft deck resulted in the least errors on the way South. The XBT profiles were used to identify the various fronts in between SA and Antarctica by the definitions listed in Table 5.

The Southern ocean is marked by strong zones, separated by several frontal systems (Belkin & Gordon, 1996). The fronts in both the South Atlantic and South Indian sectors are known to be less tense and variable when compared to regions such as the Drake Passage or the South West Indian ridge (Lutjeharms *et al.,* 1993). A consistent record of the frontal positions therefore gives an insight into the upper level circulation in the ACC and possible shifts in the predominant features. One problem however is the large variety of definitions available in the literature and therefore the need to define each feature beforehand.

Our data showed that we encountered the Subtropical front at ~41° S with a narrow band representing the Subantarctic zone before reaching the Subantarctic front at ~43° S. The APF then presented at around 51° S followed by the AAD at 55°S (see Fig.15). Fig 16 shows a similar profile for the return leg with slight modifications due to its track due west of the GoodHope line.

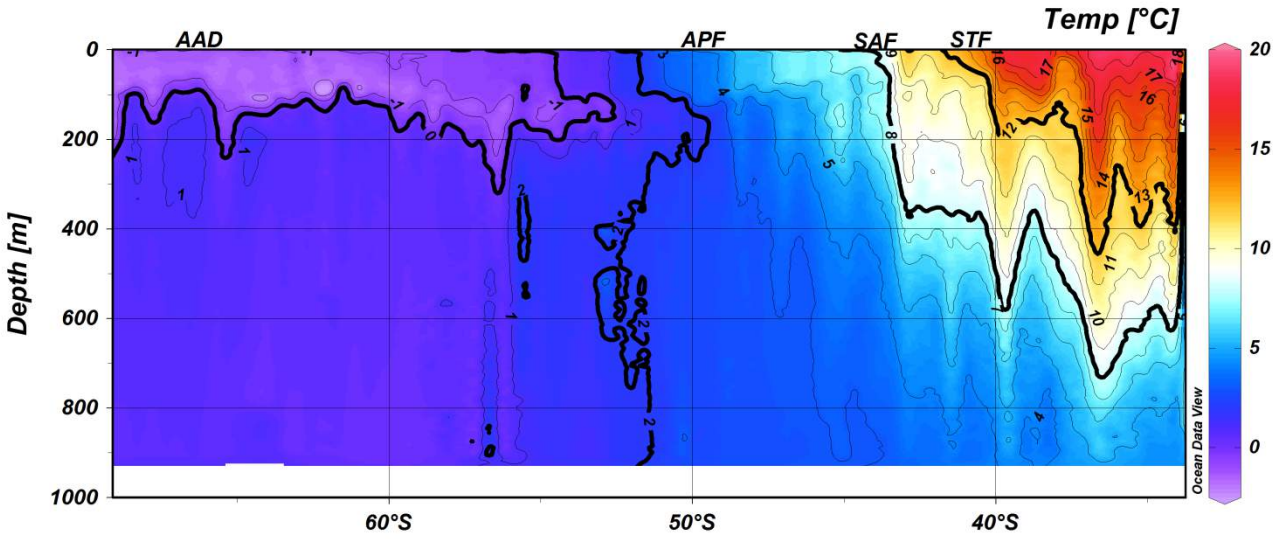

Figure 75. The temperature profile of the upper 900m as derived from XBT stations on the Southward GoodHope Line. STF: Subtropical Front; SAF: Subantarctic Front; APF: Antarctic polar front; AAD: Antarctic divergence.

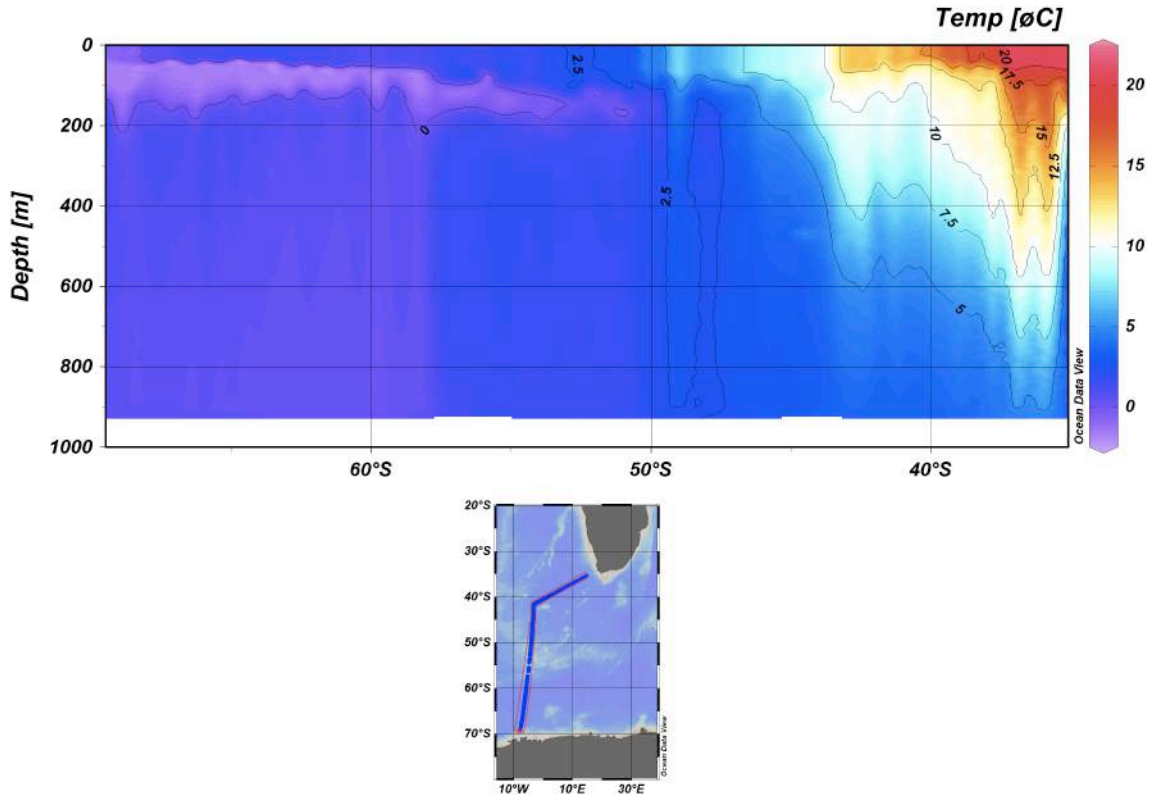

Figure 16. The temperature profile for the northward leg between Antarctica and Cape Town.

3.1.2. ARGO PROFILING FLOATS

Responsible party: Sebastiaan Swart/Gerda Du Plessis
Organization /group: CSIR
PI: S. Speich

All the Argo floats were deployed successfully. Unfortunately the data is as of yet not available online although it will be shortly. To view any of the floats please go to the proposed websites in the SOP section or noted at the end of the report.

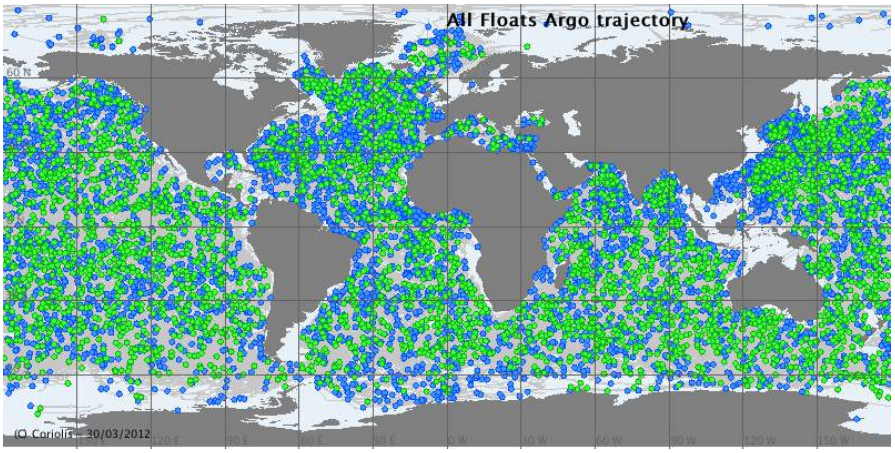

Figure 87. Argo float deployments as of Feb 2013.

3.1.3 GLIDERS

Responsible party: Sebastiaan Swart
Organization/group: CSIR
PI: Sebastiaan Swart

The deployments form a crucial part of SOCCO's Southern Ocean Seasonal Cycle Experiment (SOSCEx) from austral spring 2012 to autumn 2013, which combines measurements taken from ships, gliders and floats. The research work aims to improve the global understanding of the link between the carbon cycle and climate in the Southern Ocean. The vast Southern Ocean is one of the most important carbon-climate systems on Earth, with recent estimates being that 40% of all CO_2 emitted are stored in the Southern Ocean.

A standard glider dive between the surface and 1000 m and back to the surface again takes approximately 5 hours to complete, upon which from the surface the glider calls researchers back in the laboratory via Iridium satellites and downloads all its valuable data. Glider pilots are also able to send the glider commands in order to change a huge range of parameters, such as waypoints, sensor sampling rates and dive speeds.

The two gliders deployed during the September voyage completed a total of 600 and 594 dives with an average dive speed of of 1.43 and 2.0km/h. The tracks for all gliders are displayed in Fig. 19. Of the three deployed during the voyage 543 has completed 316 dives with an average speed of 0.70 km/hr for last 3 dives; 575 completed 304 at 0.74km/h and 542 completed 385 at 0.8km/h. The only damages that the gliders sustained that were visible on the point of retrieval are shown in Fig.18. The extent of the damage will be determined back in Cape Town as well as the influence biofouling had on the retrieved data.

Figure 9. Photo's displaying the biofouling on all glider sensors directly after retrieval.

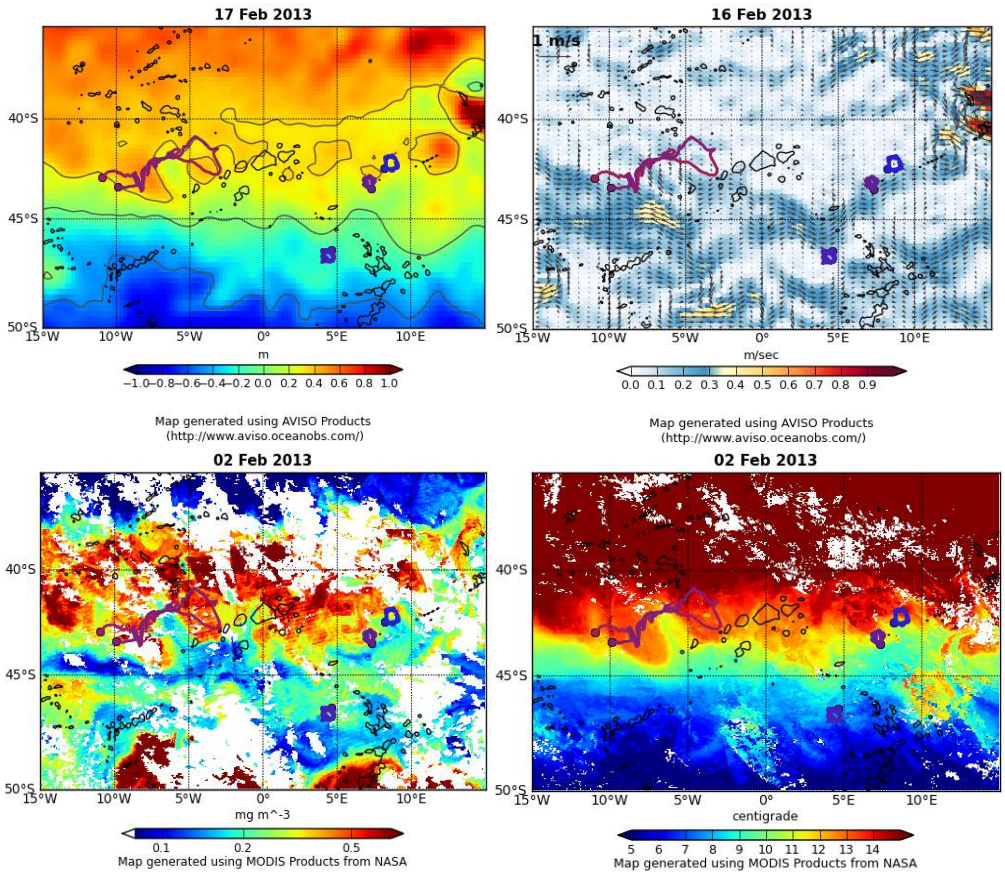

Figure 109. **Glider tracks overlaid on various parameter maps. Two pink tracks: 573 and 574. Blue and purple: 543, 575 and 542. Top Left: Glider track overlaid on the near-real time MADT (SSH in dyn m) data. The 2000m isobaths are depicted using black contours. The grey contour lines, from north to south, represent the subtropical front (STF), sub-antarctic front (SAF) and the polar front (PF). Top right: Glider track overlaid on the satellite-derived near-real time surface geostrophic velocities. The 2000m isobaths are depicted using black contours. Bottom Left: Bottom right: Glider track overlaid on MODIS 8 day Chlorophyll product, which can be 3 weeks old. The 2000m isobaths are depicted using black contours. Glider track overlaid on MODIS 4 day SST product, which can be 3 weeks old. The 2000m isobaths are depicted using black contours.**

3.1.4. BUOY'S

Responsible party: Jan Crous
Organization/group: SAWS
PI: SAWS

All but one of the buoy deployments were successful. Buoy number 109273 is not transmitting any data and is therefore not visible in the buoy tracks visualized in Fig.20. Each buoy will give us valuable data on currents, wave hight etc. for future weather predictions and help fill in data scarce areas.

For specifications regarding data supplied by individual buoy's please go to:
http://www.aoml.noaa.gov/phod/dac/deployed.html

All data can be downloaded free of charge by using the WMO numbers provided in the SOP section.

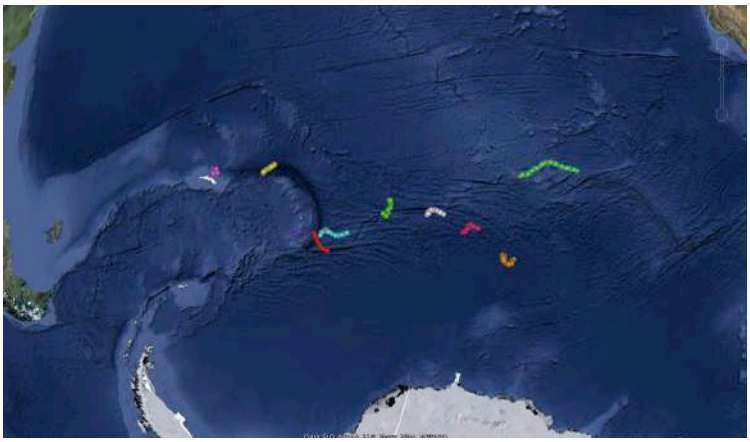

Figure 2011. Buoy tracks for the period of the voyage after deployment. The Buoy's at Southern Thule are mounted on land therefore stationary.

3.1.5. CONDUCTIVITY TEMPERATURE AND DEPTH (CTD)

Responsible party: Mfundo Lombi/Gerda Du Plessis
Organization/group: CSIR/UCT

CTD deployments were slightly disjointed during shelf science sampling, mostly due to the interference of hydraulic fluid in the moonpool. A temporary solution was reached for all errors and an error log file was created with all the tests done and the solutions to some reoccurring problems. Please find this as a separate file or contact the responsible party (information at the end of the document).

Full details on how the CTD data was processed using SeaBird Seasoft can be found in the SOP section. Details on CTD validation with independent measurements can be found in Section 2.1.5.1.

CTDs GoodHope South

Three CTD casts were conducted on the Southern leg of the GoodHope line in order to calibrate the sensors on the gliders that were deployed in the Subantarctic zone. All three CTD's were done to a depth of 1200 m as indicated by Fig. 21. The maps illustrate the positions of each CTD and the substantial difference in temperature profiles. Due to the short battery life of the two recovered gliders (much shorter than initially anticipated), it might be worthwhile to note the effect of temperature on battery life since all three were deployed in slightly different temperature locations.

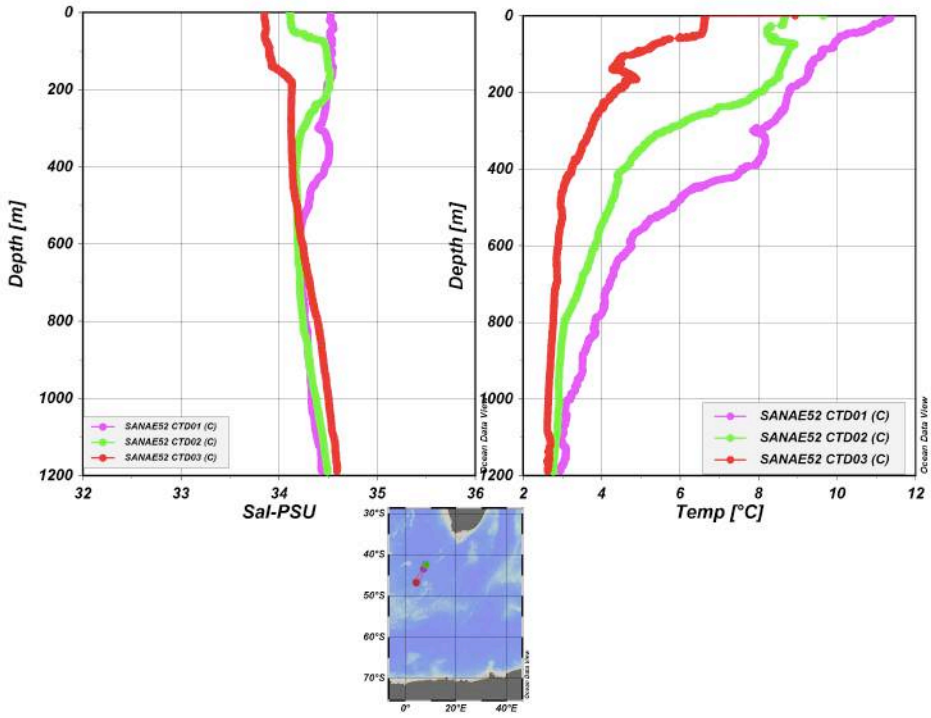

Figure 21. A diagram presenting the temperature profiles for the three CTD casts on the GoodHope south (deployed with the gliders).

CTDs Buoy run North

The temperature, salinity, oxygen, conductivity and fluorescence are displayed in Figure 22 & 23. Fluorescence profiles indicate that the primary productivity increased the further north we progressed with a substantial bloom around 60° S. This resultant bloom could not have been due to drastic temperature fluctuations, seeing that the surface temperature and oxygen stayed relatively constant at 1°C and 8ml/L respectively.

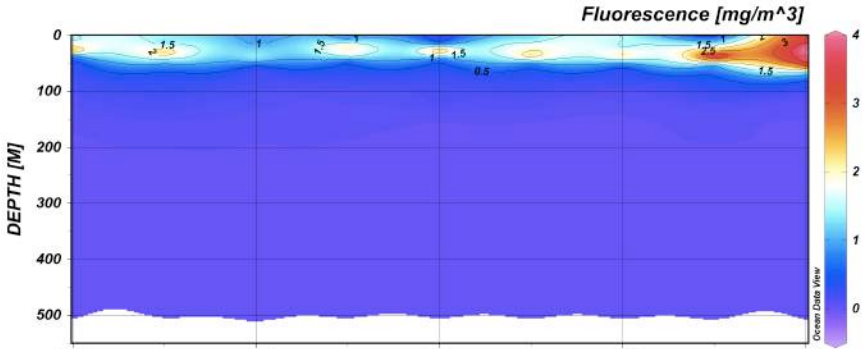

Figure 2212. The fluorescence profile for the CTD's conducted on the nothward leg of the buoy run.

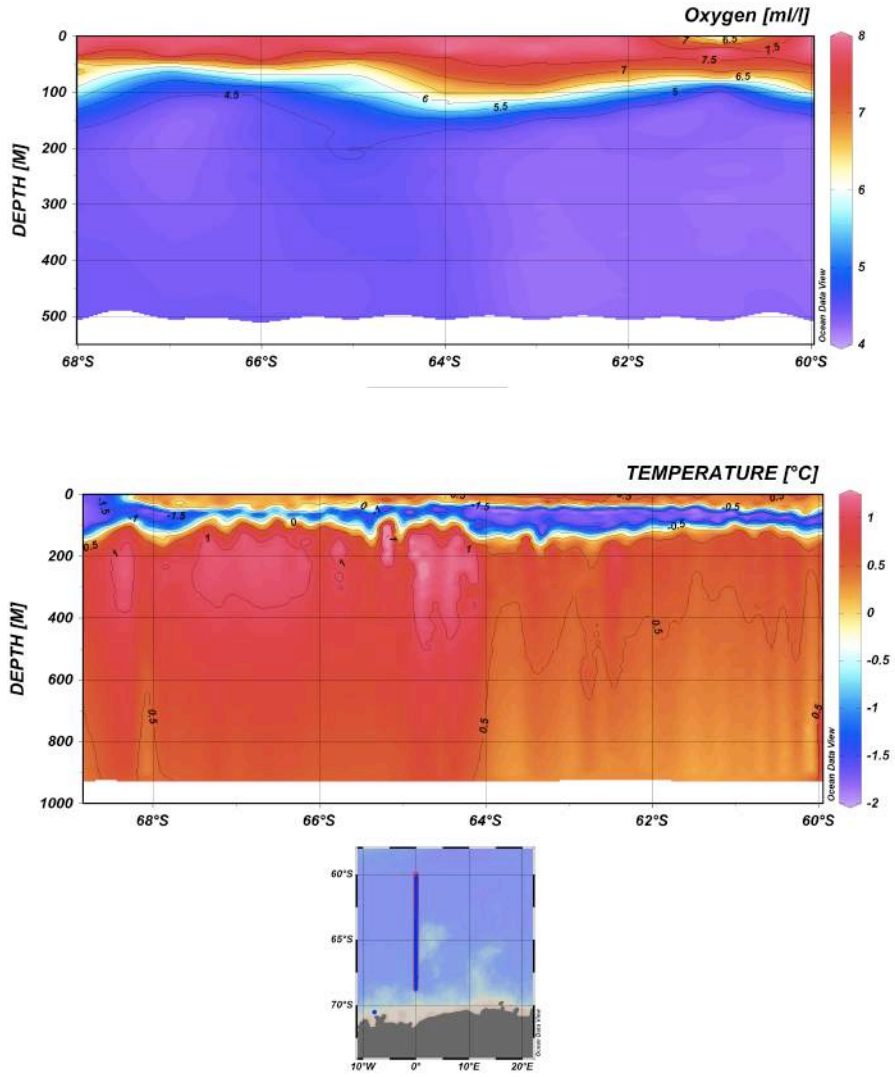

Figure 2313. The temperature and oxygen profile for the CTD's conducted on the northward leg of the Buoy run.

Shelf CTDs at RSA and Akta bukta

As previously noted the shelf CTDs are mainly a resource to document changes from year to year and capture any anomalies that might occur. During the SANAE 52 voyage, logistical operations allowed for 14 CTDs to be conducted at RSA bukta due to helicopter ops problems and a gearbox failure. Of these 14, 10 were selected that were the least disjointed and consecutive. The temperature profiles varied over time with three CTDs showing a mixed layer depth of 50m, contradictory to the average 25m (see Fig.25 Left). This could possibly be a result of the weather conditions during that time.

On return from the buoy run a quick 3 CTDs could be completed before weather closed in and sampling stopped to backload passengers at RSA bukta. The rest of the 7 CTDs were only possible between backloading operations. Three profiles showing the anomalies present at Akta are shown in Fig.25Right. All 7 CTDs had to be conducted through the moonpool due to the location being within the pack ice. The top 15 m would therefore be unreliable.

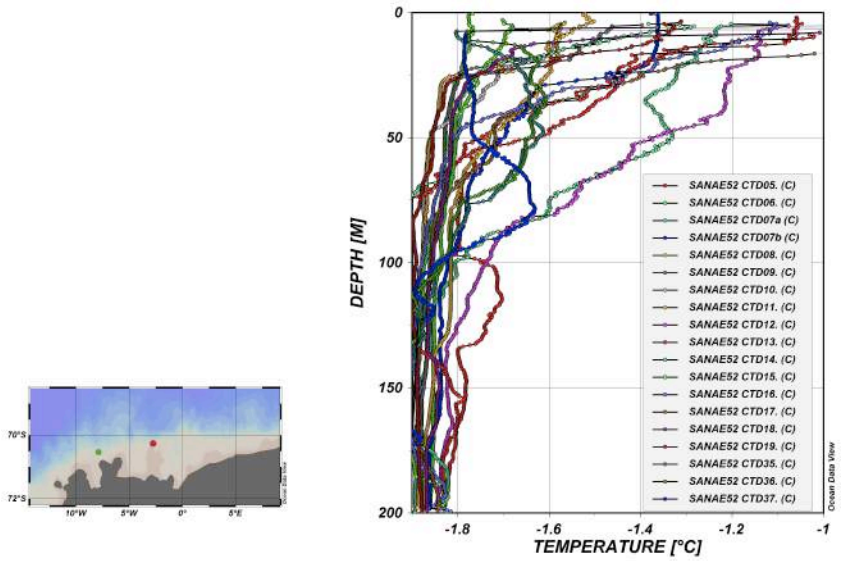

Figure 24. All CTD profiles conducted at the ice shelf and a map showing the two locations where CTDs were conducted.

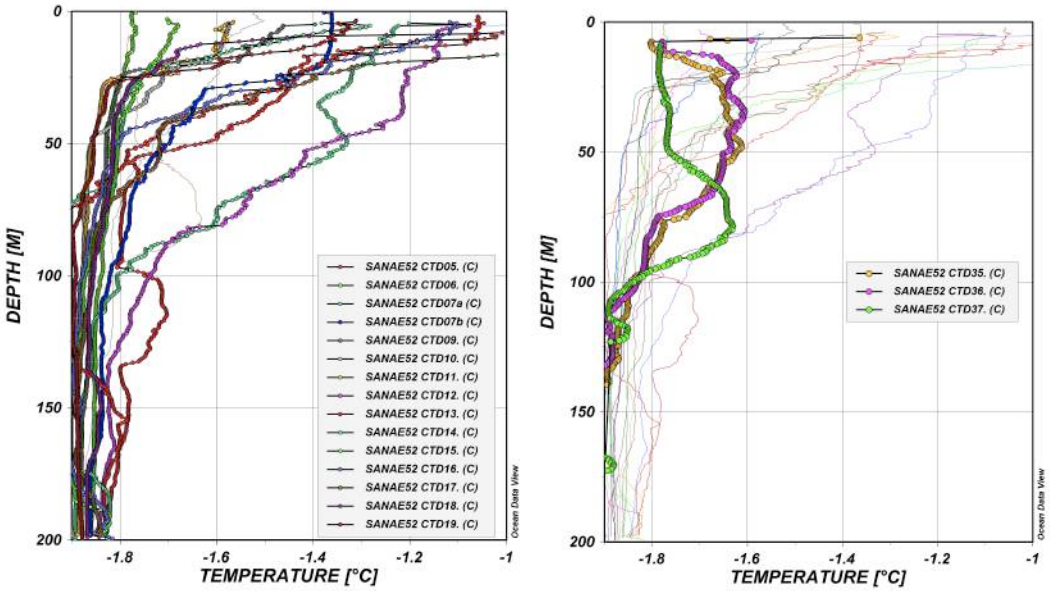

Figure 25. CTD temperature profiles of both continental shelf sites. Left: RSA bukta; Right: Akta bukta (please excuse missing profiles).

3.1.6. DISSOLVED OXYGEN

Responsible party: Khaya Siswana
Organization/group: Oceans and Coast, Department of Environmental affairs

GoodHope line South

Dissolved oxygen samples were taken at every second station resulting in a resolution of ~40nm. Observations show an increasing trend in the concentration of dissolved oxygen on the GoodHope line transect from Cape Town to Antarctica ice-shelf (Figure 26). The dissolved oxygen concentrations ranged between 5.54 (34 36.465 S; 014 12.070 E) – 8.48ml/l (61 30.561 S; 000 01.620 W) with the lowest concentrations observed within the Sub-Tropical Convergence (STC), and maximum concentrations within the Antarctic Zone (AZ).

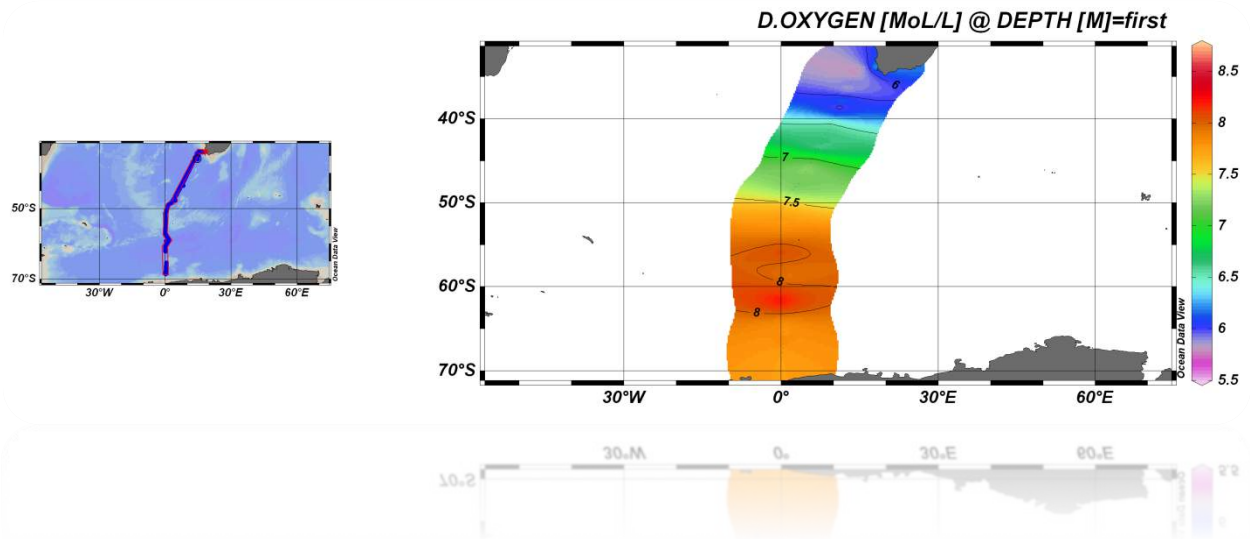

Figure 26. Dissolved oxygen concentrations for GoodHope South. The data was obtained from Winkler titrations conducted onboard.

Buoy run

During the buoy run north a 10-degree high resolution (~10nm) surface profile was concluded. The dissolved oxygen concentrations ranged between 5.95 – 10.35ml/l with a peak of 10.35ml/L just West of the GoodHope line (Fig.27). Both the upper limit and the lower limit of dissolved oxygen concentrations were observed within the Polar Front (PF) with an average of 8ml/L. The oxygen minimum was during a single station before reaching Southern Thule, and could be considered an outlier.

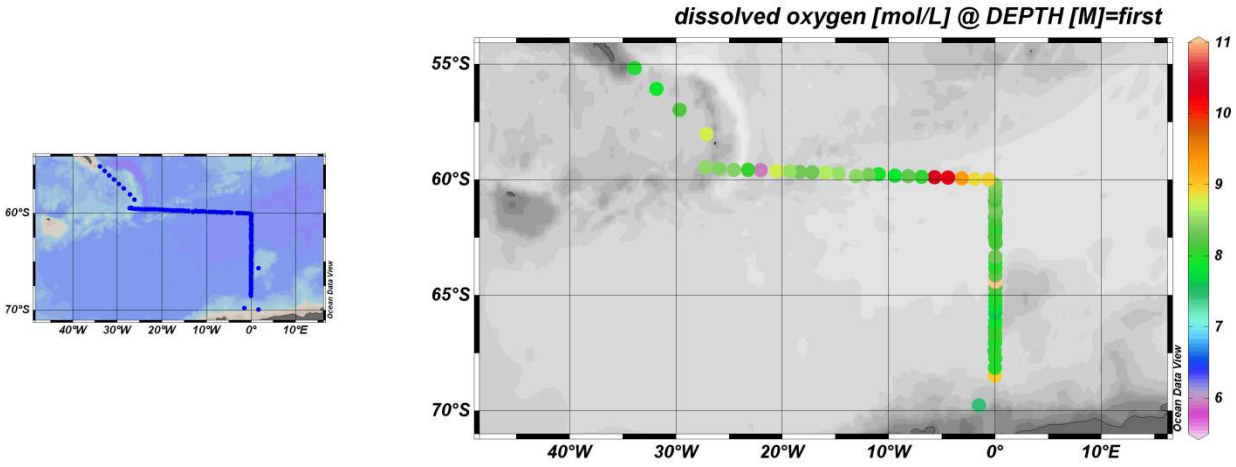

Figure 27. Dissolved oxygen concentrations for Buoy-run North.

For the leg back south on the buoy run stations were decreased to every 8 hours to accommodate sampling supplies. This resulted in a lower resolution as seen in Fig.28. The dissolved oxygen concentrations ranged between 7.69 – 9.18ml/l on the second Leg of the Buoy Run. The average dissolved oxygen concentration of 8.45 ml/l was observed between the Polar Frontal Zone and Antarctic Zone.

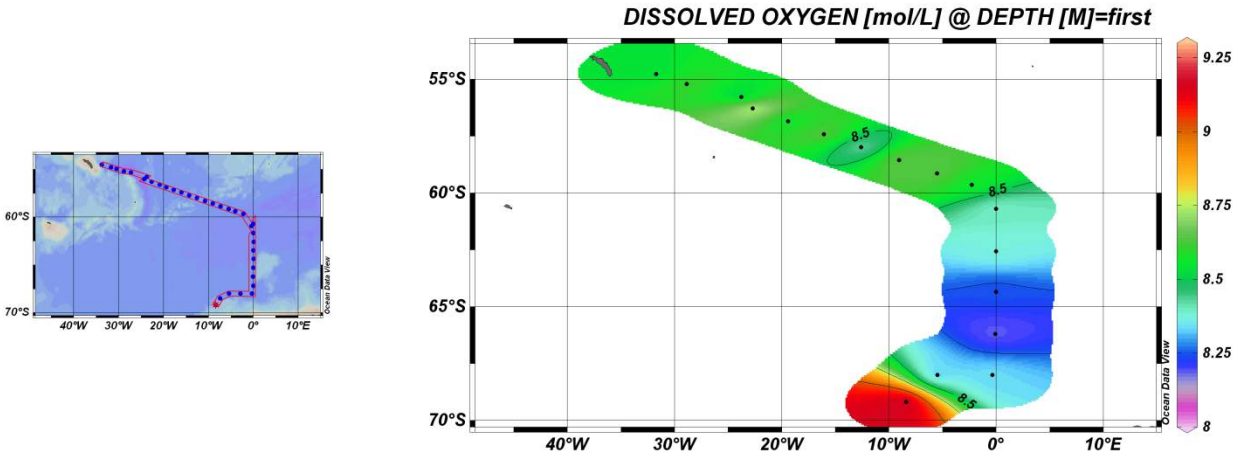

Figure 148. Dissolved oxygen concentrations for the Buoy run South.

3.1.7. TCO2

Responsible party: Precious Mongwe
Organization/group: CSIR
PI: Pedro Monteiro

Note from the Figure 29 that deep waters have very high DIC and alkalinity compared to surface waters. The high DIC in bottom waters is a result of the accumulation the sinking inorganic carbon as a result of remineralisation of organic matter after its formation by photosynthesis from surface water. In addition to the sinking inorganic carbon from the euphotic zone , colder water holds more CO_2 than warm waters hence deep and high latitudes waters have elevated DIC and AT. Note in Figure 29, surface waters at 42°S have very low DIC and high salinity. The low DIC in this region is due to warm waters from the Agalhus retroflection. Preliminary plots for underway and CDT sampled DIC and AT diagrams are given below.

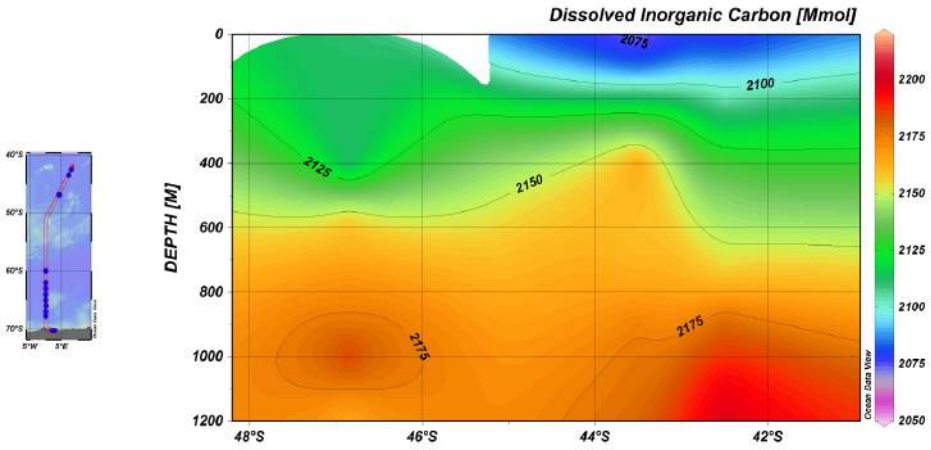

Figure 159. A preliminary plot for DIC for three CTD casts during the glider deployments on the GoodHope South.

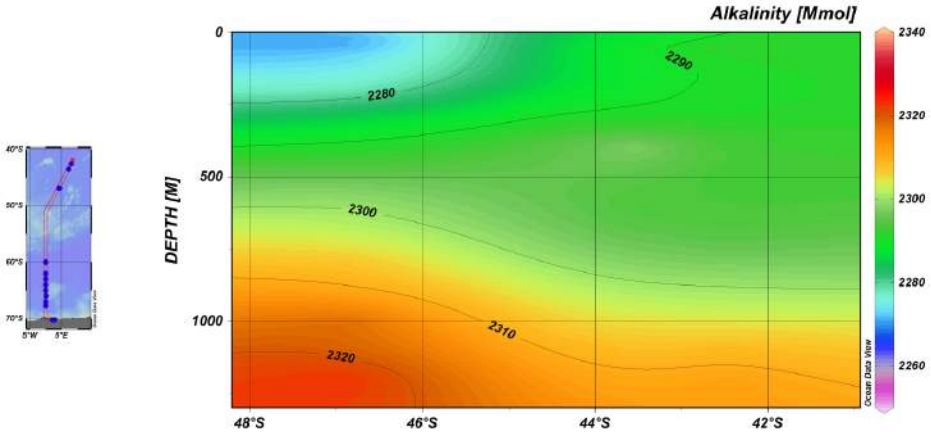

Figure 30. A preliminary plot for Alkalinity for three CTD casts on the GoodHope South.

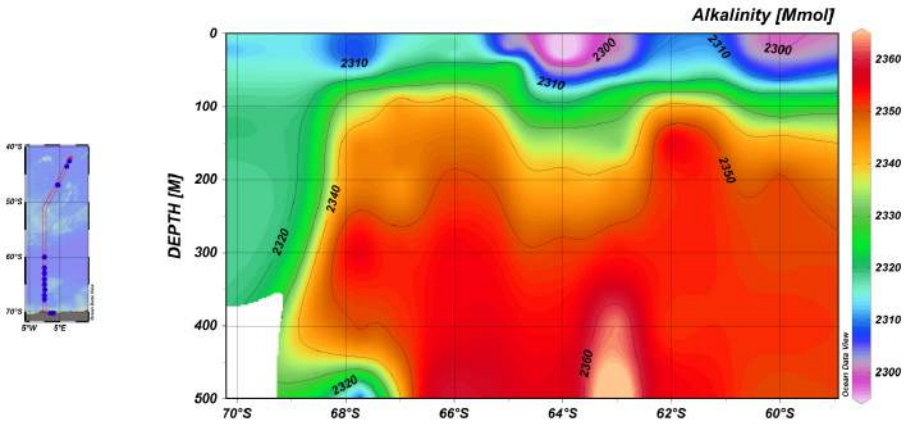

Figure 31. A preliminary Alkalinity plot for the CTDs deployed during the buoy run.

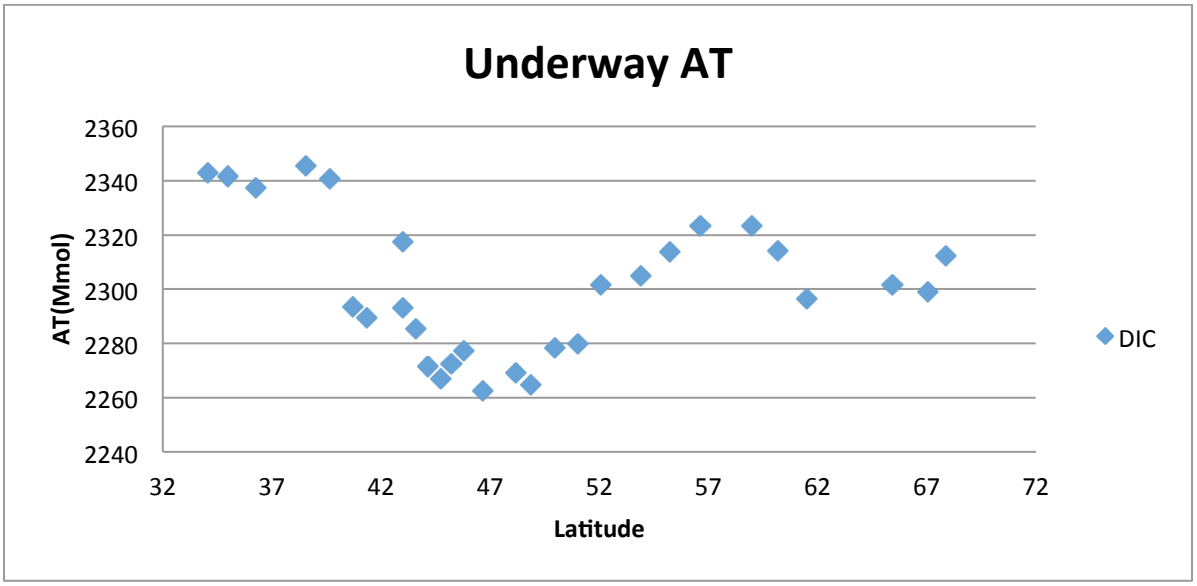

Figure 32. Underway alkalinity measurements on the GoodHope South.

3.1.8. UNDERWAY pCO2

Responsible party: Precious Mongwe
Organization/group: CSIR
PI: Pedro Monteiro

The pCO2 system logged on the log sheet the data from the TSG, underway 10 AU fluorometer, a Fluke digital thermometer for the equilibrator temperature, atmosphere CO_2 and the equilibrator measurement. For atmospheric CO_2, atmospheric air was sampled outside the ship at the bridge using a line going to the underway lab connected to the instrument. Preliminary plots are shown below. The intake and out gassing of CO_2 in the ocean is greatly influenced by the flux gradient among other factors, when ocean CO_2 is greater that of the atmosphere, the ocean release CO_2 as result of negative flux direction and when the atmospheric CO_2 is greater than the oceanic CO_2, the opposite is true. Note from the diagram (Figure 33) below that the Ocean pCO_2 increase from low to high latitudes while the atmospheric CO_2 remain constant. Among other factors this is due to the fact that colder water holds more CO_2 than warm waters, thus CO_2 is released in high latitudes and absorbed in low latitudes.

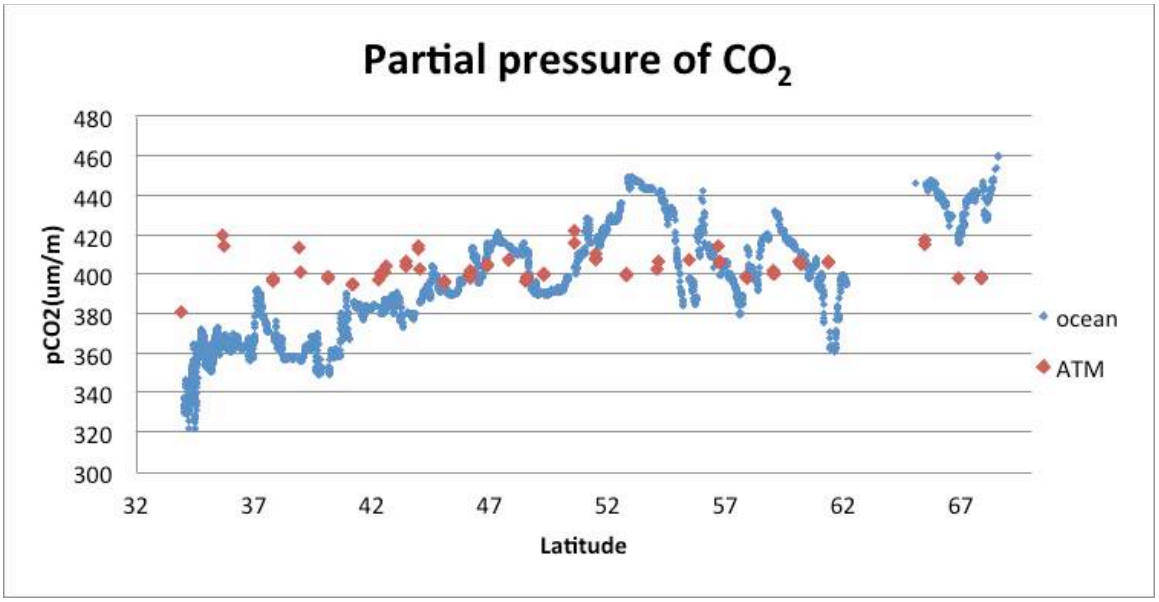

Figure 3316. Preliminary plot for the underway pCO2 system.

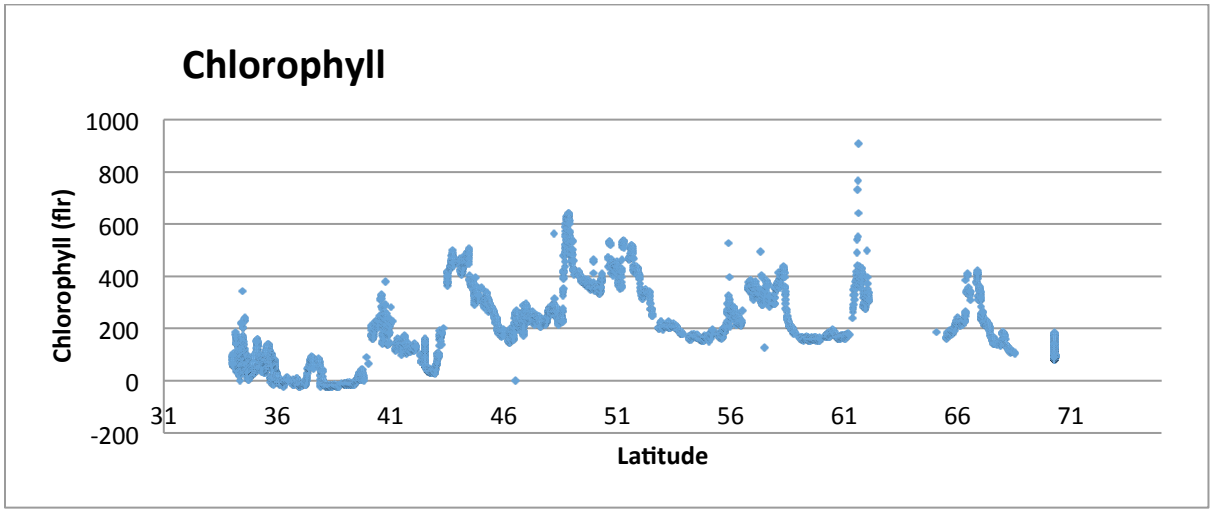

Figure 34. An estimation of chlorophyll through fluorometry as measured by the underway system.

3.2. BIOLOGICAL

3.2.1. MICROBIOLOGY

3.2.1.1. Viral biodiversity

Responsible party: G. Du Plessis, UCT
Organization/group: MCB, at University of Cape Town
PI: Dr. Ed Ryckibi

Phage or viral biodiversity in ocean surface waters is a relatively new field of study hence the interest in the field and its proposed multitude of genetic information regarding viral mutation and survival in harsh environments. The goal of analyzing comparative viral and bacterial biodiversity is to build a database of information regarding the picophytoplanktonic community.

During the course of sampling, several difficulties became apparent regarding the amount of precipitate formed and collected. An average of 8 filters (0.8 µm 142 mm) were necessary for collection of all 20L worth of precipitate and exact volumes were not possible in manageable timescales. On the northbound leg between Antarctica and Cape Town a 10 L volume was used and 0.8 µm Nitrocellulose support filters were exchanged every third polycarbonate filter. This allowed for enough precipitate to be collected and filtration time to be limited to 35min.

3.2.1.2. Bacterial biodiversity

Responsible party: G. Du Plessis, UCT
Organization/group: UCT/IMBM
PI: G. Du Plessis

All filters collected during the course of the cruise have been stored for further analyses back in Cape Town. Any requests for data can be addressed to the PI and chief scientist after processing. The culture based research provided a large array of bacterial morphologies. Two distinct fungal morphologies were apparent on one of the culture plates suggesting the Chloramphenicol concentration in the plate is either depleted or does not affect the fungal species. Some of the colonies are depicted in Fig. 35.

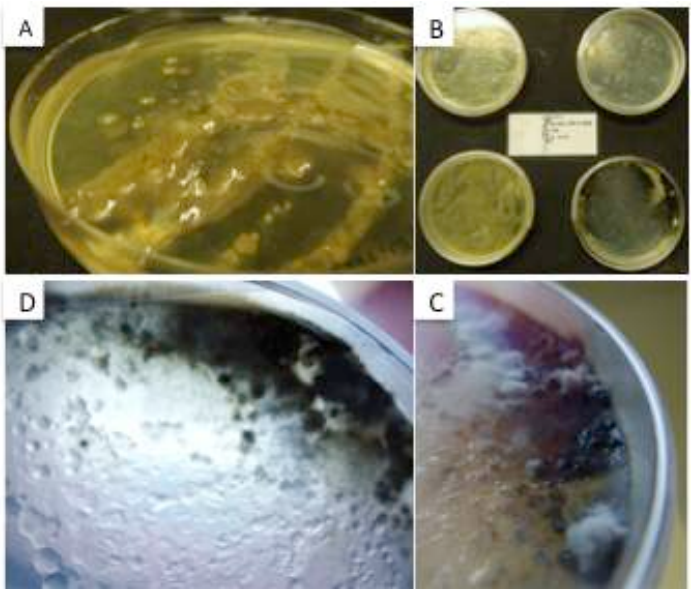

Figure 35. Photo's of bacterial growth of SAF concentrated cells on media plates. A: Closeup on colony formations. B: All four mediums used in this study. C: Fungal growth along with Gram negative colonies.

3.2.2. ORNITHOLOGICAL OBSERVATIONS

Responsible party: Andrew Schofield, Helm Van Zyl
Organization/group: **The Atlas of Seabirds at Sea**
PI: AS@S

BirdLife South Africa in association with the South African Environmental Observer Network , Egagasini Node, and SANAP the DEA and the Percy Fitzpatrick Institute started a monitoring project in the seas around southern Africa known as **The Atlas of Seabirds at Sea**, it is commonly known as AS@S, pronounced "ay-sass", the project was launched on 16 October 2009.

AS@S is the marine analogue of SABAP2, the Second Southern African Bird Atlas Project, which is gathering records of bird distribution on the mainland. The monitoring is to establish the distribution and density of seabird populations in the waters around Southern Africa and this has been extended all the way to the Antarctic and the South Sandwich Islands and South Georgia through a partnership and working relationship with the DEA.

Unfortunately the data capturing system does not allow any form of processing to be able to show the trends in species numbers or increase in counts as for the bases and islands. One graph denoting the counts at SANAE base is provided (Fig.36), however for more detailed data please contact AS@S.

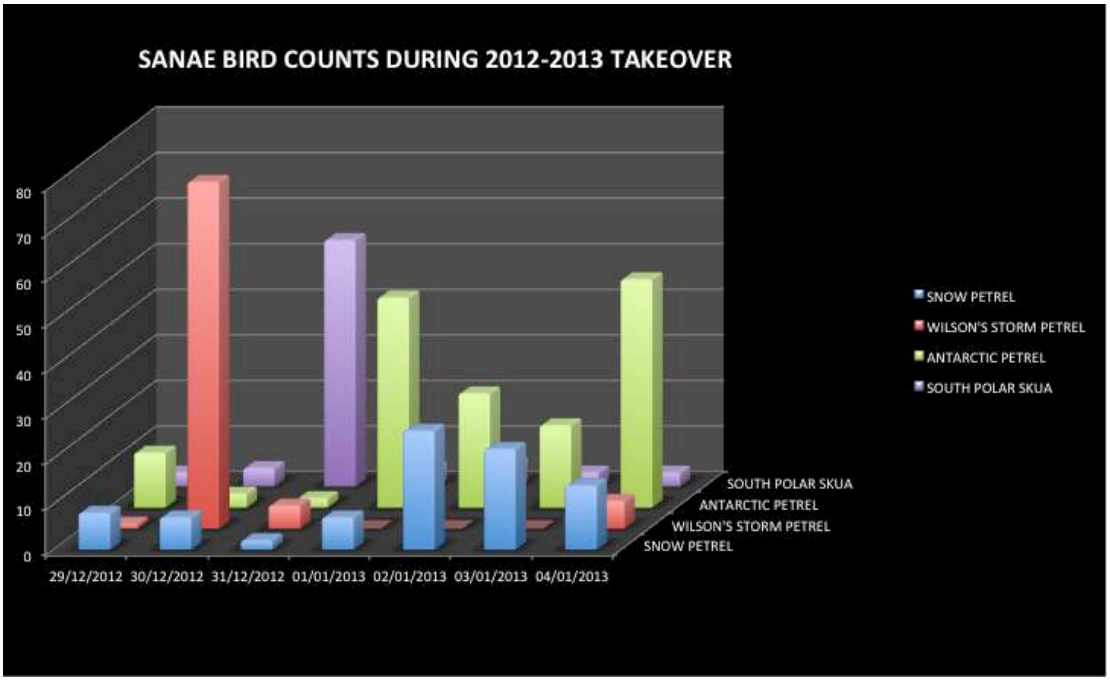

Figure 36. Bird observations during a short data capture at SANAE IV during takeover 2013.

3.2.3. Continuous Plankton Recorder

A comprehensive description of the Biological oceanography of the surveyed area during this cruise falls outside the authority and scope of this report as the sample still have to undergo further processing and analysis by the principal

investigator. The following account is a brief summary of the physical oceanography and ships trajectory during the deployment of the CPR.

Figure 37. The RBR log graph showing the depth, temperature, and salinity during the tow of cassette 189-1.

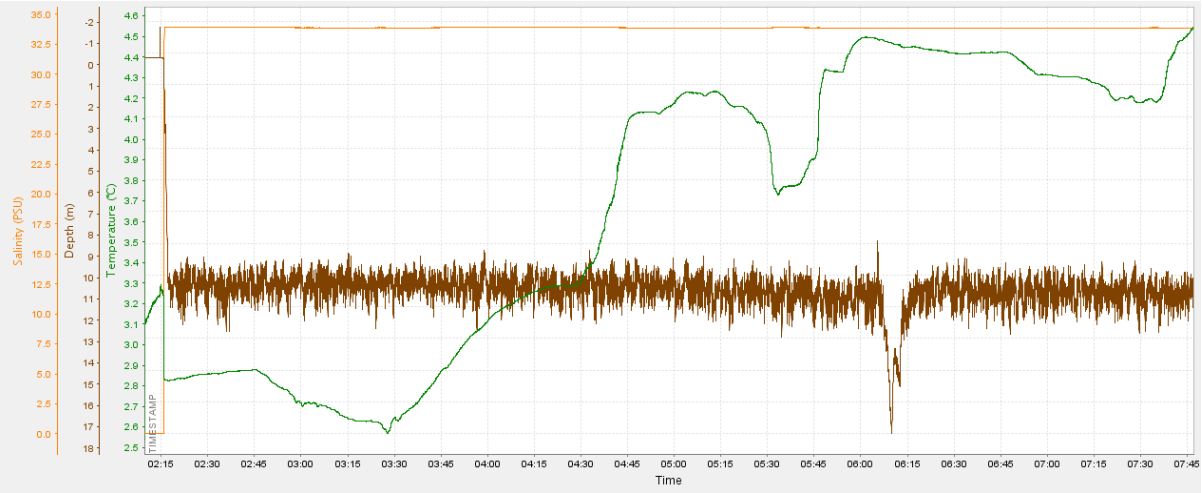

Figure 38. The RBR log graph showing the depth, temperature, and salinity during the tow of cassette 189-2.

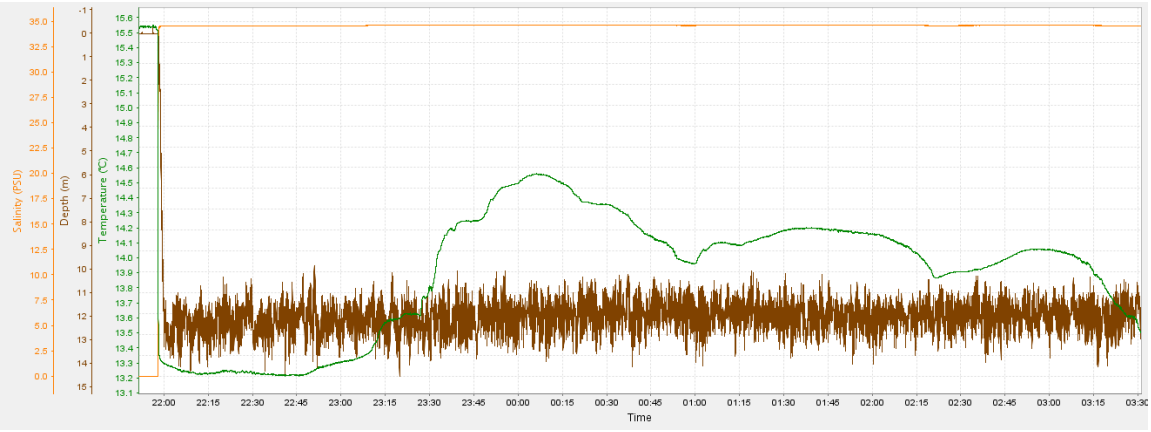

Figure 179. The sea surface temperature and trajectory during the towing of CPR.

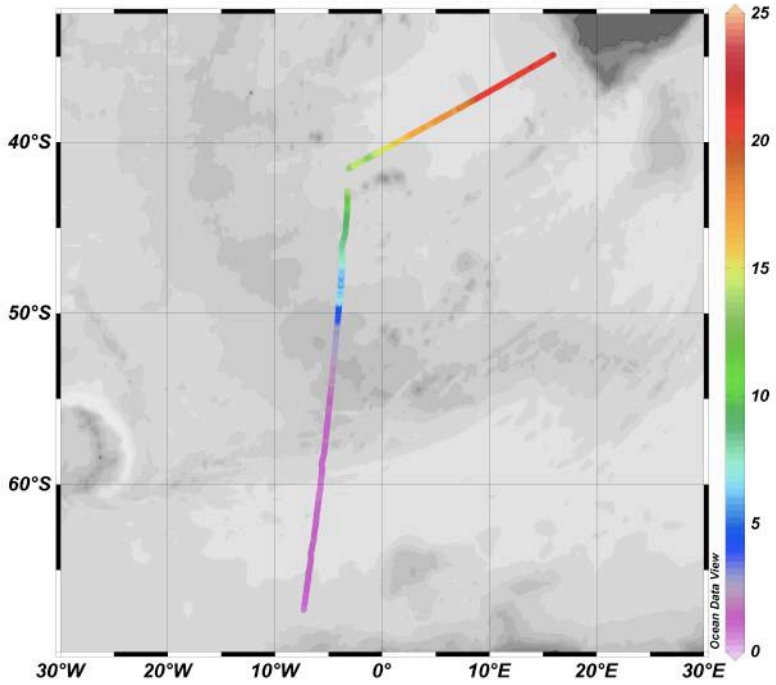

Figure 40. The RBR log graph showing the depth, temperature, and salinity during the tow of cassette 189-3.

3.3 ATMOSPHERIC

3.3.1. Atmospheric precipitation

Scalar parameters from the Parsivel and the anemometer data were matched with ship position from the Ship Data System (SDS). Figure 41 shows the predicted radar reflectivity plotted as a map and as a corresponding time-series for each phase of the voyage. Reflectivities of up to 50 dBZ are given by the Parsivel, which would represent large hailstones on a weather radar. Since no hail was experienced during the voyage, this confirms the known problem of the Parsivel incorrectly identifying precipitation type in high wind speeds. The SVI has no such limitation and should be able to provide a correct

estimate. Wind direction, speed and elevation angle are plotted for measurements sampled at one-minute intervals during the voyage. Elevation angle introduces a cosine error into wind measurements, aside from the dynamic effect of the ship's structure on the ambient wind velocity. It would appear from Figure 42 that an empirical correction for the cosine error should be possible via a simple lookup-table based on wind direction. Estimating and correcting for the ship dynamic effect on wind measurements would require a more in-depth study of the airflow over the ship.

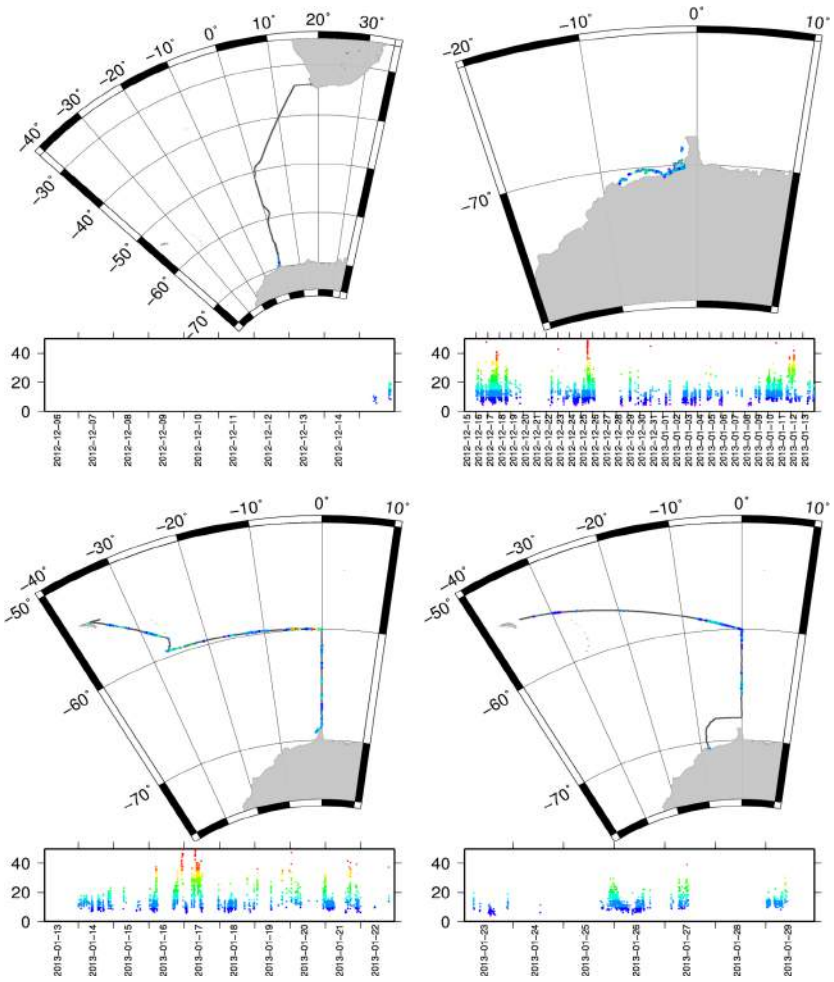

Figure 41. Predicted radar reflectivity from precipitation measured during the phases of the voyage. Top-to-bottom, left-to-right: GoodHope Southbound, Offloading, Buoy run Northbound, Buoy run Southbound.

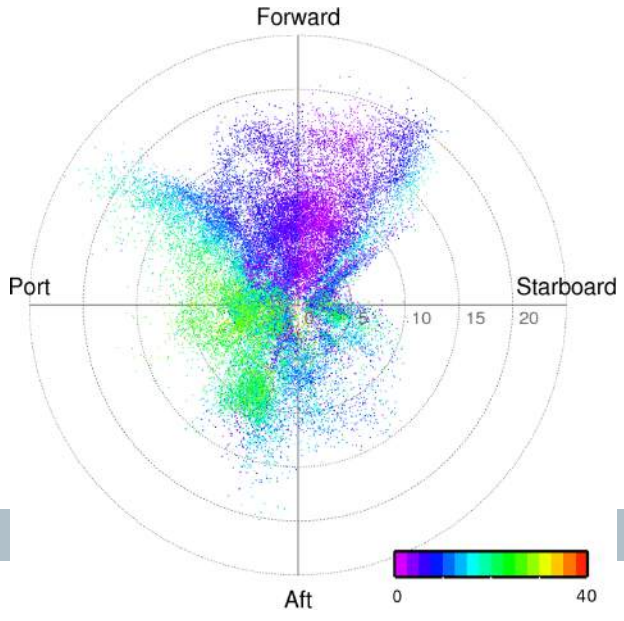

Figure 42. Wind speed (m/s) and direction relative to the ship, with elevation angle indicated by the colour of the points.

4. CONCLUSION

BIOGEOCHEMICAL CYCLE: BRINGING THE MESSAGE HOME

The Southern Ocean forms an integral part of the global climate system and is therefore a fundamentally important cornerstone in our search for knowledge. The complex interactions between the atmosphere and ocean influence the climate in ways not yet fully understood, but crucial for understanding climate change. Our current knowledge can only be enhanced if a continuous monitoring system is in place to measure physical (air-sea CO2 fluxes; temperature, salinity, dissolved oxygen, nutrients, Iron levels etc.) and biological (Birds, sea invertebrates, pico/nanophytoplankton and zooplankton, viruses and top predators) parameters accurately.

During the SANAE 52 voyage we successfully completed most underway measurements. A few logistical setbacks hampered data collection and a substantial amount of errors occurred with the pCO2 system, however we still managed to obtain a vast amount of data for the trip. The underway salinity and biological stations not only helps us to calibrate complementary instruments but gives a high resolution image of the state of the frontal features between South Africa and Antarctica. The gliders, Argo floats and weather buoy's all fill a unique gap in long-term data poor areas and helps us to understand the importance of biogeochemical fluctuations and changes in anthropogenic CO2.

When considered together these results represent important new data that allow South African oceanographic research the opportunity to begin to correctly quantify the Southern Ocean CO2 sink which will enable realistic climate simulations to be made. Our ability to tackle pertinent questions such as these will bring South African science into the forefront of a globally significant topic and improve our standing in the international science community.

Several papers regarding the data are already in progress and will be submitted to international journals in the coming months. Several PhD and Msc projects are solely based on the data collected during the voyage and will provide excellent grounds for theses work. We hope to hold a post-cruise workshop to encourage cross-discipline collaborations for future projects within the coming months and to discuss possible overlaps in various subjects.

ACKNOWLEDGEMENTS

This voyage would not have been possible without the hard work and dedication of an excellent team. Our thanks goes out to the crew and Captain of the SA Agulhas II which went out of their way to accommodate us where possible. We would also like to thank the DCO, Adriaan Dreyer for his leadership especially through trying logistical problems. A special thanks goes out to the entire DEA administrative staff who helped with medicals and passports to get us cleared in time. We would also like to thank the Chief scientist of the Polarstern with their continued effort in helping fix our pCO_2 nitrogen shortage.

Last but not least we would like to thank the technicians, especially Mfundo Lombi, engineers and electricians who worked through the night to fix our equipment for their dedication.

We are grateful to NOAA for supplying the oceanographic equipment, STX for their invaluable analyses of the ship and the NRF as well as SANAP for supplying funding for various projects.

Gerda Du Plessis

Chief Scientist (18th February 2013)

SUGGESTED READING

Baker, D.F. 2007. Reassessing carbon sinks. *Science 316*, 1708 – 1709.

Bakker DCE, Hoppema M, Schröder M, Geibert W, De Baar H. Biogeosciences A rapid transition from ice covered CO2 – rich waters to a biologically mediated CO2 sink in the eastern Weddell Gyre.

Biogeosciences. 2008. 5:1373-1386. Bellerby, R.G.J., Hoppema, M., de Baar, H.J.W., Fahrbach, E., Stoll. 2004. Interannual controls on the Weddel Sea surface fCO2 during autumn-winter transition phase. *Deep Sea Research* I, *51*, 793 – 808. Berger, W.H. and Wefer, G. 1991. Productivity of the glacial ocean: Discussion of the iron hypothesis, *Limnology and Oceanography 36(8)*, 1899 -1918.

Boyd, P.W. 2002. Review: Environmental factors controlling phytoplankton processes in the Southern Ocean. *Journal of Phycology 38*, 844-861.

Budillon G. and Rintoul S.R. (2003). Fronts and upper ocean thermal variability south of New Zealand. Ant Sci. 15, 141-152.

Carpenter, J. H. (1965a): The accuracy of the Winkler method for dissolved oxygen analysis. *Limnol. Oceanogr.,* **10,** 135–143.

Carpenter, J. H. (1965b): The Chesapeake Bay Institute technique for the Winkler dissolved oxygen method. *Limnol. Oceanogr.,* **10,** 141–143.

Caldeira, K. and Duffy, P.B. 2000. The role of the Southern Ocean in uptake and storage of anthropogenic carbon dioxide. *Science*, *287*, 620 – 622.

Caldeira and Wickett. 2005. Ocean model predictions of chemistry changes from carbon dioxide emissions to the atmosphere and ocean. *Journal of Geophysical Research 110*, C09S04, doi:10.1029/2004JC002671.

Cassar,N.,etal.2007.The Southern Ocean Biological Response to aeoli anIronde position. *Science317,1067–* 1070.

Cochlan, W.P. 2008. Nitrogen Uptake in the Southern Ocean. In: Nitrogen in the Marine Environment. Elsevier. doi:10.1016/B978-0-12-372522-6.00012-8.

Cochlan, W.P. 2008. Nitrogen Uptake in the Southern Ocean. In: Nitrogen in the Marine Environment. Elsevier. doi:10.1016/B978-0-12-372522-6.00012-8.

Doney, S.C., Fabry, V.J., Feely, R.A., Kleypas, J.A. 2009a. Ocean acidification: the other CO2 problem. Ann. Rev. *Marine Science 1*, 169–192. doi:10.1146/annurev. marine.010908.163834.

Doney, S.C., Tilbrook, B., Roy, S., Metzl, N., Le Quere, C., Hood, M., Feely, R.A., Bakker, D. 2009b. Surface ocean variability and vulnerability. *Deep Sea Research II*, doi.10.1016/j.dsr2.2008.12.016.

Feely, R.A., Sabine, C.L., Lee, K., Berelson, W., Kleypas, J., Fabry, V.J., Millero, F.J. 2004. Impact of anthropogenic CO2 on the CaCO3 system in the oceans. *Science 305 (5682)*, 362–366.

Friedlingstein, P., Cox, P., Betts, R., Bopp, L., von Bloh, W., Brovkin, V., Cadule, P., Doney, S., Eby, M., Fung, I., Bala, G., John, J., Jones, C., Joos, F., Kato, T., Kawamiya, M., Knorr, W., Lindsay, K., Matthews, H.D., Raddatz, T., Rayner, P., Reick, C.,

Roeckner, E., Schnitzler, K.-G., Schnur, R., Strassmann, K., Weaver, A.J., Yoshikawa, C., Zeng, N. 2006. Climate–carbon cycle feedback analysis: results from the C4MIP model intercomparison. *Journal of Climate 19 (14)*, 3337–3353.

Fung, I., Doney, S.C., Lindsay, K., John, J. 2005. Evolution of carbon sinks in a changing climate. *Proceedings of the National Academy of Sciences of the United States of America 102*, 11201–11206. Gordon A.L. (1986). Interocean exchange of thermocline water. J. Geophys. Res. 91, 5037-5046.

Gordon, A.L., Weiss R.F., Smethie W.M. and Warner J. (1992). Thermocline and intermediate water communication between the South Atlantic and Indian Oceans. J. Geophys. Res. 97, 7223-7240.

Grasshoff, K.M., Ehrhardt, M., Kremling, K. 1983. Determination of urea (9.5). In: *Methods of seawater analysis*, 2nd edition. Verlag Chemie, Wienheim, Germany. Pp. 158-162.

Griffiths, H.J., et al., Quantifying Antarctic marine biodiversity: The SCAR-MarBIN data portal. Deep-Sea Research II (2010),

John, S.G., Mendez, C.B., Deng, L., Poulos, B., Kauffman, A.K.M., Kern, S., Brum, J., Polz, M.F., Boyle, E.A. and Sullivan, M.B. (2011). A simple and efficient method for concentration of ocean viruses by chemical flocculation *Environ. Microbiol. Rep.*, 3(2): 195–202.

Holmes, R.M., Aminot, A., Kerouel, R., Hooker, B.A., Peterson, B.J. 1999. *A simple and precise methjod for measuring ammonium in marine and freshwater ecosystems.* Can. J. Fish.

Hall, A. and Visbeck, M. 2002. Synchronous variability in the Southern Hemisphere Atmosphere, Sea Ice, and Ocean Resulting from the Annular Mode. *Journal of Climate. 15*, 3043 – 3057.

Holeton, C.L., Nédélec, F., Sanders R., Brown, L., Moore, C.M., Stevens, D.P., Heywood, K.J., Statham. P.J., Lucas, C.H. 2005. Physiological state of phytoplankton communities in the Southwest Atlantic sector of the Southern Ocean, as measured by fast repetition rate fluorometry. *Polar Biology 29*, 44-52.

Kolber, Z, O Prasil and P G Falkowski (1998) Measurements of variable chlorophyll fluorescence using fast repetition rate techniques: defining methodology and experimental protocols *Biochimica et Biophysica Acta* 1367: 88-106

LeQuéré, C. et al. 2007. Saturation of the Southern Ocean CO2 sink due to recent climate change. *Science 316*, 1735–1738.

Lutjeharms, J.R.E., Monteiro, P.M.S., Tyson, P.D., Obura, D. 2000. The Oceans around Southern Africa and RegioBellerby, R.G.J., Hoppema, M., de Baar, H.J.W., Fahrbach, E., Stoll. 2004. Interannual controls on the Weddel Sea surface fCO2 during autumn-winter transition phase. *Deep Sea Research* I, *51*, 793 – 808.nal Effects of Global Change: START Regional synthesis. *South African Journal of Science 97 (3/4)*, 119 -130.

Lutjeharms J.R.E. and Cooper J. 1996. Interbasin leakage through Agulhas Current filaments. Deep-Sea Res. I. 43, 213-238.

Marinov, I., Gnanadesikan, A., Toggweiler, J.R. and Sarmiento, J.L. 2006. The Southern Ocean biogeochemical devide, *Nature*, *441*, 964 – 967.

Moor, J.K., Abbott, M.R. 2002. Surface chlorophyll concentrations in relation to the Antarctic Polar Front: seasonal and spatial patterns from satellite observations . *Journal of Marine Systems 37*, 69 – 86.

Orr, J.C., Fabry, V.J., Aumont, O., Bopp, L., Doney, S.C., Feely, R.A., Gnanadesikan, A., Gruber, N., Ishida, A., Joos, F., Key, R.M., Lindsay, K., Maier-Reimer, E., Matear, R., Monfray, P., Mouchet, A., Najjar, R.G., Plattner, G.-K., Rodgers, K.B., Sabine, C.L., Pierrot,D., etal. 2009. Recommendations for autonomous underway pCO2 measuring systems and data-reduction routines.

Deep Sea Research II,doi:10.1016/j.dsr2.2008.12.005 Parsons, T.R., Maita, Y., Lalli, C.M. 1984. *A manual of chemical and biological methods for seawater analysis.*

Pergamon Press, Oxford. Pp. 173. Rintoul S.R. (1991). South Atlantic interbasin exchange. J. Geophys. Res. 96, 2675-2692. Rintoul S. R. and Sokolov S. (2001). Baroclinic transport variability of the Antarctic Circumpolar Current south of Australia (WOCE repeated section SR3). J. Geophys. Res. 106, 2815-2832. Rintoul,SR, S Sokolov, J Church. 2002. A 6 year record of baroclinic transport variability of the Antarctic Circumpolar Current at 140deg E derived from expendable bathythermograph and altimeter measurements.: Journal of Geophys. Res. 107. Sarmiento, J.L., Schlitzer, R., Slater, R.D., Totterdell, I.J., Weirig, M.-F., Yamanaka, Y., Yool, A. 2005.

Anthropogenic ocean acidification over the twenty-first century and its impact on marine calcifying organisms. *Nature 437*, 681–686. Sarmiento, J.L. and Orr, J.C. 1991.

Three-dimensional simulations of the impact of Southern Ocean nutrient depletion on atmospheric CO2 and ocean chemistry, *Limnology and Oceanography 36(8)*, 1928 – 1950. Sigman, D.M., Boyle, E.A. 2000. Glacial/interglacial variations in atmospheric carbon dioxide. *Nature 407*, 859– 869.

Speich S., Blanke B., and Madec G. 2001. Warm and cold water paths of a GCM thermohaline conveyor belt.

Geophys. Res. Lett. 28, 311-314. Speich S., Blanke B., de Vries P., Döös K., Drijfhout S., Ganachaud A. and Marsh R. 2002. Tasman Leakage: A new route for the global conveyor belt. Geophys. Res. Lett. 29, 10. 1029/2001GL014586.

Sprintall J., Peterson R. and Roemmich R. 1997. High resolution XB T/XCTD measurements across DrakePassage. WOCE Newsletter 29. 18-20.

Takahashi et al., .2002. Global Sea – air CO2 flux based on climatological surface ocean pCO2 and seasonal biological and temperature effects. *Deep Sea Research II. 29:* 1601 – 1622.

Toggweiler, J.R., Murmane, R., Carson, S., Gnanadesikan, A., Sarmiento, J.L. 2003. Representation of the carbon cycle in box models and GCM's: 2. Organic pump, *Global biogeochemical cycles*, *17(1)*, 1027, doi:10.1029/2001GB001841

Toggweiler, J.R., Russel, J.L., Carson, S.R. 2006. Midlatitude westerlies, atmospheric CO2, and climate change during the ice ages, *Paleoceanography*, *21*, doi: 10.1029/2005PA001154

CONTACT INFORMATION/IMPORTANT SITES

BUOY DEPLOYMENTS AND DATA:	http://www.aoml.noaa.gov/phod/dac/deployed.html	
GLIDER DEPLOYMENTS AND DATA:	http://access.oceansafrica.org	
ARGO DEPLOYMENTS AND DATA:	Coriolis:	http://www.coriolis.eu.org/
	USGODAE:	http://www.usgodae.org/argo/argo.html
XBT RAW DATA:	http://www.aoml.noaa.gov/phod/hdenxbt/ax25_feb13.html	
CTD RAW DATA:	Dr. Isabelle Ansorge : i.ansorge@uct.ac.za	
pCO_2 AND TCO_2 DATA:	Dr. Pedro Monteiro	
MICROBIOLOGY DATA:	Gerda Du Plessis: gdp.safrica@gmail.com	
SUN PHOTOMETER DATA:	aeronet.gsfc.nasa.gov	
ATMOSPHERIC DATA:	Dr. Stephen Broccardo, University of Potchefstroom	

APPENDIX A

Standard Operating Procedure

Isolating Bacterial Strains From Environmental Samples

Media Needed:

- Marine Agar
- Sea Water Agar
- GYM Streptomyces Medium
- Ashby's Nitrogen Free Agar

Procedure

1. Mix 1 part sample with 9 parts sterile sea water
2. Preform serial dilutions until approx. 10^6 cells per ml
3. Spread 100ul onto 2 plates of each of the above media
4. Incubate at room temperature (approx. 21C)
5. Check plates every day
6. As colonies appear they should be numbered, picked and spread onto the same media the colony was isolated from
7. For slow growing strains additionally plate onto marine agar
8. Once in pure culture pick a single colony and grow in 5ml of the appropriate liquid culture.
9. Concentrate to 500ul in centrifuge and add 500ul of 50% glycerol
10. Freeze at -80C

Recipes

Marine Broth/Agar

Used to isolate a wide range of fast growing non-fastidious bacteria from marine samples.

- Difco Marine Broth 2216 37.5g
- Agar (Optional) 15g
- dH2O 1000ml

Sea Water Agar

Used to isolate slow growing fastidious bacteria from marine samples

- Sea Water 750ml
- dH_2O 250ml
- Agar (optional) 15g
- Wolf's Mineral Mix 5ml
- Wolf's Vitamin Mix 10ml

Wolfe's Mineral Mix

- Nitrilotriacetic acid 1.5g
- $MgSO_4$-$7H_2O$ 3g
- $MnSO_4$-H_2O 05g
- NaCl 1g
- $FeSO_4$-$7H_2O$ 0.1g
- $CaCl_2$ 0.1g
- $CoCl_2$-$6H_2O$ 0.1g
- $ZnSO_4$-$7H_2O$ 0.1g
- $CuSO_4$-$5H_2O$ 0.01g
- $AlK(SO)_4$-$12H_2O$ 0.01g
- H3BO3 (Boric Acid) 0.01g
- Na2MoO4-2H2O 0.01g
- dH2O 1000ml

Wolf's Vitamin Mix

- Pyridoxine hydrochloride 10mg
- Thiamine-HCl 5.0mg
- Riboflavin 5.0mg
- Nicotinic acid 5.0mg
- Calcium D-(+)-pantothenate 5.0mg
- p-Aminobenzoic acid 5.0mg
- Thioctic acid 5.0mg
- Biotin 2.0mg
- Folic Acid 2.0mg
- Vitamin B12 0.1mg
- dH2O 1000ml

GYM Streptomyces Medium (DSMZ Media 65) – Modified

Used to isolate Actinomyces species. Modified to increase salt concentrations to represent that of a marine environment. Cycloheximide used to retard the growth of fungus

- D-Glucose 4g
- Yeast Extract 4g
- Malt Extract 10g
- $CaCO_3$ 2g
- NaCl 24g
- $MgCl_2 * 6H_2O$ 5.3g
- KCl 0.7g
- $CaCl_2$ 0.1g
- Agar (Optional) 15g
- dH_2O 1000ml

- 20mg/ml Cycloheximide 1.25ml

Ashby's Nitrogen Free Medium – Modified

Used to isolate cyanobacteria which are able to fix nitrogen from the atmosphere. Modified to increase salt concentrations close to those of a marine environment.

- Mannitol 15g
- $CaCl_2 * 2H_2O$ 0.3g
- K_2HPO_4 0.2g
- $MgSO_4 * 7H_2O$ 0.2g
- 694mM Sodium Molybdate solution 0.1ml
- $FeCl_3$ (10% w:v solution) 0.05ml
- NaCl 24g
- $MgCl_2 * 6H_2O$ 5.3g
- KCl 0.7g
- Agar (Optional) 15g
- dH_2O 1000ml

APPENDIX B

Measurements dates for the sun photometer and precipitation measurements. **Data available at the time of writing. Blue-green: AIMMS, Orange: Microtops, Cyan: SDS, Vermillion: Parsivel**

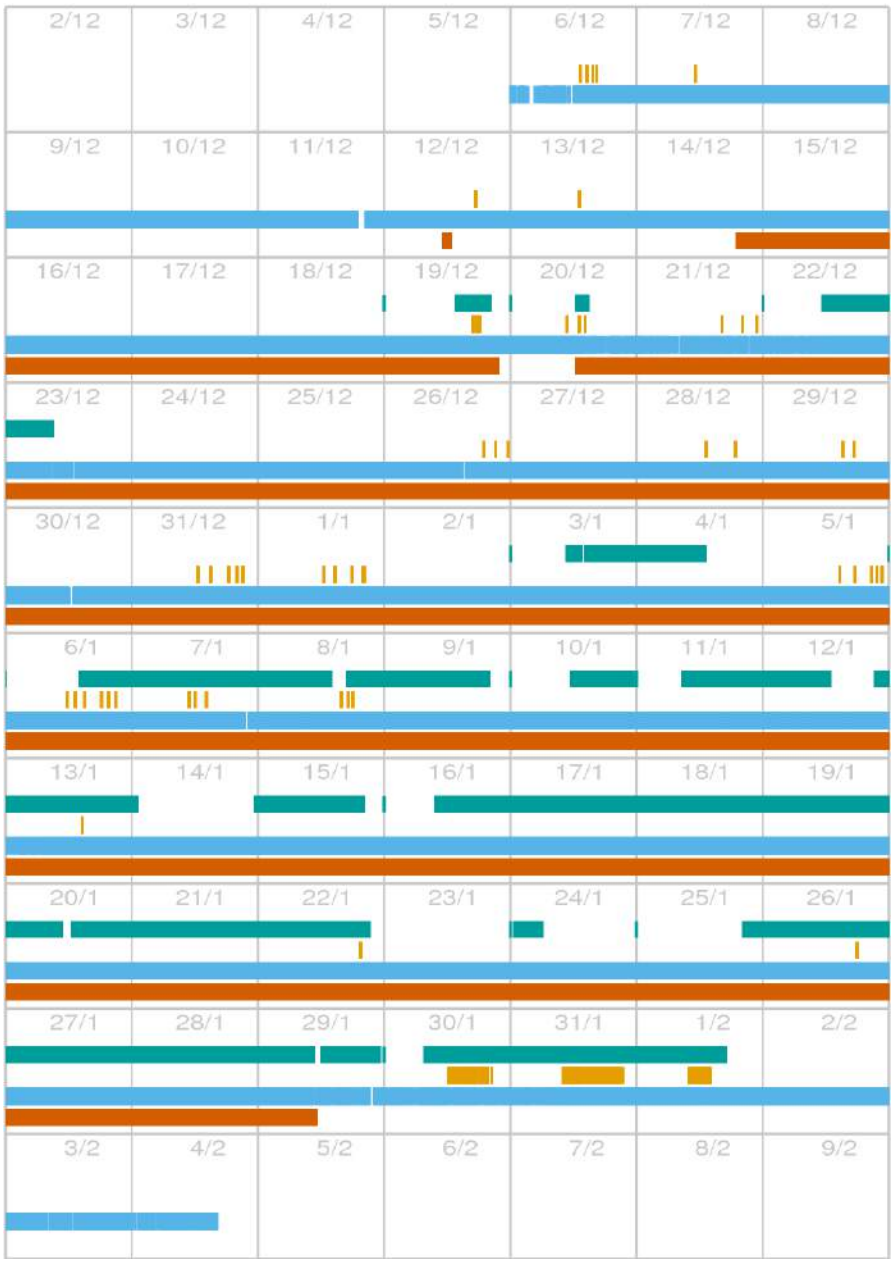

APPENDIX C

Date	Time	Type	Station	Filename	Latitude	NS	Longitude	EW	Station	Salinity	DO	Chla	TCO2	Nutrient
12/06/2012	22:17	XBT	GHS001	X121206N01	33 52.52	S	017 53.97	E		*	*	*	*	*
12/06/2012	23:38	XBT	GHS002	X121206N02	33 53.50	S	017 27.35	E			*			*
12/07/2012	01:15	XBT	GHS003	X121207N01	33 55.00	S	017 00.00	E		*	*	*	*	*
12/07/2012	01:25	XBT		X121207N02	33 55.17	S	016 56.67	E			*			*
12/07/2012	02:35	XBT	GHS004	X121207N03	33 55.44	S	016 37.70	E			*	*	*	*
12/07/2012	04:03	XBT	GHS005	X121207N04	33 56.32	S	016 12.80	E		*	*			*
12/07/2012	05:43	XBT	GHS006	X121207N05	33 58.02	S	015 46.71	E		*	*	*	*	*
12/07/2012	07:05	XBT	GHS007	X121207N06	33 59.29	S	015 24.82	E		*	*			*
12/07/2012	08:37	XBT	GHS008	X121207N07	34 00.22	S	015 00.29	E			*	*	*	*
12/07/2012	10:07	XBT	GHS009	X121207N08	34 02.70	S	014 37.44	E		*	*			*
12/07/2012	11:33	XBT	GHS010	X121207N09	34 19.48	S	014 24.56	E			*	*	*	*
12/07/2012	13:02	XBT	GHS011	X121207N10	34 36.47	S	014 12.07	E		*	*			*
12/07/2012	14:32	XBT	GHS012	X121207N11	34 54.07	S	013 59.02	E			*	*	*	*
12/07/2012	16:03	XBT	GHS013	X121207N12	35 10.47	S	013 47.09	E	Micro	*	*			*
12/07/2012	17:35	XBT	GHS014	X121207N13	35 27.51	S	013 34.11	E	Micro		*	*	*	*
12/07/2012	19:05	XBT	GHS015	X121207N14	35 43.48	S	013 22.01	E	Micro	*	*			*
12/07/2012	20:35	XBT	GHS016	X121207N15	35 59.34	S	013 09.85	E	Micro		*	*	*	*
12/07/2012	22:06	XBT	GHS017	X121207N16	36 16.92	S	012 57.02	E		*	*			*
12/07/2012	23:08	XBT	GHS018	X121207N17	36 28.32	S	012 48.22	E			*	*	*	*
12/08/2012	00:37	XBT	GHS019	X121208N01	36 46.37	S	012 34.49	E		*	*			*
12/08/2012	02:06	XBT	GHS020	X121208N02	37 03.47	S	012 21.20	E			*	*	*	*
12/08/2012	03:38	XBT	GHS021	X121208N03	37 21.79	S	012 07.32	E		*	*			*
12/08/2012	05:05	XBT	GHS022	X121208N04	37 38.95	S	011 53.59	E			*	*	*	*
12/08/2012	06:38	XBT	GHS023	X121208N05	37 56.62	S	011 40.01	E		*	*			*
12/08/2012	08:03	XBT	GHS024	X121208N06	38 14.37	S	011 27.81	E			*	*	*	*
12/08/2012	09:34	XBT	GHS025	X121208N07	38 31.51	S	011 13.59	E		*	*			*
12/08/2012	11:06	XBT	GHS026	X121208N08	38 49.02	S	010 59.02	E			*	*	*	*

12/08/2012	12:35	XBT	GHS027	X121208N09	39 04.50	S	010 47.55	E		*	*			*
12/08/2012	14:00	XBT	GHS028	X121208N10	39 20.88	S	010 33.85	E			*	*	*	*
12/08/2012	15:31	XBT	GHS029	X121208N11	39 39.01	S	010 20.10	E		*	*			*
12/08/2012	17:01	XBT	GHS030	X121208N12	39 56.46	S	010 05.84	E			*	*	*	*
12/08/2012	18:33	XBT	GHS031	X121208N13	40 14.08	S	009 52.83	E	Micro	*	*			*
12/08/2012	20:00	XBT	GHS032	X121208N14	40 29.95	S	009 39.45	E	Micro		*	*	*	*
12/08/2012	21:32	XBT	GHS033	X121208N15	40 46.82	S	009 26.09	E	Micro	*	*			*
12/08/2012	23:00	XBT	GHS034	X121208N16	41 02.54	S	009 13.38	E	Micro		*	*	*	*
12/09/2012	00:02	XBT	GHS035	X121209N01	41 14.14	S	009 03.95	E	Micro		*			*
12/09/2012	01:34	XBT	GHS036	X121209N02	41 31.54	S	008 49.78	E		*	*	*	*	*
12/09/2012	03:01	XBT	GHS037	X121209N03	41 48.34	S	008 36.06	E			*			*
12/09/2012	04:32	XBT	GHS038	X121209N04	42 05.28	S	008 22.13	E	Micro	*	*	*	*	*
12/09/2012	06:00	XBT	GHS039	X121209N05	42 21.37	S	008 08.86	E	Micro		*			*
12/09/2012	07:30	XBT	GHS040	X121209N06	42 30.04	S	008 01.63	E	CTD001 GLIDER Micro	*	*	*	*	*
12/09/2012	12:06	XBT	GHS041	X121209N07	42 40.40	S	007 53.10	E	Micro		*			*
12/09/2012	13:31	XBT	GHS042	X121209N08	43 06.46	S	007 39.70	E		*	*	*	*	*
12/09/2012	15:05	XBT	GHS043	X121209N10	43 14.28	S	007 24.80	E			*			*
12/09/2012	17:53	XBT	GHS044	X121209N11	43 30.01	S	007 11.17	E	CTD002 GLIDER Micro		*	*	*	*
12/09/2012	17:58	XBT	GHS044	X121209N12	43 30.01	S	007 11.17	E	Micro		*			*
12/09/2012	19:37	XBT	GHS045	X121209N13	43 35.12	S	007 07.19	E	Micro		*	*	*	*
12/09/2012	21:04	XBT	GHS046	X121209N14	43 50.67	S	006 54.10	E	Micro	*	*			*
12/09/2012	22:33	XBT	GHS047	X121209N15	44 07.54	S	006 39.76	E	Micro		*	*	*	*
12/10/2012	00:01	XBT	GHS050	X121210N01	44 24.05	S	006 25.66	E		*	*			*
12/10/2012	01:32	XBT	GHS051	X121210N02	44 41.18	S	006 10.95	E			*	*	*	*
12/10/2012	02:59	XBT	GHS052	X121210N03	44 56.90	S	005 57.41	E		*	*			*
12/10/2012	04:29	XBT	GHS053	X121210N04	45 12.87	S	005 43.60	E			*	*	*	*
12/10/2012	06:01	XBT	GHS054	X121210N05	45 29.93	S	005 28.75	E		*	*			*

12/10/2012	07:29	XBT	GHS055	X121210N06	45 47.30	S	005 13.55	E			*	*	*	*
12/10/2012	09:04	XBT	GHS056	X121210N07	46 05.70	S	004 58.97	E		*	*			*
12/10/2012	10:31	XBT	GHS057	X121210N10	46 21.84	S	004 43.14	E			*	*	*	*
12/10/2012	12:01	XBT	GHS058	X121210N11	46 38.81	S	004 28.05	E		*	*			*
12/10/2012	15:51	XBT	GHS059	X121210N14	46 51.11	S	004 16.82	E	CTD003 GLIDER Micro		*	*	*	*
12/10/2012	16:48	XBT	GHS060	X121210N15	47 00.87	S	004 08.32	E	Micro		*			*
12/10/2012	18:03	XBT	GHS061	X121210N16	47 13.96	S	003 55.46	E	Micro	*	*	*	*	*
12/10/2012	19:33	XBT	GHS062	X121210N17	47 29.95	S	003 42.11	E	Micro		*			*
12/10/2012	21:03	XBT	GHS063	X121210N18	47 44.90	S	003 26.34	E		*	*	*	*	*
12/10/2012	22:33	XBT	GHS064	X121210N19	47 58.27	S	003 09.17	E			*			*
12/11/2012	00:03	XBT	GHS065	X121211N01	48 11.31	S	002 52.09	E		*	*	*	*	*
12/11/2012	01:32	XBT	GHS066	X121211N02	48 21.78	S	002 34.12	E			*			*
12/11/2012	03:01	XBT	GHS067	X121211N03	48 31.28	S	002 14.94	E		*	*	*	*	*
12/11/2012	04:33	XBT	GHS068	X121211N04	48 41.79	S	001 53.65	E			*			*
12/11/2012	06:00	XBT	GHS069	X121211N05	48 52.07	S	001 32.14	E		*	*	*	*	*
12/11/2012	07:29	XBT	GHS070	X121211N06	49 01.89	S	001 10.80	E			*			*
12/11/2012	08:58	XBT	GHS071	X121211N07	49 17.71	S	000 54.12	E		*	*	*	*	*
12/11/2012	10:33	XBT	GHS072	X121211N08	49 38.49	S	000 46.79	E			*			*
12/11/2012	12:04	XBT	GHS073	X121211N09	49 59.49	S	000 39.66	E	Micro		*	*	*	*
12/11/2012	13:39	XBT	GHS074	X121211N10	50 18.33	S	000 32.76	E	Micro		*			*
12/11/2012	15:05	XBT	GHS075	X121211N11	50 37.60	S	000 23.49	E	Micro	*	*	*	*	*
12/11/2012	16:31	XBT	GHS076	X121211N12	50 55.76	S	000 14.67	E	Micro		*			*
12/11/2012	18:00	XBT	GHS077	X121211N14	51 18.40	S	000 03.40	E	Micro	*	*	*	*	*
12/11/2012	19:29	XBT	GHS078	X121211N15	51 33.00	S	000 00.00	E			*			*
12/11/2012	21:00	XBT	GHS079	X121211N16	51 52.87	S	000 00.01	E		*	*	*	*	*
12/11/2012	22:33	XBT	GHS080	X121211N17	52 13.59	S	000 00.00	E			*			*
12/12/2012	00:06	XBT	GHS081	X121212N01	52 31.40	S	000 00.01	E		*	*	*	*	*
12/12/2012	01:35	XBT	GHS082	X121212N02	52 53.15	S	000 00.21	E			*			*
12/12/2012	03:02	XBT	GHS083	X121212N03	53 13.60	S	000 00.20	E		*	*	*	*	*

12/12/2012	04:33	XBT	GHS084	X121212N04	53 34.19	S	000 00.01	E			*			*
12/12/2012	05:58	XBT	GHS085	X121212N05	53 54.17	S	000 00.00	E		*	*	*	*	*
12/12/2012	07:28	XBT	GHS086	X121212N06	54 14.75	S	000 00.01	E			*			*
12/12/2012	08:58	XBT	GHS087	X121212N07	54 35.08	S	000 00.01	E	Micro	*	*	*	*	*
12/12/2012	10:32	XBT	GHS088	X121212N08	54 55.96	S	000 00.08	E	Micro		*			*
12/12/2012	12:02	XBT	GHS089	X121212N09	55 15.74	S	000 00.04	E	Micro	*	*	*	*	*
12/12/2012	13:38	XBT	GHS090	X121212N11	55 36.49	S	000 00.01	E	Micro		*			*
12/12/2012	15:03	XBT	GHS091	X121212N12	55 56.44	S	000 00.00	E		*	*	*	*	*
12/12/2012	16:05	XBT	GHS092	X121212N14	56 10.21	S	000 00.00	E			*			*
12/12/2012	17:11	XBT	GHS093	X121212N16	56 23.89	S	000 00.02	E			*	*	*	*
12/12/2012	18:02	XBT	GHS094	X121212N17	56 36.98	S	000 00.01	E		*	*			*
12/12/2012	19:46	XBT	GHS095	X121212N19	56 57.43	S	000 01.73	E			*	*	*	*
12/12/2012	21:07	XBT	GHS096	X121212N20	57 15.47	S	000 12.10	E		*	*			*
12/12/2012	22:35	XBT	GHS097	X121212N21	57 33.14	S	000 26.04	E			*	*	*	*
12/13/2012	00:00	XBT	GHS098	X121213N01	57 48.29	S	000 41.44	E		*	*			*
12/13/2012	01:31	XBT	GHS099	X121213N02	58 05.75	S	000 58.75	E			*	*	*	*
12/13/2012	03:03	XBT	GHS100	X121213N03	58 22.93	S	001 15.57	E		*	*			*
12/13/2012	04:28	XBT	GHS101	X121213N04	58 40.05	S	001 29.15	E			*	*	*	*
12/13/2012	06:01	XBT	GHS102	X121213N05	58 59.60	S	001 31.06	E		*	*			*
12/13/2012	07:29	XBT	GHS103	X121213N06	59 16.47	S	001 21.56	E			*	*	*	*
12/13/2012	08:58	XBT	GHS104	X121213N07	59 31.95	S	001 03.37	E		*	*			*
12/13/2012	10:32	XBT	GHS105	X121213N08	59 50.13	S	000 46.43	E			*	*	*	*
12/13/2012	12:03	XBT	GHS106	X121213N09	60 09.59	S	000 36.16	E		*	*			*
12/13/2012	13:34	XBT	GHS107	X121213N10	60 27.94	S	000 17.19	E			*	*	*	*
12/13/2012	15:00	XBT	GHS108	X121213N11	60 47.17	S	000 00.55	W		*	*			*
12/13/2012	16:30	XBT	GHS109	X121213N12	61 08.65	S	000 02.48	E			*	*	*	*
12/13/2012	18:11	XBT	GHS110	X121213N13	61 30.56	S	000 01.02	W		*	*			*
12/13/2012	19:42	XBT	GHS111	X121213N15	61 47.40	S	000 00.69	W			*	*	*	*
12/13/2012	22:31	XBT	GHS113	X121213N18	62 21.18	S	000 04.14	W			*			*
12/13/2012	23:27	XBT	GHS114	X121213N19	62 31.74	S	000 03.41	W			*	*	*	*
12/14/2012	00:06	XBT	GHS115	X121214N01	63 36.76	S	000 05.00	E			*			*

12/14/2012	01:26	XBT	GHS116	X121214N02	62 43.50	S	000 03.49	W			*	*	*	*
12/14/2012	02:59	XBT	GHS117	X121214N03	62 52.64	S	000 03.18	W			*			*
12/14/2012	03:09	XBT	GHS118	X121214N04	62 53.83	S	000 03.39	W			*	*	*	*
12/14/2012	04:29	XBT	GHS119	X121214N05	63 01.91	S	000 03.69	W			*			*
12/14/2012	04:39	XBT	GHS120	X121214N06	63 03.23	S	000 03.63	W			*	*	*	*
12/14/2012	05:59	XBT	GHS121	X121214N07	63 13.69	S	000 04.29	W			*			*
12/14/2012	07:38	XBT	GHS122	X121214N08	63 31.30	S	000 01.97	E		*	*	*	*	*
12/14/2012	09:02	XBT	GHS123	X121214N09	63 48.17	S	000 00.20	W			*			*
12/14/2012	10:32	XBT	GHS124	X121214N10	64 01.34	S	000 02.72	W			*	*	*	*
12/14/2012	12:03	XBT	GHS125	X121214N11	64 18.67	S	000 05.09	W			*			*
12/14/2012	15:57	XBT	GHS126	X121214N12	64 59.55	S	000 04.16	E			*	*	*	*
12/14/2012	18:02	XBT	GHS127	X121214N13	65 24.70	S	000 30.30	E		*	*			*
12/14/2012	20:04	XBT	GHS128	X121214N14	65 53.81	S	000 29.23	E			*	*	*	*
12/14/2012	21:03	XBT	GHS129	X121214N15	66 07.25	S	000 28.24	E		*	*			*
12/14/2012	22:30	XBT	GHS130	X121214N16	66 28.10	S	000 23.20	E			*	*	*	*
12/14/2012	22:30	XBT	GHS130	X121215N01	66 28.10	S	000 23.20	E			*			*
12/15/2012	00:02	XBT	GHS131	X121215N02	66 49.09	S	000 20.21	E		*	*	*	*	*
12/15/2012	01:30	XBT	GHS132	X121215N04	67 02.90	S	000 25.27	E			*			*
12/15/2012	03:00	XBT	GHS133	X121215N06	67 21.86	S	000 29.70	E		*	*	*	*	*
12/15/2012	04:29	XBT	GHS134	X121215N07	67 34.55	S	000 22.36	E			*			*
12/15/2012	05:58	XBT	GHS135	X121215N08	67 50.78	S	000 08.83	E		*	*	*	*	*
12/15/2012	06:23	XBT	GHS136	X121215N10	67 56.68	S	000 05.38	E			*			*
12/15/2012	07:33	XBT	GHS137	X121215N12	68 11.73	S	000 01.64	E			*	*	*	*
12/15/2012	09:01	XBT	GHS138	X121215N13	68 31.94	S	000 08.68	W		*	*			*
12/15/2012	10:32	XBT	GHS139	X121215N14	68 46.94	S	000 10.32	W			*	*	*	*
12/15/2012	13:15	XBT	GHS140	X121215N15	69 06.06	S	000 13.45	W			*			*
12/24/2012	23:52	XBT	ICE141	X121224N01	70 15.61	S	002 44.25	W	CTD004		*	*	*	*
12/25/2012	12:02	XBT	ICE142	X121225N01	70 15.58	S	002 43.89	W	CTD005		*			*
12/26/2012	23:52	XBT	ICE143	X121226N01	70 15.61	S	002 44.27	W	CTD006		*	*	*	*
12/27/2012	12:56	XBT	ICE144	X121227N01	70 16.25	S	002 45.27	W	CTD007 test		*			*
12/27/2012	23:49	XBT	ICE145	X121227N02	70 15.61	S	002 44.24	W	CTD007		*	*	*	*

12/28/2012	11:50	XBT	ICE146	X121228N01	70 15.65	S	002 44.17	W	CTD008		*			*
12/28/2012	23:54	XBT	ICE147	X121228N02	70 15.65	S	002 44.63	W	CTD009		*	*	*	*
12/29/2012	23:54	XBT	ICE148	X121229N01	70 15.61	S	002 44.24	W	CTD010		*			*
12/29/2012	23:59	XBT	ICE149	X121230N01	70 15.61	S	002 44.24	W	CTD010		*	*	*	*
12/30/2012	23:58	XBT	ICE150	X121231N01	70 15.60	S	002 44.33	W	CTD011		*			*
12/31/2012	11:56	XBT	ICE151	X121231N02	70 15.58	S	002 44.36	W	CTD012		*	*	*	*
01/02/2013	12:21	XBT	ICE152	X130102N01	70 15.70	S	002 44.46	W	CTD013		*			*
01/02/2013	23:52	XBT	ICE153	X130102N02	70 15.57	S	002 44.45	W	CTD014		*	*	*	*
01/03/2013	11:54	XBT	ICE154	X130103N01	70 15.54	S	002 44.15	W	CTD015		*			*
01/03/2013	23:56	XBT	ICE155	X130103N02	70 15.52	S	002 44.25	W	CTD016		*	*	*	*
01/04/2013	12:01	XBT	ICE156	X130104N01	70 15.53	S	002 44.27	W	CTD017		*			*
01/05/2013	00:02	XBT	ICE157	X130105N01	70 15.58	S	002 44.34	W	CTD018		*	*	*	*
01/09/2013	23:58	XBT	ICE158	X130110N01	70 15.58	S	002 44.27	W	CTD019		*			*
01/10/2013	11:56	XBT	ICE159	X130110N02	70 15.59	S	002 44.32	W	CTD020		*	*	*	*
01/10/2013	12:00	XBT	ICE159	X130110N02	70 15.57	S	002 44.31	W			*			*
01/13/2013	14:36	XBT	BR161	X130113N04	69 53.89	S	001 36.26	W			*	*	*	*
01/13/2013	14:44	XBT	BR162	X130113N05	69 53.89	S	001 36.26	W		*	*			*
01/14/2013	06:00	XBT	BR164	X130114N01	68 47.46	S	000 02.67	W			*	*	*	*
01/14/2013	07:27	XBT	BR165	X130114N02	68 29.47	S	000 00.55	W			*			*
01/14/2013	08:22	XBT	BR166	X130114N03	68 17.85	S	000 00.97	E			*	*	*	*
01/14/2013	08:40	XBT	BR167	X130114N04	68 13.43	S	000 00.20	W		*	*			*
01/14/2013	09:04	XBT	BR168	X130114N05	68 08.17	S	000 00.69	W			*	*	*	*
01/14/2013	09:50	XBT	BR169	X130114N06	68 00.35	S	000 00.17	W			*			*
01/14/2013	11:25	XBT	BR170	X130114N07	67 52.82	S	000 03.61	E		*	*	*	*	*
01/14/2013	12:03	XBT	BR171	X130114N08	67 44.65	S	000 00.90	E			*			*
01/14/2013	12:54	XBT	BR172	X130114N09	67 33.23	S	000 04.57	W		*	*	*	*	*
01/14/2013	13:35	XBT	BR173	X130114N10	67 24.06	S	000 02.68	W			*			*
01/14/2013	14:23	XBT	BR174	X130114N11	67 13.38	S	000 00.38	E		*	*	*	*	*
01/14/2013	15:01	XBT	BR175	X130114N12	67 04.46	S	000 00.78	E			*			*
01/14/2013	15:28	XBT	BR176	X130114N13	66 59.84	S	000 00.07	W		*	*	*	*	*
01/14/2013	17:20	XBT	BR177	X130114N15	66 45.04	S	000 00.15	W			*			*

01/14/2013	18:01	XBT	BR178	X130114N16	66 37.53	S	000 00.41	W		*	*	*	*	*
01/14/2013	18:41	XBT	BR179	X130114N17	66 30.85	S	000 00.86	W			*			*
01/14/2013	19:32	XBT	BR180	X130114N18	66 22.18	S	000 01.42	W		*	*	*	*	*
01/14/2013	20:14	XBT	BR181	X130114N19	66 14.90	S	000 00.51	W			*			*
01/14/2013	21:02	XBT	BR182	X130114N20	66 06.94	S	000 00.24	W		*	*	*	*	*
01/14/2013	21:45	XBT	BR183	X130114N21	66 00.00	S	000 00.00	E			*			*
01/14/2013	23:15	XBT	BR184	X130114N22	65 53.50	S	000 00.23	W		*	*	*	*	*
01/15/2013	00:38	XBT	BR185	X130115N01	65 39.51	S	000 00.45	W			*			*
01/15/2013	00:54	XBT	BR186	X130115N02	65 36.92	S	000 00.53	W		*	*	*	*	*
01/15/2013	01:37	XBT	BR187	X130115N03	65 29.78	S	000 00.31	W			*			*
01/15/2013	02:18	XBT	BR188	X130115N04	65 22.97	S	000 00.06	W		*	*	*	*	*
01/15/2013	03:05	XBT	BR189	X130115N05	65 15.06	S	000 00.10	W			*			*
01/15/2013	03:52	XBT	BR190	X130115N06	65 07.21	S	000 00.10	E		*	*	*	*	*
01/15/2013	04:28	XBT	BR191	X130115N07	65 00.91	S	000 00.12	W			*			*
01/15/2013	05:55	XBT	BR192	X130115N08	64 56.15	S	000 00.47	E		*	*	*	*	*
01/15/2013	06:44	XBT	BR193	X130115N09	64 48.36	S	000 00.24	E			*			*
01/15/2013	07:30	XBT	BR194	X130115N10	64 39.66	S	000 00.33	W		*	*	*	*	*
01/15/2013	08:17	XBT	BR195	X130115N11	64 31.67	S	000 00.25	W			*			*
01/15/2013	09:01	XBT	BR196	X130115N12	64 24.02	S	000 00.01	E		*	*	*	*	*
01/15/2013	09:45	XBT	BR197	X130115N13	64 16.48	S	000 00.28	W			*			*
01/15/2013	10:30	XBT	BR198	X130115N14	64 08.55	S	000 00.01	W		*	*	*	*	*
01/15/2013	11:28	XBT	BR199	X130115N15	63 59.99	S	000 00.08	W			*			*
01/15/2013	13:32	XBT	BR200	X130115N16	63 49.65	S	000 00.06	W		*	*	*	*	*
01/15/2013	14:16	XBT	BR201	X130115N17	63 42.31	S	000 00.99	W			*			*
01/15/2013	15:02	XBT	BR202	X130115N18	63 34.98	S	000 00.10	W		*	*	*	*	*
01/15/2013	15:47	XBT	BR203	X130115N19	63 27.33	S	000 00.63	E			*			*
01/15/2013	16:32	XBT	BR204	X130115N20	63 19.78	S	000 00.29	W		*	*	*	*	*
01/15/2013	17:17	XBT	BR205	X130115N21	63 12.28	S	000 00.42	E			*			*
01/15/2013	18:01	XBT	BR206	X130115N22	63 04.72	S	000 00.21	E		*	*	*	*	*
01/15/2013	18:31	XBT	BR207	X130115N23	63 00.06	S	000 00.29	E			*			*
01/15/2013	20:09	XBT	BR208	X130115N24	62 59.45	S	000 00.65	E			*	*	*	*

01/15/2013	20:57	XBT	BR209	X130115N25	62 44.52	S	000 01.47	E		*	*			*
01/15/2013	21:51	XBT	BR210	X130115N26	62 36.39	S	000 00.40	E			*	*	*	*
01/15/2013	23:05	XBT	BR211	X130115N27	62 28.44	S	000 00.48	W		*	*			*
01/15/2013	23:29	XBT	BR212	X130115N28	62 19.97	S	000 00.29	W			*	*	*	*
01/16/2013	00:03	XBT	BR213	X130116N01	62 14.53	S	000 00.09	W		*	*			*
01/16/2013	00:51	XBT	BR214	X130116N02	62 06.97	S	000 01.07	W			*	*	*	*
01/16/2013	01:33	XBT	BR215	X130116N03	62 00.20	S	000 00.23	W		*	*			*
01/16/2013	03:07	XBT	BR216	X130116N04	61 53.06	S	000 00.85	W			*	*	*	*
01/16/2013	04:01	XBT	BR217	X130116N05	61 43.39	S	000 00.06	W		*	*			*
01/16/2013	04:33	XBT	BR218	X130116N06	61 38.38	S	000 01.97	W		*	*	*	*	*
01/16/2013	05:15	XBT	BR219	X130116N07	61 32.10	S	000 01.51	W			*			*
01/16/2013	05:58	XBT	BR220	X130116N08	61 24.77	S	000 03.75	E		*	*	*	*	*
01/16/2013	06:47	XBT	BR221	X130116N09	61 16.94	S	000 02.13	E			*			*
01/16/2013	07:31	XBT	BR222	X130116N10	61 09.80	S	000 01.48	E		*	*	*	*	*
01/16/2013	08:41	XBT	BR223	X130116N11	60 59.95	S	000 00.01	E			*			*
01/16/2013	10:33	XBT	BR224	X130116N12	60 54.30	S	000 00.48	E		*	*	*	*	*
01/16/2013	11:17	XBT	BR225	X130116N13	60 47.80	S	000 00.51	W			*			*
01/16/2013	12:00	XBT	BR226	X130116N14	60 41.06	S	000 00.16	E		*	*	*	*	*
01/16/2013	12:48	XBT	BR227	X130116N15	60 33.39	S	000 00.39	E			*			*
01/16/2013	13:32	XBT	BR228	X130116N16	60 26.45	S	000 00.13	W		*	*	*	*	*
01/16/2013	14:18	XBT	BR229	X130116N17	60 18.67	S	000 00.05	W			*			*
01/16/2013	15:02	XBT	BR230	X130116N18	60 11.62	S	000 00.15	E		*	*	*	*	*
01/16/2013	15:48	XBT	BR231	X130116N19	60 04.20	S	000 00.13	W			*			*
01/16/2013	16:24	XBT	BR232	X130116N20	60 00.02	S	000 00.18	E			*	*	*	*
01/30/2013	00:04	XBT	ICE233	X130130N01	70 32.02	S	007 51.94	W	CTD031		*			*
01/30/2013	12:32	XBT	ICE234	X130130N02	70 32.02	S	007 51.89	W	CTD032		*	*	*	*
01/31/2013	12:56	XBT	ICE235	X130131N01	70 32.01	S	007 51.89	W	CTD034		*			*
02/08/2013	23:55	XBT	ICE236	X130208N01	70 32.01	S	007 51.86	W	CTD035		*	*	*	*
02/08/2013	12:14	XBT	ICE237	X130208N02	70 32.00	S	007 51.86	W	CTD036		*			*
02/09/2013	00:03	XBT	ICE238	X130209N01	70 32.00	S	007 51.84	W	CTD037		*	*	*	*
02/10/2013	22:34	XBT	SN001	X130210N01	69 13.01	S	007 58.63	W		*	*			*

02/11/2013	00:05	XBT	SN002	X130211N01	68 54.85	S	007 49.42	W		*	*	*	*
02/11/2013	01:36	XBT	SN003	X130211N02	68 38.08	S	007 41.21	W	*	*			*
02/11/2013	02:59	XBT	SN004	X130211N03	68 22.12	S	007 34.79	W		*	*	*	*
02/11/2013	04:31	XBT	SN005	X130211N04	68 01.18	S	007 29.99	W	*	*			*
02/11/2013	06:06	XBT	SN006	X130211N05	67 38.97	S	007 24.21	W		*	*	*	*
02/11/2013	07:32	XBT	SN007	X130211N06	67 18.81	S	007 18.51	W	*	*			*
02/11/2013	09:02	XBT	SN008	X130211N07	66 57.02	S	007 14.10	W		*	*	*	*
02/11/2013	10:32	XBT	SN009	X130211N08	66 35.04	S	007 08.68	W	*	*			*
02/11/2013	12:01	XBT	SN010	X130211N09	66 14.25	S	007 03.53	W		*	*	*	*
02/11/2013	13:33	XBT	SN011	X130211N10	65 52.39	S	006 58.82	W	*	*			*
02/11/2013	13:43	XBT	SN011	X130211N11	65 52.39	S	006 58.82	W		*	*	*	*
02/11/2013	15:07	XBT	SN012	X130211N12	65 30.49	S	006 52.89	W		*			*
02/11/2013	16:33	XBT	SN013	X130211N13	65 09.82	S	006 51.08	W	*	*	*	*	*
02/11/2013	18:05	XBT	SN014	X130211N14	64 48.78	S	006 44.21	W		*			*
02/11/2013	19:33	XBT	SN015	X130211N15	64 27.98	S	006 38.92	W	*	*	*	*	*
02/11/2013	21:03	XBT	SN016	X130211N16	64 05.55	S	006 38.98	W		*			*
02/11/2013	22:32	XBT	SN017	X130211N17	63 44.96	S	006 32.87	W	*	*	*	*	*
02/12/2013	00:02	XBT	SN018	X130212N01	63 27.19	S	006 27.46	W		*			*
02/12/2013	00:10	XBT	SN018	X130212N02	63 25.97	S	006 26.86	W		*	*	*	*
02/12/2013	01:29	XBT	SN019	X130212N03	63 11.08	S	006 22.40	W	*	*			*
02/12/2013	03:00	XBT	SN020	X130212N04	62 53.42	S	006 19.32	W		*	*	*	*
02/12/2013	04:32	XBT	SN021	X130212N05	62 31.36	S	006 14.72	W	*	*			*
02/12/2013	06:02	XBT	SN022	X130212N06	62 07.90	S	006 09.95	W		*	*	*	*
02/12/2013	07:32	XBT	SN023	X130212N07	61 43.73	S	006 06.22	W	*	*			*
02/12/2013	09:00	XBT	SN024	X130212N08	61 20.58	S	006 00.38	W		*	*	*	*
02/12/2013	10:30	XBT	SN025	X130212N09	60 56.38	S	005 55.08	W	*	*			*
02/12/2013	12:03	XBT	SN026	X130212N10	60 31.71	S	005 50.81	W		*	*	*	*
02/12/2013	13:33	XBT	SN027	X130212N11	60 07.90	S	005 45.39	W	*	*			*
02/12/2013	15:02	XBT	SN028	X130212N12	59 44.08	S	005 42.97	W		*	*	*	*
02/12/2013	16:31	XBT	SN029	X130212N13	59 20.37	S	005 37.66	W	*	*			*
02/12/2013	19:34	XBT	SN031	X130212N15	58 32.80	S	005 32.56	W	*	*	*	*	*

02/12/2013	21:03	XBT	SN032	X130212N16	58 09.11	S	005 24.02	W		*			*
02/12/2013	22:33	XBT	SN033	X130212N17	57 44.67	S	005 19.25	W	*	*	*	*	*
02/13/2013	00:02	XBT	SN034	X130213N01	57 21.26	S	005 16.24	W		*			*
02/13/2013	01:40	XBT	SN035	X130213N02	56 55.73	S	005 11.49	W	*	*	*	*	*
02/13/2013	02:57	XBT	SN036	X130213N03	56 35.00	S	005 07.99	W		*			*
02/13/2013	04:40	XBT	SN037	X130213N05	56 12.55	S	005 04.03	W	*	*	*	*	*
02/13/2013	06:04	XBT	SN038	X130213N06	55 52.49	S	005 00.95	W		*			*
02/13/2013	07:29	XBT	SN039	X130213N07	55 29.47	S	004 57.17	W	*	*	*	*	*
02/13/2013	09:01	XBT	SN040	X130213N08	55 05.14	S	004 52.62	W		*			*
02/13/2013	12:07	XBT	SN041	X130213N10	54 15.60	S	004 45.31	W	*	*	*	*	*
02/13/2013	13:32	XBT	SN042	X130213N11	53 52.49	S	004 41.10	W		*			*
02/13/2013	15:01	XBT	SN043	X130213N12	53 29.43	S	004 37.37	W	*	*	*	*	*
02/13/2013	16:34	XBT	SN044	X130213N13	53 04.74	S	004 33.48	W		*			*
02/13/2013	18:03	XBT	SN045	X130213N14	52 40.66	S	004 29.71	W	*	*	*	*	*
02/13/2013	19:36	XBT	SN046	X130213N15	52 16.34	S	004 25.95	W		*			*
02/13/2013	21:02	XBT	SN047	X130213N16	51 53.08	S	004 22.37	W	*	*	*	*	*
02/13/2013	22:33	XBT	SN048	X130213N17	51 29.34	S	004 18.74	W		*			*
02/13/2013	23:58	XBT	SN049	X130214N01	51 07.28	S	004 15.93	W	*	*	*	*	*
02/14/2013	00:03	XBT	SN050	X130214N02	51 07.28	S	004 15.94	W		*			*
02/14/2013	01:30	XBT	SN051	X130214N03	50 43.21	S	004 11.79	W	*	*	*	*	*
02/14/2013	02:59	XBT	SN052	X130214N04	50 19.34	S	004 08.25	W		*			*
02/14/2013	04:18	XBT	SN053	X130214N05	49 59.20	S	004 05.29	W	*	*	*	*	*
02/14/2013	06:05	XBT	SN054	X130214N06	49 30.38	S	004 01.07	W		*			*
02/14/2013	07:27	XBT	SN055	X130214N07	49 10.12	S	003 58.10	W	*	*	*	*	*
02/14/2013	08:59	XBT	SN056	X130214N08	48 44.57	S	003 54.46	W		*			*
02/14/2013	10:30	XBT	SN057	X130214N09	48 20.75	S	003 51.07	W	*	*	*	*	*
02/14/2013	12:02	XBT	SN058	X130214N10	47 56.36	S	003 47.61	W		*			*
02/14/2013	13:36	XBT	SN059	X130214N11	47 31.70	S	003 44.15	W	*	*	*	*	*
02/14/2013	15:02	XBT	SN060	X130214N12	47 07.88	S	003 40.83	W		*			*
02/14/2013	16:33	XBT	SN061	X130214N13	46 44.09	S	003 41.48	W	*	*	*	*	*
02/14/2013	16:39	XBT	SN061	X130214N14	46 44.08	S	003 41.47	W		*			*

02/14/2013	18:05	XBT	SN062	X130214N15	46 21.56	S	003 47.13	W			*	*	*	*
02/14/2013	19:35	XBT	SN063	X130214N16	45 57.81	S	003 42.70	W		*	*			*
02/14/2013	21:05	XBT	SN064	X130214N18	45 39.60	S	003 34.53	W			*	*	*	*
02/14/2013	23:57	XBT	SN066	X130215N01	45 04.27	S	003 24.00	W		*	*			*
02/15/2013	01:26	XBT	SN067	X130215N02	44 46.12	S	003 21.57	W			*	*	*	*
02/15/2013	01:31	XBT	SN067	X130215N03	44 46.12	S	003 21.57	W		*	*			*
02/15/2013	02:59	XBT	SN068	X130215N04	44 26.74	S	003 19.01	W			*	*	*	*
02/15/2013	03:04	XBT	SN068	X130215N05	44 26.74	S	003 19.01	W			*			*
02/15/2013	04:32	XBT	SN069	X130215N07	44 09.19	S	003 16.69	W		*	*	*	*	*
02/15/2013	05:57	XBT	SN070	X130215N08	43 51.30	S	003 14.56	W			*			*
02/15/2013	07:27	XBT	SN071	X130215N09	43 34.12	S	003 14.49	W		*	*	*	*	*
02/15/2013	09:30	XBT	SN072	X130215N10	43 08.34	S	003 14.50	W			*			*
02/15/2013	10:31	XBT	SN073	X130215N11	42 44.14	S	003 14.51	W		*	*	*	*	*
02/15/2013	12:02	XBT	SN074	X130215N12	42 19.02	S	003 14.50	W			*			*
02/15/2013	13:27	XBT	SN075	X130215N13	41 55.43	S	003 14.50	W		*	*	*	*	*
02/15/2013	14:59	XBT	SN076	X130215N14	41 31.75	S	003 08.89	W			*			*
02/15/2013	17:54	XBT	SN077	X130215N15	41 32.97	S	003 07.90	W	CTD038 /GLIDE RS		*	*	*	*
02/15/2013	21:02	XBT	SN078	X130215N16	41 23.95	S	002 47.17	W			*			*
02/15/2013	22:36	XBT	SN079	X130215N18	41 15.28	S	002 21.02	W		*	*	*	*	*
02/16/2013	00:00	XBT	SN080	X130216N01	41 07.06	S	001 56.31	W			*			*
02/16/2013	00:45	XBT	SN081	X130216N02	41 03.76	S	001 46.41	W		*	*	*	*	*
02/16/2013	01:58	XBT	SN082	X130216N03	40 55.91	S	001 22.89	W			*			*
02/16/2013	03:46	XBT	SN083	X130216N04	40 45.18	S	000 50.78	W		*	*	*	*	*
02/16/2013	05:01	XBT	SN084	X130216N05	40 38.06	S	000 29.63	W			*			*
02/16/2013	06:28	XBT	SN085	X130216N06	40 29.86	S	000 05.13	W		*	*	*	*	*
02/16/2013	08:03	XBT	SN086	X130216N08	40 21.07	S	000 20.95	W			*			*
02/16/2013	09:31	XBT	SN087	X130216N09	40 12.11	S	000 47.51	E		*	*	*	*	*
02/16/2013	11:02	XBT	SN088	X130216N10	40 03.08	S	001 14.29	E			*			*
02/16/2013	12:30	XBT	SN089	X130216N11	39 54.33	S	001 40.10	E		*	*	*	*	*
02/16/2013	14:00	XBT	SN090	X130216N12	39 45.40	S	002 06.40	E			*			*

02/16/2013	15:34	XBT	SN091	X130216N13	39 36.14	S	002 33.64	E	*	*	*	*	*
02/16/2013	17:03	XBT	SN092	X130216N14	39 26.97	S	003 00.76	E		*			*
02/16/2013	18:32	XBT	SN093	X130216N15	39 17.75	S	003 27.42	E	*	*	*	*	*
02/16/2013	20:04	XBT	SN094	X130216N16	39 08.52	S	003 54.42	E		*			*
02/16/2013	21:34	XBT	SN095	X130216N17	38 59.48	S	004 21.65	E	*	*	*	*	*
02/16/2013	23:01	XBT	SN096	X130216N18	38 50.58	S	004 47.16	E		*			*
02/17/2013	00:29	XBT	SN096	X130217N01	38 41.57	S	005 12.58	E		*	*	*	*
02/17/2013	01:59	XBT	SN097	X130217N02	38 32.73	S	005 38.47	E	*	*			*
02/17/2013	03:33	XBT	SN098	X130217N03	38 23.29	S	006 05.69	E		*	*	*	*
02/17/2013	05:02	XBT	SN099	X130217N04	38 14.01	S	006 32.16	E	*	*			*
02/17/2013	06:25	XBT	SN100	X130217N05	38 05.79	S	006 55.75	E		*	*	*	*
02/17/2013	08:03	XBT	SN101	X130217N06	37 56.29	S	007 24.24	E	*	*			*
02/17/2013	09:30	XBT	SN102	X130217N07	37 47.18	S	007 49.15	E		*	*	*	*
02/17/2013	11:01	XBT	SN103	X130217N08	37 37.69	S	008 16.84	E	*	*			*
02/17/2013	12:31	XBT	SN104	X130217N09	37 28.72	S	008 43.69	E		*	*	*	*
02/17/2013	12:38	XBT	SN104	X130217N10	37 28.72	S	008 42.69	E		*			*